FACULDADE DE ENGENHARIA DA UNIVERSIDADE DO PORTO

MODEL FOR EDUCATIONAL SIMULATION OF THE NEONATAL ELECTROCARDIOGRAM

MODELO PARA SIMULAÇÃO EDUCATIVA DO ELECTROCARDIOGRAMA NEONATAL

José Rodolfo Polónia Pinto
(Licenciature degree in Electrical and Computer Engineering by Engineering Faculty, University of Porto, Portugal)

Thesis submitted in fulfilment of the requirements for the degree of master of science in Biomedical Engineering

Supervised by:

Prof. Willem van Meurs (Ph.D), principal researcher at Instituto de Engenharia Biomédica (INEB)

Porto, March 2005

Much importance is given to the cost of building something.
And none to the cost of not building it.

Philip Kotler

Acknowledgments…

… to Prof. Willem van Meurs, for all the support, interest, exciting motivation, and friendship during the elaboration of this thesis, and for the given opportunities to develop and present this work abroad.

… to Nicole de Beer (PhD), for the essential co-orientation, collaboration and friendship during my stage in Eindhoven – The Netherlands.

… to Peter Andriessen (MD, PhD), from Maxima Medical Center – Veldhoven, The Netherlands, for the interest, availability, and expert feedback on neonatology.

… to Prof. Marques de Sá, for stimulating this work and facilitating my stage in Eindhoven.

… to the Technische Universiteit Eindhoven and the colleagues from the Signal Processing Systems group - Department of Electrical Engineering, for the excellent working conditions, financial support, facilities given and friendship.

… to Instituto de Engenharia Biomédica, for the excellent working conditions, and financial and logistic support.

… to the physiologic modelling and simulation team, at Instituto de Engenharia Biomédica, for all the collaboration and friendship.

… to my family, for the eternal patience, accompaniment, and (rather than technical) support. ;)

Abstract

In the first weeks of life, cardiac rhythm disturbances may represent - or evolve into - life threatening situations. Electrocardiography is an essential tool in the often time-critical diagnosis and management of rhythm abnormalities. Traditional education in neonatal electrophysiology is based on didactic teaching and the use of sample electrocardiogram (ECG) strips, and on practical training of acute care skills in the clinical setting. These are less than ideal learning environments for a number of reasons, among them the lack of control over the training situation, limited possibility to intervene, and potential risks to (real) patients. In other areas of acute care medicine, simulator based training is rapidly becoming the standard for addressing these educational challenges.

The general goal of this work was to design a model for educational simulation of the neonatal ECG, which may become part of a full-body, model-driven neonatal simulator. In the limited time frame of this study, we focused on a screen-based application.

We present a brief review of neonatal cardiovascular physiology and electrophysiology. A rigorous methodology for the design of simulators and simulator based training, presented in the military context, consists of subsequent training needs analysis, training program design, and training media specification (TMS). We adapted and applied this methodology to outline a simulator based training program and to set detailed requirements for a neonatal ECG simulator.

A screen-based, model-driven simulator: Neonatal Electrocardiogram Generator for Rhythm Analysis (NEGRA) was developed to meet these requirements. It displays action potentials in a number of cardiac structures and a corresponding lead II ECG in real-time. A number of rhythms can be selected, and several physiologic parameters can be manipulated and their effect on action potentials and ECG wave forms observed. Specifications for the required underlying model of electrophysiology were also set as part of the TMS.

A detailed review of the literature and subsequent classification of encountered models led to selection of a published model for the adult which came closest to meeting the requirements. We expanded this model with a more flexible structure for representing cardiac conduction phenomena, derived parameters and ECG wave form templates for the neonate, and filled in several blanks left by the authors.

The simulation results emphasize the power of a model-driven approach for generation of a large variety of cardiac rhythms, associated action potentials, and ECG time signals. Simultaneous display of action potentials and ECG helps build a "mental model" of impulse conduction through the heart and its relationship to surface ECG. The adapted and followed design methodology is a foundation for further work on all educational acute care simulators.

Sumário

Durante as primeiras semanas de vida, diferentes perturbações do ritmo cardíaco podem representar (ou desenvolver-se em) situações de risco de vida. A electrocardiografia é uma ferramenta essencial no diagnóstico e controlo de anomalias rítmicas, muitas vezes em fracções de tempo críticas. A aprendizagem tradicional da electrofisiologia neonatal tem sido baseada no ensino didáctico com apoio de exemplos de electrocardiogramas (ECGs) e treino de práticas de cuidados intensivos em situações reais de ambiente clínico-hospitalar. Estas condições estão longe ser as ideais: são dificilmente controláveis, as possibilidades de intervenção são sempre limitadas, e acarretam riscos reais para os pacientes. Noutras áreas de cuidados intensivos, o treino com simuladores tem-se vindo a revelar fundamental para dar resposta a estes desafios educacionais.

O objectivo geral deste trabalho consiste na concepção de um modelo para a simulação educativa do ECG neonatal, que poderá vir a fazer parte de um simulador neonatal em tamanho real, mediado por um ou mais modelos ("model driven"). No tempo limitado deste estudo, os objectivos foram centrados na construção de uma aplicação "model driven" para uso em computador.

Começamos por apresentar uma revisão sucinta sobre a fisiologia cardiovascular neonatal. Depois, aplicamos e adaptamos uma metodologia rigorosa na concepção de um programa de treino simulado e na definição detalhada dos requisitos para um simulador do ECG neonatal. Esta metodologia consiste numa análise das necessidades de treino, no desenho e concepção do programa de treino, e especificação dos meios a serem utilizados ("training media specification" - TMS).

Desenvolvemos um simulador "model driven" para uso em computador – Neonatal Electrocardiogram Generator for Rhythm Analysis (NEGRA) – baseado nos requisitos estabelecidos. A aplicação fornece em tempo real os potenciais de acção em algumas estruturas cardíacas, e o electrocardiograma, "lead II". Permite também seleccionar alguns ritmos pré-definidos, bem como manipular alguns parâmetros fisiológicos. Os efeitos podem ser observados nos potenciais de acção e ECG correspondentes. As especificações para o modelo de electrofisiologia requerido foram definidas como parte da TMS.

Fazemos uma descrição integrada e consequente classificação dos modelos resultantes da pesquisa de literatura, que permitiu a selecção de um modelo para o adulto que melhor pudesse satisfazer os requisitos propostos para um modelo do recém-nascido. Expandimos o modelo com uma estrutura mais flexível para uma melhor representação dos fenómenos de condução, derivamos parâmetros e formas de onda típicas do ECG neonatal, e preenchemos ainda mais algumas lacunas deixadas pelos autores.

Os resultados das simulações realçam o poder de uma abordagem "model-driven" na geração de uma variedade de ritmos cardíacos, potenciais de acção associados, e sinais electrocardiográficos. A apresentação simultânea de potenciais de acção e o ECG é uma ajuda efectiva na construção de um modelo mental para a condução de impulsos eléctricos no coração e a sua relação com o ECG à superfície do corpo. A metodologia seguida e adaptada constitui um "exemplo a seguir" em futuros desenvolvimentos de este e outros simuladores educacionais em cuidados intensivos.

Contents

List of Figures

List of Tables

List of Abbreviators

AP	Action potential
AV	Atrio-ventricular
BPM	Beats per minute
CAH	Combined atrial hypertrophy
CHD	Congenital heart disease
CVH	Combined ventricular hypertrophy
DA	Ductus arteriosus
DV	Ductus venosus
ECG	Electrocardiogram
FO	Foramen ovale
HR	Heart rate
II	Instructor interface
IVC	Inferior vena cava
LA	Left atrium
LAH	Left atrial hypertrophy
LBBB	Left bundle branch block
LQTS	Long QT syndrome
LV	Left ventricle
LVH	Left ventricular hypertrophy
MRI	Magnetic resonance imaging
NEGRA	Neonatal electrocardiogram generator for rhythm analysis
NSR	Normal sinus rhythm
PAC	Premature atrial contraction
PL	Placenta
PVC	Premature ventricular contraction
RA	Right atrium
RAD	Right axis deviation
RAH	Right atrial hypertrophy
RAVT	Reciprocating AV tachycardia
RBBB	Right bundle branch block
RV	Right ventricle
RVH	Right ventricular hypertrophy
SE	Simulation engine
SVT	Supraventricular tachycardia
TI	Trainee interface
TMS	Training media specification
TNA	Training needs analysis
TPD	Training program design
UA	Umbilical arteries
UV	Umbilical vein
VT	Ventricular tachycardia
WPW	Wolff-Parkinson-White

Chapter 1

Introduction

The evolution from the intrauterine fetus to the extrauterine neonate, infant, child, adolescent and adult, results in major changes of body size and shape, and with this, the size and position of the heart relative to the body and cardiac physiology [Tipple, 1999]. The most dramatic of these changes occur at birth and within the first year of life, in which the first weeks are particularly precarious. In most children, serious heart disease presents early in the first month of life [Klaus, 2001]. More deaths occur due to cardiac defects than any other birth defect [Stat, 2002]. Underlying the most serious heart complications in neonates are congenital heart defects (CHD) and/or cardiac rhythm disturbances, which may represent - or evolve into - life threatening situations. CHD is one of the most common causes of morbidity and mortality in a pediatric hospital [Klaus, 2001].

During the critical neonatal period, a thorough physical and physiological examination is essential to identify potential problems and institute early interventions. Several diagnostic tools are commonly used: chest radiography, electrocardiography, echocardiography, cardiac catheterisation and angiography, and magnetic resonance imaging (MRI). From these tools, electrocardiography is the most valuable for the diagnosis and management of arrhythmias [Avery, 1999].

Neonatal electrocadiography

Electrocardiography is a useful tool in the management of pediatric heart disease. So far, neonatal ECGs are requested relatively infrequently. This situation may change, however, as some european countries have begun to consider the possibility of introducing in their National Health Services an ECG during the first month of life in all newborns as part of a cardiovascular screening programme [Schwartz, 2002]. The rational for this evolution is diverse, but it is mainly based on the realization that early identification of life-threatening arrhythmogenic disorders may allow initiation of effective preventive therapy. This confirms the importance of electrocardiography in the diagnosis of neonatal cardiac abnormalities, particularly in the case of rhythm disturbances.

Neonatal ECG interpretation requires practice due to evolving norms, brought about by physiological changes in the circulatory system in this age group [Tipple, 1999]. Unless the patient's age and additional clinical information is known, the ECG cannot be interpreted. For these reasons, teaching and training medical personnel in reading neonatal ECGs, diagnosis and deciding on consequent interventions is a complex, and not completely resolved topic. This is also underlined by the European Society of Cardiology, which considers medical education and the improvement of clinical practice concerning neonatal electrocardiography among its major focus points [Schwartz, 2002].

So far, teaching neonatal electrophysiology has been based on the use of sample ECG strips in databases or the literature [Andriessen, 2001, Park, 1992, Schwartz, 2002, Tipple, 1999]. This allows for training ECG interpretation and diagnosis, but is not ideal for learning to recognize dynamic rhythm changes. Practical training in acute care skills often takes place in the clinical setting. This is a less than ideal learning environment for a number of reasons, among them the lack of control over the training situation, limited possibility to intervene, and potential risks to (real) patients.

Acute care educational simulation

Factors contributing to errors in acute care medicine include: 1. complex underlying physiology and pharmacology, 2. a short time interval available for diagnosis, decision making, and intervention, 3. complex interactions in health care teams and systems, and 4. malfunction and improper use of medical equipment. In an attempt to reduce these errors, there is an increasing use of recently developed acute care educational simulators.

The first full-body acute care educational simulators were anesthesia simulators [Couto, 2002]. These learning systems have evolved significantly over the past two decades. Reactivity and realism of these simulators was enhanced by including simulation engines based on mathematical and physical models of human physiology and pharmacology [Meurs, 1997]. Adult full-body, model-driven simulators are now used world-wide in a number of acute care domains, allowing for:

- Teaching and evaluation of integrated knowledge and skills by alternation of hands-on experience and didactic teaching, and selective or integrated teaching of basic diagnostic and therapeutic skills, advanced medical decision making, resource management, group dynamics, etc.,
- Optimisation of the educational environment by practicing through frequent repetition (even of rare situations), and student paced learning, all without risks to real patients.

The advantages of simulator-based training in neonatal acute care will be obvious from the above. Halamek et al. [Halamek, 2000], referring to neonatal resuscitation, state that: “Realistic simulation-based training in neonatal resuscitation offers benefits not inherent in traditional paradigms of medical education.” To date, no full-body, model-driven neonatal acute care simulator is available on the market.

Goals and objectives

The general goal of this work is to design a model for educational simulation of the neonatal ECG, which may become part of a full-body, model-driven neonatal simulator. In the limited time frame of this study we will focus on a somewhat less ambitious screen-based application. The formulation of simulator and model requirements adapts and follows a rigorous methodology presented in the context of the design of combat helicopters [Farmer, 1999]. To our knowledge, this study represents the first time this methodology is applied to medical simulators.

Outline

Chapter 2 summarizes essential concepts of neonatal cardiovascular physiology and electrocardiography for a biomedical engineering target audience. It includes an extensive list of normal and abnormal ECGs of the neonate.

Chapter 3 presents a training needs analysis for neonatal electrophysiology and electrocardiography. This is followed by the specification of a compact set of requirements for a simulator based training program. Requirements for trainee and instructor interfaces, as well as for a model-driven simulation engine are derived based on these analyses.

Chapter 4 describes a literature research on neonatal and adult ECG simulation models. The resulting models are classified according to purpose, structure, and capabilities. Based on the simulator and model requirements derived in Chapter 3, a model for simulation of the adult ECG was chosen as a basis for adaptation to the neonatal context.

Chapter 5 describes the selected adult model, and its adaptation to reflect the neonate. This chapter also includes a section on model parameter estimation and manipulation for the generation of different rhythms.

Chapter 6 describes the software of the developed screen-based model-driven simulator.

Chapter 7 presents results of the model-driven simulation engine and the developed trainee and instructor interfaces.

In Chapter 8 we discuss the presented results in view of the broader training program requirements. Simulation results are analysed and compared to target data. We comment on the strategy for parameter estimation and rhythm generation, and provide detailed suggestions for possible future extensions.

Chapter 9 includes conclusions and future perspectives.

Chapter 2

Neonatal cardiovascular physiology and electrocardiography

We introduce neonatal cardiovascular physiology as resulting from the changes that occur at birth, based on the framework by [Couto, 2002]. The characteristics of normal and abnormal neonatal electrocardiograms are described with specific references to the scientific literature. Basic aspects of general electrophysiology and electrocardiography are available in Appendix I.

2.1 Transition from fetal to neonatal heart and circulation

2.1.1 Specific anatomy of fetal circulation

The fetal heart and circulatory system operate in a considerably different fashion from the adult (Fig. 2.1). Because the lungs are non-functional during fetal life and the liver is only partially functional, it is not necessary for the heart to pump much blood through either organ. On the other hand, the fetal heart must pump a large blood volume through the placenta (PL), which provides a low resistance circuit to the systemic circulation. It receives blood with low oxygen saturation from the two umbilical arteries (UA) and returns oxygenated blood to the fetus by a single umbilical vein (UV). Right to left shunting occurs from the pulmonary artery to aorta via the ductus arteriosus (DA) and from the right atrium to the left atrium via the foramen ovale (FO). The ductus venosus (DV) creates a partial bypass of the liver from the umbilical vein to the inferior vena cava (IVC).

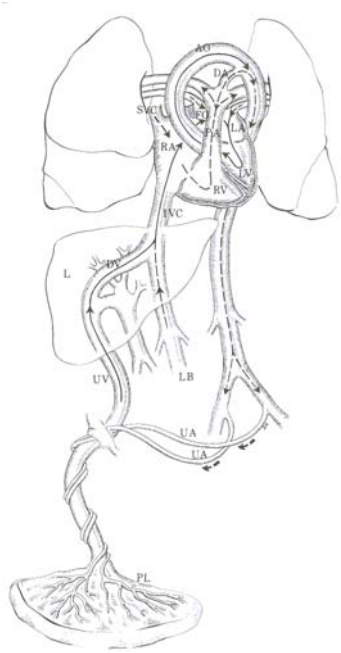

Figure 2.1 – *Specific elements of fetal circulation [Bell, 1997].*

Ventricular pressures are equal and the pulmonary resistance is much higher than systemic resistance, resulting in a larger size and mass of the right ventricle (RV) as compared to the left ventricle (LV), starting at 35 weeks of gestation [Tipple, 1999].

2.1.2 Changes in fetal heart and circulation after birth

With the onset of labor, the fetus begins its transition to postnatal life. Hence, critical adjustments must be performed: gas exchange is transferred from the placenta

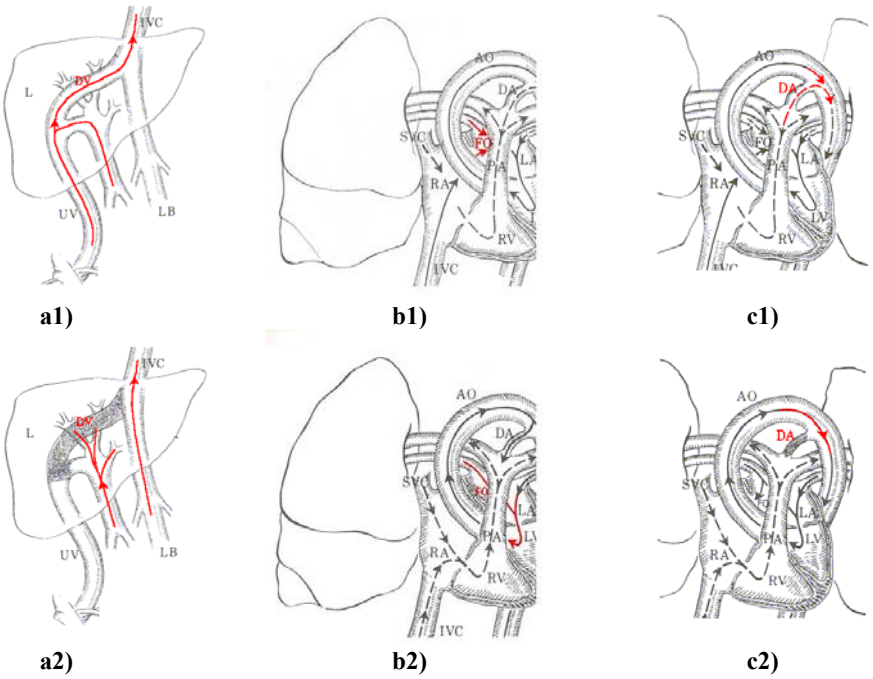

Figure 2.2 - *Closure of DV, FO and DA. a1), b1), c1): circulation during fetal life; a2), b2), c2): circulation immediately after birth [Bell, 1997].*

to the lungs and an adequate pulmonary circulation must be established and maintained. This requires significant physiological adaptation: the low resistance placental circulation is removed, the pulmonary resistance falls as the lungs open and the DA, DV and FO functionally close (Fig. 2.2).

These changes occur rapidly over the first few hours and days of life. The LV grows rapidly. By 1 month of age the LV/RV ratio has changed to 1.5:1 from the birth ratio 0.8:1, by 6 months to 2:1, and then slowly to the adult ratio of 2.5:1 [Tipple, 1999].

In normal conditions, the heart and circulation of the neonate, after the closure of DV, FO, and DA, within 1 or 2 weeks after birth, may be considered as behaving approximately like in the adult.

2.1.3 Neonatal heart and circulatory system

The general structure of the healthy neonatal circulation is the same as in the adult [Couto, 2002], Fig. 2.3. Poorly oxygenated blood from the entire body is transported to the right atrium through the superior and inferior venae cavae. When the right atrium (RA) contracts, the blood is forced into the RV. Blood is prevented from returning into the atrium by the tricuspid valve. Contraction of this ventricle drives the blood to the lungs. In its passage through the lungs, the blood is oxygenated; it then flows back to the heart (left atrium - LA) via four pulmonary veins. When the LA contracts, blood is forced into the LV and then by ventricular

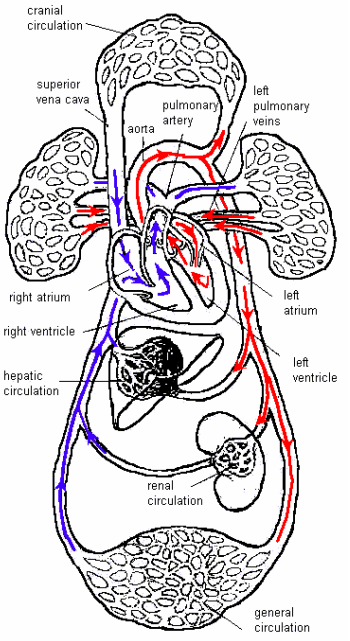

Figure 2.3 – *Neonatal (adult) circulatory system [Stedman, 1997].*

contraction into the aorta. The mitral valve prevents the blood from flowing back into the atrium and the semilunar valves between the LV and the aorta prevent it from flowing back into the ventricle. Similar valves are present between the RV and the pulmonary artery.

From the aorta oxygenated blood is conducted all over the body through an elaborate series of increasingly thinner vessels and capillaries. At the capillary level blood releases oxygen to the tissues, furnishes nutrients and other essential substances to the cells, and takes up waste products from the tissues. It returns to the heart through an analogous path of increasingly larger veins, entering into the RA conducted by the superior and inferior venae cavae.

2.1.4 Congenital heart diseases (CHD)

A congenital defect occurs when the heart or its associated vessels are malformed during fetal life. CHD is one of the most common causes of morbidity and mortality in a pediatric hospital [Klaus, 2001]. Basically, congenital anomalies of the heart or its vessels may be classified into four major types [Couto, 2002]:

- **Left-to-right shunt:** is an abnormal connection between the left heart or aorta and the right heart or pulmonary artery, allowing the blood to bypass the systemic circulation. Examples of this type of CHD are: ventricular *septal defect, atrial septal defect (open foramen ovale)* or *patent ductus arteriosus*.
- **Right-to-left shunt:** is an abnormality that allow blood to flow from the right heart to the left heart, bypassing the lung. Thus, the LV ejects venous blood to the systemic circulation. This usually results in cyanotic (blue) babies. The most common example of this type of CHD is the *tetralogy of Fallot*.
- **Obstructive lesions** at some point in the heart can prevent ventricular outflow, from either side of the heart, diminishing cardiac output into the pulmonary or systemic vasculature and causing ventricular failure [Bell, 1997, Guyton, 1991]. Examples of obstructive lesions are the *coarctation of the aorta*, *aortic stenosis* or *mitral stenosis*.
- **Complex shunts:** are cardiac defects where venous and arterial blood is mixed before being ejected from the heart. There may or not be obstruction to flow. Examples of complex shunts are the *hypoplastic left heart syndrome* or the *D-transposition of the great arteries*.

2.2 Normal and abnormal neonatal ECG

Changes occur in the human ECG from birth to adult life. They are related to the haemodynamic changes at birth, see section 2.1.2, developmental changes in physiology, body size, the position and size of the heart relative to the body, and variations in the size and position of the cardiac chambers relative to each other. Most of these changes occur rapidly over the first few hours and days of life but continue throughout early childhood and more gradually into adulthood. Unless the patient's age is known, the paediatric ECG cannot be interpreted or considered normal or abnormal. With the age in mind, the tracing may then be read objectively but additional clinical information is required for a full interpretation, including indication clinical diagnosis (cardiac and other), medications and electrolytes [Tipple, 1999]. In this section, we introduce commonly obtained tracings of normal neonatal electrocardiograms and selected abnormal neonatal ECGs.

2.2.1 Normal neonatal ECG

The normal neonatal ECG changes rapidly over the first few weeks of life and it is not until 3 years of age that it begins to resemble that of an adult [Tipple, 1999]. The ECG of newborns and infants younger than 1 month normally show right axis deviation (RAD) and right ventricular dominance. Between 1 month and 3 years, ECGs are intermediate, showing neither right nor left dominance. Children 3 years of age and older should have an ECG that resembles an adult ECG. Table 2.1, includes an overview of the typical characteristics of normal neonatal ECGs. Detailed descriptions of normal values for pediatric electrocardiograms for different age groups is available in [Davignon, 1979, Park, 1992, Rijnbeek, 2001, Schwartz, 2002].

Table 2.1 – *Characteristics of normal ECGs for newborn, neonate and infants [Davignon, 1979, Park, 1992, Rijnbeek, 2001, Schwartz, 2002].*

ECG characteristic		Description
Heart Rate (HR)		. normally high, normal neonates may have rates up to around 200 beats per minute (bpm). Varies with age, status (awake, sleeping, crying) and other physical factors, such as fever.
Rhythm		. the normal rhythm for any age is sinus rhythm, in which the SA node is the pacemaker of the entire heart. P-waves are always present in front of QRS-complexes.
P-wave	P amplitude	. is generally pointed on lead II and aVF. It may vary from 0.15 to 0.30mV.
	P duration	. normal average duration is 60 ± 20ms in children. Maximal durations are 100ms in children and 80ms in infants less than 1 year.
	P axis	. ranges from 0° to +90° at any age.
PR interval		. normally measured in lead II, increases with age and decreases with HR. Normal values range from 70 to 140ms, with mean 100ms.
QRS Complex	QRS amplitude	. vary with the lead and the age. Q-waves may be absent in many leads. R and S waves are taller in precordial leads.
	QRS duration	. increases with age and may vary from 40ms in premature infants to 70ms in 3 year old children
	QRS axis	. newborn infants normally have RAD comparing to the adult. Normal full-term neonates may have an axis between 55° and 200°. After um month, it falls to less than 160°.
	R/S ratio	. because of right heart dominance, the R/S ratio is large in right precordial leads (V1, V2) and small in left precordial leads (V5,V6)
ST segment		. normally horizontal and isoelectric. Elevation or depression up to 0.1mV in limb leads is not necessary abnormal.
T-wave	T amplitude	. normally very variable in first week of life. It is best measured in left precordial leads. After 1 week, is negative in lead V1.
	T axis	. the mean is +25° with a range of [-40°, +100°] in the first week of life. In infants with 1 month of age, it almost reaches the adult mean of 45°.
QRS-T angle		. in general, falls in the same range as the T axis. However, in early infancy the QRS-T angle is normally wider.
QT interval		. varies with HR but not with the age, therefore must be interpreted in relation to the HR. The corrected QT interval (QTc) is given by $QTc = \frac{QT}{\sqrt{RR}}$ (Bazett's formula) and relates the QT interval to heart rate. It should not exceed 0.44s, except in infants.

2.2.2 Abnormal neonatal ECG

Many abnormal neonatal ECG tracings can be attributed to changes in rhythm and/or shapes of ECG waves or baseline. They can occur due to serious cardiac conditions, like heart disease, or due to simple non-threatening phenomena, such as crying, sleeping or fever. As a basis for this work, but also for future reference, in the remaining six pages of this chapter, we present a quite extensive list of abnormal ECGs and their descriptions. Classification refers to the origin of the abnormalities: hypertrophy, conduction disturbances, ventricular repolarisation, reentry and disrhythmias [Andriessen, 2001, Park, 1992, Schwartz, 2002].

a) Hypertrophy

Due to the nature of heart disease in children (structural abnormalities with volume and/or pressure overload), hypertrophy is the most common abnormality seen in pediatric electrocardiograms [Park, 1992]. Different kinds of hypertrophy are common manifestations of almost all of the congenital diseases mentioned in section 2.1.4. Depending on the location of pressure overload, atrial or ventricular hypertrophy may result.

Atrial hypertrophy [Park, 1992]

Volume and/or pressure overload is located on the atria. Changes in the ECG with atrial hypertrophy are increased amplitude and/or duration of the P-wave. Different criteria are adopted for classifying atrial hypertrophy from ECG tracings:

- **RAH - Right atrial hypertrophy:** produces tall P-waves in any lead, but more often in leads II and V1/V2. It is called "p-pulmonale" since it is frequently associated with cor pulmonale[1].
- **LAH - Left atrial hypertrophy:** is characterized by a prolongation of the P-wave duration in all leads. It is also common to observe a broad and notched P-wave in limb-leads or diphasic P-wave in lead V1.
- **CAH - Combined atrial hypertrophy:** produces a combination of RAH and LAH, which means increases in amplitude and duration of the P-waves.

Ventricular hypertrophy [Schwartz, 2002]

Similarly, ventricular hypertrophy is associated to volume and/or pressure overload of the ventricle(s). Right ventricular hypertrophy (RVH), left ventricular hypertrophy (LVH) and combined ventricular hypertrophy (CVH) reflect the location of the volume/pressure overload. Criteria for classification from ECG tracings are based on QRS-complex morphology: changes in QRS axis, voltage, duration and R/S ratio.

b) Conduction disturbances

Disturbances in electrical conduction in the heart are one of the most common sources of electrocardiographic abnormalities in pediatric patients [Park, 1992]. They may occur between the normal sinus impulse and the ventricular response (AV blocks), or in the ventricular conduction. AV blocks are classified in three categories according to severity: 1st, 2nd, 3rd degree AV blocks. Ventricular blocks occur most frequently dues to lack of conduction in one of the bundle branches.

[1] **Cor Pulmonale –** Failure of the right side of the heart caused by prolonged high blood pressure in the pulmonary artery and right ventricle.

b.1) AV nodal conduction disturbances

1st-Degree AV block [Park, 1992]

It is the result of a conduction disturbance between the SA node and the ventricles, produced by an abnormal delay in the AV node. This results in prolongation of the PR interval beyond the age dependent upper limit for a normal interval. It is sometimes seen in healthy children with infectious diseases.

2nd-Degree AV block [Park, 1992]

Some dropped beats occur in which P-waves are not followed by QRS-complexes. Different types of 2nd-degree AV blocks are classified as: Mobitz type I, Mobitz type II and Two-to-One AV block.

3rd-Degree (Complete) AV block [Schwartz, 2002]

Complete AV block implies complete absence of conduction from atria to ventricles. The ECG shows normal atrial activation and slower, asynchronous, but regular ventricular activation. QRS-complexes can be normal or abnormal, depending on where the ventricular pacemaker is located. P-waves are normal.

Atrioventricular dissociation [Park, 1992]

Atria and ventricles beat independently, which means that P-wave and QRS-complex are completely asynchronous. Such independency may be caused by (1) slowed rate of the SA node; (2) accelerated rate of normally slower or latent pacemakers (AV node or ventricle); or (3) complete or advanced AV block.

b.2) Ventricular conduction disturbances

RBBB – Right bundle branch block [Park, 1992]

The depolarisation of the ventricular septum is normal, but the right ventricle is not depolarised directly through the Purkinje system. The RV is depolarised through the centricular myocardium at a much slower rate. This slower rate results in prolongation of the terminal portion of the QRS-complex, called *terminal slurring*.

LBBB – Left Bundle Branch Block [Park, 1992]

When the left bundle branch is interrupted, there is an abnormality in septal depolarisation: it proceeds leftward from the RV. The LV is depolarised through the ventricular myocardium at a much slower rate. Abnormalities are found not only in the terminal phase but also in the initial phase of ventricular depolarisation, affecting the entire QRS-complex.

WPW – Wolff-Parkinson-White syndrome [Schwartz, 2002]

This is a classic form of pre-excitation, accelerated atrioventricular conduction through an accessory pathway (also considered as a type *accessory reciprocating AV tachycardia* – section d.2). In this case, that pathway is the "Kent bundle" and is located between the atrium and the ventricle (either side), bypassing the AV node without its normal delay (Fig. 2.4). As a consequence, the affected ventricle depolarises prematurely, but slower, producing a short PR interval. Conduction through the AV node and the accessory pathway results in collision of two electrical wavefronts at the ventricular level causing a delta wave and a fused QRS-complex with prolonged duration. This phenomena will be illustrated in Fig III.1.

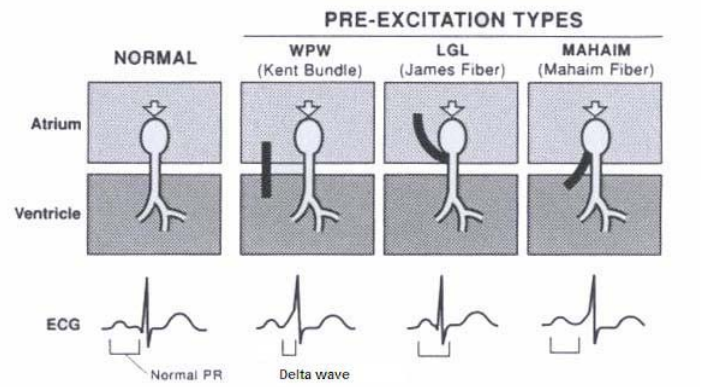

Figure 2.4 – *Schematic diagram of accessory pathways and the electrocardiogram in preexcitation. In the normal subject, the atrial impulse (open arrow) reaches the ventricle through the AV node and bundle of His. In preexcitation, abnormal pathways partially bypass the normal conduction system. The bundle of Kent is responsible for the most cases of WPW syndrome. James fibers bypass the the upper AV node in LGL syndrome. Mahaim fibers bypass the bundle of His and "short-circuit" into the right ventricle [Park, 1992].*

Hemiblocks (Fascicular Blocks) [Park, 1992]

The left bundle branch consists of three divisions (fascicles): septal, anterior-superior and posterior-inferior. In infants, only the anterior fascicle is of clinical significance. Hemiblocks are diagnosed when delay or block occurs in this fascicle. The superior anterior portion of the LV is depolarised last and the QRS vector is directed supero-anteriorily.

Intraventricular Block [Park, 1992]

A diffuse conduction delay throughout the ventricles occurs and results in prolonged QRS-complexes. This is distinct from the characteristic block in one of the bundle branches of either LBBB or RBBB.

Ventricular pacemaker [Park, 1992]

One ventricle in which the pacemaker is implanted is depolarised first, followed by the other through myocardial transmission. This mode of artificial pacing is recognized in the ECG by vertical pacemaker spikes initiating ventricular depolarisation with wide QRS-complexes. The electronic spike has no fixed relationship with atrial activity, and there is usually no P-wave in front of the spike, except by coincidence.

Atrial pacemaker [Park, 1992]

An atrial pacemaker is recognized by a pacemaker spike followed by an atrial complex. With normal AV conduction, a QRS-complex of normal duration will follow. When there is complete AV block in addition to sinus node dysfunction with sinus bradycardia, a ventricular pacemaker may also be required.

P-wave-triggered ventricular pacemaker [Park, 1992]

This pacemaker may be recognized by pacemaker spikes that follow the patient's own P-waves, with regular PR intervals and wide QRS-complexes. The patient's own P-waves are sensed, which triggers a ventricular pacemaker after an electronically preset PR interval. This type of pacemaker reproduces natural physiology and is indicated when there is an AV block, but the sinus mechanism is normal.

c) Ventricular repolarisation

Ventricular repolarisation can be evaluated on the surface ECG by measuring the QT interval duration and by analysing the morphology of the ST segment and the T-wave. Changes in QT interval, ST segment and T-wave may be pathologic or nonpathologic, with different degrees of significance. The most common ways of abnormal ventricular repolarisation are: QT interval prolongation, Long QT syndrome and ST segment elevation/depression [Schwartz, 2002].

QT interval prolongation [Schwartz, 2002]

QT duration may change over time. Accordingly, it is recommended to repeat the ECG exam in those infants found to have a prolonged QTc on the first ECG. It can yield lengthening of ST segment, decrease of T-wave amplitude, decrease/increase of T-wave duration and T-wave inversion. Effective QT prolongation beyond the normal values for the age group may be caused by electrolyte disturbances, hypocalcaemia, vomiting, diarrhoea, central nervous system abnormalities, drugs, or Long QT syndrome (LQTS).

LQTS - Long QT syndrome [Schwartz, 2002]

LQTS is a genetic disease characterized by the occurrence of syncopal episodes due to *torsades de pointes ventricular tachycardia*[2] and by a high risk of sudden cardiac death among untreated patients. Although the likelihood of having LQTS increases with increasing QTc, the correlation between QT prolongation and the presence of this syndrome is not absolute. If a first ECG shows a QTc above the upper limit of normal, diagnosis requires scrutinizing the family history for familial (hereditary?) LQTS, information about episodes of sudden death, fainting spells, seizures-eplilepsy, and further ECG exams. QTc close to 600ms, T-wave alternans and 2:1 AV block secondary to major QT prolongation identify infants at an extremely high risk.

ST segment elevation/depression [Park, 1992]

Abnormal ST segment shifts usually assume one of the following two forms:

- downward slanting followed by biphasic or inverted T-wave,
- straight /horizontal sustained ST segment.

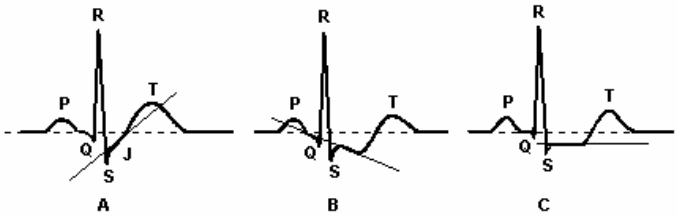

Figure 2.5 - *Nonpathologic (A) and pathologic (B, C) ST and T changes.* ***A*** *– characteristic ST segment with upward ST slope (J-depression).* ***B,C*** *– pathologic (ischemic) ST segment alterations; note a downward ST segment slope in (B), and horizontal segment is sustain in (C) [Park, 1992].*

There are multiple causes of ST segment elevation/depression in infancy, with or without T-wave abnormalities: LVH or RVH with "strain", digitalis effect,

[2] **Torsades de pointes –** Cardiac disrhythmia, which may cause blackouts or even sudden death in individuals with mutations in genes that control expression of sodium or potassium channels. Its name ("twisting the points") refers to the characteristic appearance of the ECG with long QT interval.

pericarditis, myocarditis, myocardial ischemia, myocardial infarction and electrolyte disturbances (hypo and hyperkalemia).

d) Disrhythmias

All forms of cardiac disrhythmias can occur in neonates, even if their frequency and clinical significance differ from adults. Many disrhythmias are benign, occurring in normal hearts and of no hemodynamic consequence. Others may result in significant cardiovascular compromise, particularly if they are sustained, recur frequently, or occur in the presence of structural/functional heart disease. Rarely disrhythmias are a sign of cardiac abnormalities such as cardiomyopathy. One should also keep in mind that disrhythmias may result from noncardiac disease, occurring in association with preceding severe hypoxemia, hypotension, acidosis, electrolyte disturbance, or drug toxicity (e.g., digitalis) [Avery, 1999]. In this section we describe neonatal disrhythmias with clearly defined mechanisms.

d.1) Disrhythmias originated on the SA Node

Sinus Tachycardia [Schwartz, 2002]

The HR is faster than normal limits for the infant's age - 166 bpm in the first week and 179 bpm in the first month. Newborn infants may transiently reach a heart rates up to 230 bpm. ECG shows normal or eventually overlapping atrial and ventricular activity.

Sinus Bradycardia [Schwartz, 2002]

The heart rate is slower than normal for the infant's age, around 90 bpm in the first week and 110 bpm in the first month. At the first month the lower limit increases to 121 bpm and declines to approximately 100 bpm in the following months. P-wave and QRS-T complexes are normal.

It happens rarely in healthy infants and may be caused by increased intracranial pressure, hypothyroidism, hypothermia, profound hypoxia, "sick sinus" syndrome, hiperkalemia and drugs. During a slow sinus rhythm, the AV node or ventricles may capture the pacing role by virtue of a higher rate of automaticity.

Sinus Arrhythmia [Park, 1992]

The HR is irregular, rising during inspiration and decreasing during expiration. However, the normal P-QRS-T configuration is maintained. The cardiovascular system is under vagal (not sympathetic) control, which is a sign of good cardiac reserve.

Sinus Pause [Park, 1992, Schwartz, 2002]

The SA node has a momentary failure in initiating an impulse. Neither atrial nor ventricular activation takes place and no P-wave or QRS-complex is present. It is, however, of short duration. Sinus pauses in newborns may last from 800 to 1000 ms. They can be due to increased vagal tone, hypoxia or digitalis.

Sinus Arrest [Park, 1992]

Is similar to sinus pause, but of longer duration, resulting in escape beats from other pacemakers.

d.2) Disrhythmias originating in the atria and AV node

Park et al. [Park, 1992], in agreement with several other authors, define ectopic rhythms as rhythms in which the pacemaker is not the SA node. Other possible pacemakers can be in the atria, AV node and ventricles. The next section will introduce rhythms originating in the ventricles; here we will present rhythms originating in the atria and/or the AV node.

PAC – Premature Atrial Contraction [Park, 1992]

An premature ectopic beat originates in the atrium. Since the SA node is depolarised by atrial activation, the SA node "clock" resets so that the following RR interval is usually normal. PACs may have no significance in healthy infants. However, they may also be associated with structural heart diseases.

Wandering Pacemaker[Park, 1992]

This is a benign disrhythmia. The site of the impulse formation gradually shifts from the SA node to an ectopic atrial focus over several cardiac cycles. There are also gradual changes in the configuration of P-waves and PR intervals. QRS-complexes are normal.

Atrial Tachycardia [Park, 1992]

There are uncommon cases of very rapid tachycardia (240 ± 40 bpm) produced by firing of a single focus in the atrium. Very often, the P-wave is buried in the previous T-wave so that the atrial tachycardia is difficult to separate from the less frequent nodal tachycardia. This lead to the use of the term *supraventricular tachycardia* (SVT) to include both of these disrhythmias.

Atrial Flutter [Schwartz, 2002]

Atrial flutter is characterized by a rapid, regular form of atrial depolarisation: the 'flutter wave'. The "picket fence" morphology is similar to adults. However, the flutter wave durations are generally 0,09 to 0,18s with atrial rates in infants between 300-500 bpm. In general, there is variable AV conduction from 1:1 to 4:1 yielding an irregular ventricular rate. The QRS-complex is usually the same as in sinus rhythm although there may be occasional aberrancy.

Atrial Fibrillation [Park, 1992]

The atrial rate ranges from 350 to 600 bpm. Ventricular response is irregular and may be fast or slow. Atrial waves on ECG are totally irregular and vary in size and shape from beat to beat. The QRS-complex is usually normal. This disrhythmia is usually associated with structural heart defects or can occur after intra-atrial surgery.

Nodal Premature Beat [Park, 1992]

A premature ectopic beat originates in the AV node. If the SA node is triggered prematurely by retrograde activation of the atria, there is an incomplete compensatory pause as a result of resetting the SA node "clock". If not, there is a complete compensatory pause. Normal QRS-complexes occur prematurely and are followed by normal or inverted P-waves.

Nodal Escape Beat [Park, 1992]

The impulse from the SA node fails to reach the AV node in time and it depolarises spontaneously. The escape beat comes later than the anticipated normal

beat. The ECG shows a normal QRS-complex with or without a subsequent P-wave. This disrhythmia is common after surgical procedures involving the atria.

Accelerated Nodal Rhythm [Park, 1992]

Sinus rate and AV conduction are normal. An AV node with enhanced automaticity overtakes the pacing role at a rate that is higher than normal (60 to 120 bpm).

Nodal Tachycardia [Park, 1992]

The nodal rate can vary from 120 to 200 bpm. The QRS-complex is usually normal and regular and may be followed by an inverted P-wave. As observed above, it may be difficult to separate nodal tachycardia from atrial tachycardia.

Aberrancy [Park, 1992]

When a supraventricular impulse prematurely reaches the AV node or bundle of His, it may find one bundle branch excitable and the other still refractory. It will be conducted down one bundle branch only. The resulting QRS-complexes are similar to those of RBBB.

SVT - Supraventricular Tachycardia [Park, 1992]

As mentioned for atrial tachycardia, SVT includes both atrial and AV tachycardia. The most common mechanism of SVT (reciprocating AV tachycardia - RAVT) is the result of the presence of an abnormal pathway connecting atria and ventricles besides the AV node (Fig. 2.6). The extra pathway may be anatomically separate (such as the bundle of Kent - Fig. 2.4), resulting in *Accessory Reciprocating AV Tachycardia*; or only functionally separate (such as a dual AV node pathways), resulting in *Nodal Reciprocating AV Tachycardia*. The typical infant with SVT has an extremely regular RR interval after 10-20 beats, most often at rates greater than 230 bpm. P-waves are sometimes visible with morphology that differs from sinus rhythm. QRS-complexes are normal and possibly narrow.

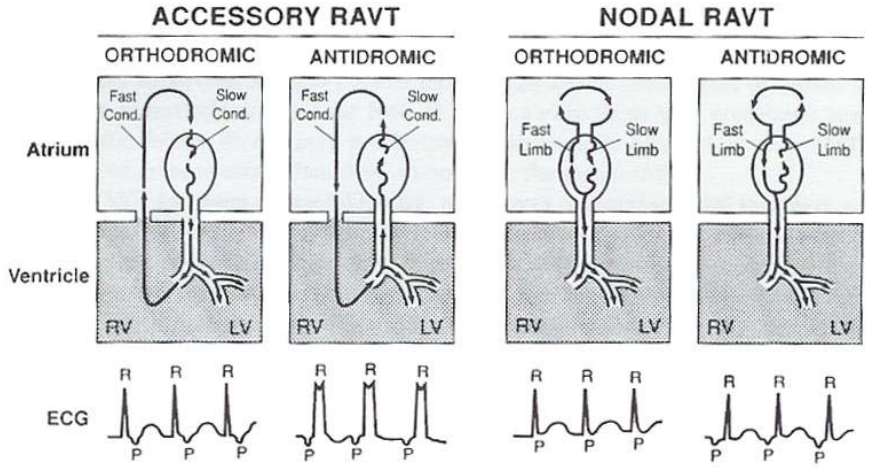

Figure 2.6 - *Diagrams showing the mechanisms of reciprocating AV tachycardias (RAVT) in relation to ECG findings [Park, 1992].*

d.3) Disrhythmias originated in the ventricles

PVC - Premature Ventricular Contraction [Park, 1992]

A PVC is manifested in the ECG by a bizarre, wide QRS-complex occurring before the expected QRS in a regular rhythm. There is no P-wave preceding the premature QRS. The retrograde impulse generated in the ventricle is usually blocked in the AV node, and thus the SA node "clock" keeps its original pace.

VT - Ventricular Tachycardia [Schwartz, 2002]

Ventricular tachycardia is rare in infants and children but is a very serious disrhythmia and can deteriorate into ventricular fibrillation. It consists of a series of three or more PVCs occurring at a rate of 120 to 180 bpm. In teh ECG it is often difficult to differentiate VT from supraventricular tachycardia with aberrant (intraventricular) conduction. A reliable sign of ventricular disrhythmia is the presence of a *ventricular fusion complex*. This is a QRS-complex produced in part by a normally conducted supraventricular impulse and in part by an ectopic ventricular impulse. The resulting QRS-complex is intermediate in appearance between the respective QRSs. Since aberrancy is rare in children, wide QRS tachycardia without visible P-waves should be considered VT.

Ventricular Fibrillation [Park, 1992]

This is usually a terminal disrhythmia and successful resuscitation depends on prompt recognition and cardiac defibrillation. It is characterized by a bizarre ventricular QRS pattern of varying size and configuration. The rate is rapid and irregular.

Chapter 3

Simulator and model requirements[3]

Farmer et al. [Farmer, 1999] present a systematic approach to the specification of educational simulators for military applications. Training needs analysis (TNA) considers the target learners and results in an explicit set of training objectives (*what* to train). Training program design (TPD) looks at *how* training objectives can be addressed, and results in a set of program requirements. A typical TPD strikes a balance between constraint-driven and need-driven strategies. For rapid implementation of a program with existing simulation technology, the former will dominate, for the design of new programs or simulators, the latter. Training media specification (TMS) translates program requirements into functional simulator requirements. Specific requirements can be formulated for trainee and instructor interfaces and for the simulation engine.

A complete TNA-TPD-TMS for a full-body neonatal acute care simulator, or even for a screen-based simulator of neonatal electrophysiology is beyond the scope of the present masters project. The purpose of this chapter is to summarize essential elements of TNA and TPD, and interface aspects of TMS. The requirements for the simulation engine will be addressed in more detail. The simulation engine is the component of a simulator that provides reactivity to actions by the trainee and/or instructor. For educational acute care simulators it typically consists of a combination of time-and-event-based scripts and mathematical and/or mechanical models of human physiology and pharmacology [Meurs, 1997, Schwid, 1987]. Requirements for the physiologic model underlying a screen-based simulator of neonatal electrophysiology will be formulated and form the basis for the subsequent literature search and model design and evaluation.

This approach provides structure to the design and validation processes, and it is our hope that it will lead to training programs, acute care simulators and physiological models that are better suited to meet specific educational needs.

3.1 TNA: Training Needs Analysis

The primary target audience for neonatal ECG simulation, particularly as part of a full-body training environment for neonatal resuscitation, consists of residents in pediatrics. Beyond the specific resuscitation purpose, other medical personnel could be included in the target audience:

- medical students,
- post-graduate training participants and residents in obstetrics, cardiology or anesthesia,

[3] First sections co-authored by W.L. van Meurs, N.A.M. de Beer, P. Andriessen in view of submission of an abstract to the 2004 conference of the Society in Europe for Simulation Applied to Medicine.

- specialized nurses (*e.g.* neonatal nurse practitioners),
- midwifes.

Three main categories of learning objectives are considered:

Recognition of normal and abnormal rhythms in the ECG:

Timely and accurate recognition of dynamic rhythm changes into potentially life threatening conditions, like the change from sinus rhythm to supraventricular disrhythmias or atrioventricular blockade, is highly relevant to clinical practice, and represents an educational challenge that is difficult to meet in traditional educational settings.

Recognition of abnormal, but stable ECGs, even those corresponding to serious pathologic conditions, can be learned "off-line" from printed 12-lead ECG strips, and does not necessarily require simulator-based training. Examples of these ECGs and corresponding guidelines for interpretation are available in literature [Andriessen, 2001, Park, 1992, Tipple, 1999].

Understanding underlying electrophysiology:

All target groups need to understand the electrophysiology underlying specific rhythms and their ECG manifestations. The basis of electrical activity in the heart is the cellular action potential (AP) and its propagation between heart cells. These phenomena and the propagation to the thorax surface are the main determinants of the resulting ECG.

Clinical decision making, therapeutic and diagnostic interventions:

Some rhythms are life threatening and require prompt intervention, e.g. drug administration and/or defibrillation. Recognition of abnormal ECGs may also lead to requests for additional diagnostic interventions, for example, 24-h Holter monitoring.

Combining the first and last categories of learning objections, the simulation should support training quick diagnosis of dynamically evolving situations and prompt initiation of treatment.

Because of time constraints associated to a masters project, rather than for educational reasons, we decided to focus on 1 week to 3 months old neonates, i.e., after completion of the significant cardiovascular and electrophysiological changes following birth and during the first week of life.

3.2 TPD: Training Program Design

To meet the above outlined learning objectives, especially in the first and third categories, a fully immersive simulator based training would probably be ideal. A computer based trainer that guides the students through a number of exercises without instructor intervention could be envisioned as well. The training program proposed below relies on a somewhat less ambitious, but more easily achievable configuration.

After introductory didactic lessons about neonatal electrophysiology, electrocardiography, and available therapeutic and diagnostic interventions, an instructor, in a small classroom setting, provides interactive computer based demonstrations, frequently inviting the students to comment on displayed conditions and concepts.

Recognition of normal and abnormal rhythms on the ECG will be trained by displaying static waveforms and dynamic changes, and asking the students for their diagnosis. The relationships between action potentials, conduction, lead location and ECG tracings will be demonstrated on a rhythm per rhythm basis, and/or as a separate block in a different class. By making changes in selected parameters, and observing the consequences on the ECG in real time, the instructor guides the students in building a mental model for these relationships. Clinical decision making can initially be trained up to the level of the identification of the action to be undertaken. The instructor presents rhythms requiring intervention and probes the trainees for their suggestions.

3.3 TMS: Training Media Specification

In the training program outlined above the instructor makes use of an interactive demonstration tool. General requirements for this tool are:

- real-time presentation of the neonatal ECG for a number of rhythms and dynamic rhythm changes,
- visualization of relevant aspects of action potential, conduction, and propagation to lead location,
- ability to change underlying physiology and observe the effects on the ECG.

To meet these requirements, we propose developing a screen-based application that generates underlying physiology and ECG tracings in real-time. Below, we will formulate specific requirements for trainee and instructor interfaces, and for the simulation engine.

3.3.1 Trainee interface (TI)

Trainees should be able to observe ECG tracings and underlying electrophysiological phenomena on the screen. Other information required to make a diagnosis based on the simulated ECGs can be provided by the instructor. In the application referred to above, the instructor is the only one directly interacting with the device. The trainee interface requirements can be summarized as follows:

- graphical display of relevant underlying AP tracings,
- graphical display of ECG tracing(s), see below,
- display of a numerical value for heart rate.

Full clinical interpretation of the neonatal ECG requires a 12-lead configuration. However, educational goals in acute care training include prompt decision making, which is based on a more limited set of leads. Leads in the frontal plane are important for rhythm and P-wave analysis, and for the localization of firing foci in the frontal plane, and should therefore be included in the generated and displayed tracings. Two limb leads, for example, lead I or II, and aVF, are the minimal requirement for the screen-based simulator.

Beyond the scope of a simple rhythm generator for acute care, more complex simulators would demand the inclusion of precordial leads, allowing the complete localization of firing foci and detection of possible abnormalities in the horizontal plane.

3.3.2 Instructor Interface (II)

The instructor interface should allow for the selection of a set of rhythms with prepared parameter settings. Essential parameters for instructor control over rhythm generation include automaticity, refractory periods and conduction times. Besides the selection of one out of the set of rhythms, instructor interface requirements further include the control over a state machine allowing for simulating gradual or abrupt rhythm changes. Table 3.1 lists the selected rhythms, other than normal sinus rhythm, that should be included in this simulator. This list is a subset of the abnormal neonatal rhythms introduced in Chapter 2. It is limited to rhythms that represent potentially serious threats, or that could lead to life-threatening situations. For that reason, some less threatening rhythms like sinus tachy- or bradycardia are included together with more dangerous disrhythmias, such as ventricular fibrillation. As mentioned in the specification of learning objectives, stable rhythms, even if representing serious pathologies, are usually not included. However, some rhythms, like AV blocks or disrhythmias due to reentry, highlight aspects of conduction and automaticity, and can assist in building a mental model of neonatal electrophysiology. They are included to support these educational objectives. Table 3.1 is followed by a detailed discussion of specific rhythms.

Table 3.1 – *List of rhythms for a screen based neonatal ECG simulator.*

SA nodal disrhythmias	**AV nodal conduction disturbances**
Sinus Tachycardia	1st-Degree AV Block
Sinus Bradycardia	2nd-Degree AV Block
Sinus Pause	3rd-Degree (Complete) AV Block
Sinus Arrest	Atrioventricular Dissociation
Atrial and AV nodal disrhythmias	**Ventricular conduction disturbances**
Atrial Tachycardia	WPW – Wolff-Parkinson-White syndrome
Atrial Flutter	Ventricular pacemaker
Atrial Fibrillation	Atrial pacemaker
Nodal Tachycardia	P-wave-triggered pacemaker
SVT - Supraventricular Tachycardia	**Ventricular repolarisation**
Ventricular disrhythmias	QT interval prolongation
PVC - Premature Ventricular Contraction	Long QT syndrome
Ventricular Tachycardia	ST segment depression/elevation
Ventricular Fibrillation	

We excluded the stable rhythms associated to atrial and ventricular hypertrophy, RBBB and LBBB, hemiblocks and intraventricular block. From the list of sinus disrhythmias, we excluded respiratory sinus arrhythmia, which is frequently reported as a sign of good cardiac reserve and not a serious threat. Sinus pause and sinus arrest and are included because they occasionally develop into SSS – Sick Sinus Syndrome [Park, 1992] in children who undergo extensive cardiac surgery. The Atrial and AV nodal disrhythmias: PACs, wandering pacemaker, nodal premature beat, nodal escape beat and accelerated nodal rhythm are not reported as life-threatening in neonates and are not included in Table 3.1. Atrial and nodal tachycardia (and also WPW syndrome) are sometimes grouped as supraventricular tachycardias [Park, 1992], which may be associated with serious congenital heart failure, and like atrial flutter, may evolve into atrial fibrillation and some degree of AV block. Atrial and ventricular pacemakers, and P-wave-triggered pacemakers are used for correcting different kinds of heart block. We consider the delicate heart response and ECG analysis after surgery as important enough to require rhythm demonstrations. Ventricular tachycardia is a rare

but serious disrhythmia and may indicate myocardial damage or dysfunction. It possibly deteriorates into terminal ventricular fibrillation, requiring prompt recognition and cardiac defibrillation. Occasional PVCs are benign in children, but when they are multifocal and/or frequent, they become significant and possibly part of more complex ventricular disrhythmias. Some reasons for including AV blocks were already mentioned above. Additional reasons are that mortality rates in neonates with complete AV block are still high [Schwartz, 2002]. In some cases, second degree AV block may progress into complete heart block, representing a potentially life-threatening situation. First degree AV block does not usually signify a serious condition. However, it can be associated with some serious cardiac threats, such as cardiomyopathy or atrial septal defect [Park, 1992]. Abnormal ventricular repolarisations can evolve into life-threatening disrhythmia [Schwartz, 2002].

3.3.3 Simulation Engine (SE)

The training objectives and interface requirements include simulation of a number of rhythms, Table 3.1, with associated conduction events and action potential and ECG waveform signals. Transitions in waveforms can be gradual and continous or abrupt and discrete. These requirements virtually rule out the use of a signal data base. A simulation engine in the form of a mathematical representation of electrophysiologic phenomena could generate these events and variables. It would also facilitate creation of different rhythms through manipulation of model parameters. The current requirements do not include response to therapeutic interventions, but using a model based simulation engine would allow for such an extension. A state machine running scripts setting model parameters should be used in conjunction with the model to generate rhythm transitions, resulting in a script-controlled, model-driven simulation engine [Meurs, 1997].

Both as basic model requirements and for future reference in the model design section, we further include specific lead II ECG data for a normal sinus rhythm in the 3 week-old male neonate, Table 3.2 and Fig. 3.1.

Table 3.2 - *Typical settings for standard lead II ECG in 3 week-old neonates at normal sinus rhythm*

ECG Settings			Target Data	Format	Reference
Heart Rate (bpm)			149 (107, 182)	median (lower, upper)	[Davignon, 1979]
P-wave	Amplitude (mV)		0.2	median (upper)	[Davignon, 1979]
	Duration (ms)		78 (64, 85)	median (lower, upper)	[Rijnbeek, 2001]
PR interval (ms)			100 (70, 140)	median (lower, upper)	[Davignon, 1979]
QRS complex	Duration (ms)		67 (50, 85)	median (lower, upper)	[Rijnbeek, 2001]
	Amplitude (mV)	Q wave	0.14 (0.23)	median (upper)	[Rijnbeek, 2001]
		R wave	0.64 (1.28)	median (upper)	[Rijnbeek, 2001]
		S wave	0.24 (0.46)	median (upper)	[Rijnbeek, 2001]
QT interval (ms)			250 (280)	average (upper)	[Park, 1992]
T-wave	Amplitude (mV)		0.3	-	*
	Duration (ms)		120	-	*

** - values taken from visual observation of real ECG tracings provided by Maxima Medical Center - Dep. of Perinatology, Veldhoven, The Netherlands*

Examples of waveform data for all rhythms listed in Table 3.1 are included in Appendix II.

Figure 3.1 - *Example lead II ECG showing a normal sinus rhythm of a 3 week-old neonate, HR ≈ 150 bmp [provided by Maxima Medical Center - Dep. of Perinatology, Veldhoven, The Netherlands].*

Chapter 4

Literature review

Note that the nature of this chapter requires citing many sources. For reasons of style and compactness, references will only include the author and year for the first time they are cited.

4.1 Search and selection strategy

A limited number of references on (adult) ECG modeling and simulation were available at the start of this master's project. A literature search specifically aimed at models for educational simulation of the neonatal ECG did not yield any results, confirming the need for the present master's work. The search goal was extended to all models for ECG simulation, including those for the adult, and those not specifically applied in educational simulations. The following databases were searched: Medline, Web of science, TU/e library, Elsevier/Sciencedirect. Various sets of key words were used. Of the encountered references, we rejected articles that were not in English, and focused on papers that were available through the TU/e library system. The resulting references are listed in Appendix together with a brief, personal summary of their contents.

A first selection among the resulting articles was made based on the perceived ability to adapt the models to neonatal conditions and the specific requirements of the educational application as outlined in the previous chapter. Papers describing models of which ECG waveform generation was but one out of many represented phenomena, were rejected.

For a number of "key articles" this was followed by in-depth forward and reverse searches. The former looks at the articles referenced in the key article, the latter uses the Science Citation Index, which provides a list of all publications that cite the key article. Although quite time consuming, the reverse search procedure is a relatively efficient way to find articles that were overlooked in key word and/or forward searches.

4.2 Analysis and classification

4.2.1 Chronology

Simulation of human ECGs is not a recent research topic. It started sometime in the 70's and since then has known an evolution that can be divided in 3 phases:

Analog wave form generators

The first models for ECG simulation were designed as single wave form generators (Fig 4.1), normally with electronic circuits controlled by microprocessors [Burke, 2001, Howlett, 1978, Nowotny, 1976, Schwid, 1988]. Some of them did not have an (explicit or implicit) underlying mathematical model but were based on ECG wave forms read from databases. Wave form parameters such as frequency, wave amplitudes and time intervals, etc., are reflected in the components of the electronic circuits, or in characteristics of the mathematical representation of the ECG. In most cases, the goal of these models and simulators was study of the basic electrical activity of the heart (generating i.e. simple arrhythmias) as well test and calibration of electrocardiographs.

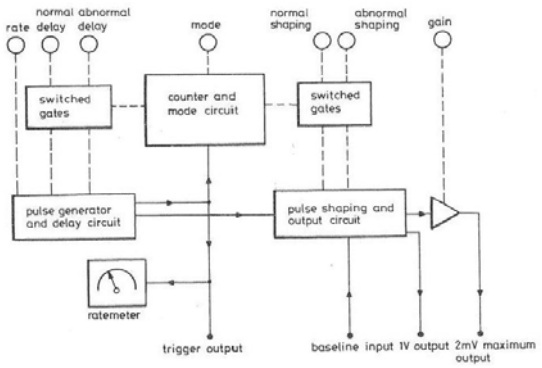

Figure 4.1 - *Block diagram of the ECG arrhythmia simulator proposed by [Howlett, 1978].*

2D heart models

In the 80's, the approach to ECG modelling and simulation became broader. The focus shifted from relatively simple wave form generators to models representing the conduction system and heart muscle at the cellular level, introducing physiologic parameters, such us action potential characteristics, conduction times etc. [Ahlfeldt, 1987, Fukushima, 1984, Malik, 1986, Takeuchi, 1998] started with 2D models for the conduction system (Fig. 4.2), and the resulting signals were single (Malik, Fukushima) or multi channel (Ahlfeldt) ECG tracings.

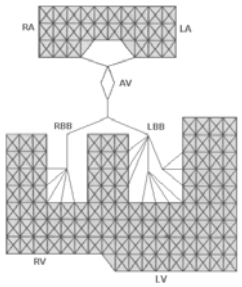

Figure 4.2 – *Ahlfeldt et al's 2D network for heart modelling [Ahlfeldt, 1987].*

3D heart and thorax models

A 3D approach was the next step in this evolution [Berenfeld, 1996, Clayton, 2002, Hernandez, 2000, Hsiao, 2000, Lu, 1993, Miller, 1978, Miller, 1978, Siregar, 1998, Weixue, 1996], building on the great advance in the computer capabilities. Despite these advances, such models are still quite time-consuming. Works by Miller, one of the first authors working on this kind of models, is cited in many articles. 3D models for heart (ventricles) and torso of the human body were constructed as groups of single cells with particular characteristics and surface potentials calculated. Besides the above mentioned physiological parameters, the models now also contain physical parameters, such as heart and/or body dimensions. Not only ECG tracings, but also

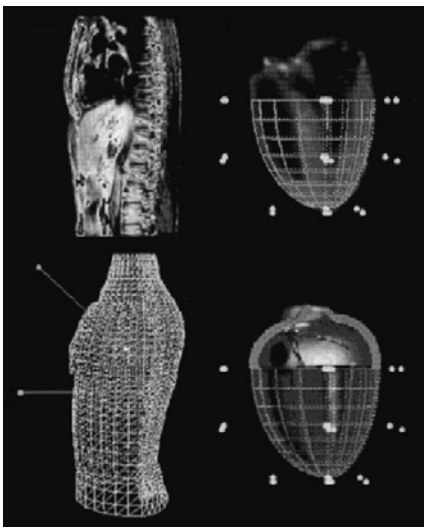

Figure 4.3 - *3D heart and torso models used by [Siregar, 1998].*

isopotential surfaces and body surface potential maps as well as other useful graphical representations of electical activity could be generated. Recent innovations include modeling and simulation of electrical conduction in an inhomogeneous torso (Siregar – Fig. 4.3), excitation propagation (Lu), epicardial surface potentials (Weixue), rotational anisotropy (Berenfeld) or mesh models (Hsiao). At present, a significant number of powerful 3D models of the heart, designed for different purposes, are available.

4.2.2 Model complexity

In general, the more recent the models, the more complex. The first simple ECG waveform generators need only a few equations or simple algorithms to represent the normal heart and some variations in rhythm and wave shape. Changes in the simulated ECG are created by changing parameters representing features of the typical ECG wave from, such as time intervals, amplitudes, etc. Powerful computing capabilities allowed for the inclusion of, for example, the conduction system of the heart and torso models, leading to a fast increase in model complexity, first in 2D and later in 3D.

It will be clear from the above that the more recent complex models are much more than simple ECG wave form generators; they simulate much of the electrical activity of the heart, and the ECG measured on the chest is one among many possible output variables. An exception to this rule is the model by [McSharry, 2003], which is a simple wave form generator based on a set of nonlinear dynamic equations.

4.2.3 Purpose and capabilities

The encountered models were designed for a number of different purposes, and even though a lot of them can be applied to educational simulation, only (Fukushima, Schwid, Hernandez, Siregar, Takeushi) specifically refer to that goal. Howlett and Nowotny designed models for comparative studies of the automatic detection of arrhythmias with patient monitoring equipment, Burke's model focused on testing, evaluation and calibration of electrocardiographic equipment and McSharry developed a model for assessing biomedical signal processing techniques, which are used to compute clinical statistics from the ECG. The remaining models were designed to study cardiac fields and electrical activity, rhythms, the conduction system, and general behavior of the whole heart.

It will be obvious that all of the models are able to generate a "normal" adult ECG including typical P, QRS and T-waves, without any changes.

Concerning "abnormal" conditions, almost all models are able to generate a number of arrhythmias and some of them are specifically designed for that purpose (Ahlfeldt, Clayton, Fukushima, Howlett, Takeushi). Siregar simulate a number of ventricular arrhythmias, as well as fibrillation. Ahlfeldt and Fukushima's models allow for the simulation of various types of AV block. Ahlfeldt also simulate particular abnormal occurrences, like modulated parasystole, escape rhythms, macro and micro reentry and reflection.

Changes in wave shape are often related to pathologies, for example, congenital heart diseases. Berenfeld, Miller II, Lu and Schwid specifically refer to normal and ischemic conditions of the heart. Myocardial infarction is represented in Hsiao and Miller II's work and Weixue presents WPW syndrome simulations. Siregar's model reproduces a set of particular pathologies and abnormal occurrences in the ECG,

including: hypertrophy, LVH, LBBB, atrial flutter and other rhythmic disorders in the atria, ventricles, and conduction pathways. Lu presents simulation results on the pathologies: bundle branch block, ventricular hypertrophy and pre-excitation.

The fact that a particular condition is not explicitly listed in a publication, does not imply that the presented model does not have the capability to simulate it. For example, hypertrophy and conduction disturbances on congenital heart diseases are detected on the ECG by a set of typical changes in the wave shapes and time intervals that can be reproduced by altering selected model parameters, if available, even if the model was not specifically designed for this purpose.

A few models are designed around a single specific pathology, for example, Clayton specifically simulated the ECG of ventricular tachyarrhythmias. To meet our requirements, we are more interested in "general purpose" ECG simulation models, and therefore, such models received less attention.

4.2.4 Suitability for reflecting neonatal electrophysiology

As mentioned before, the educational simulation of the neonatal ECG is a quite specific topic, and therefore no such models were found. However, in this section we will discuss the possibility to adapt the chosen models to the neonatal condition (more precisely, from 1 week-old neonate on, skipping the first days of intensive changes of the heart).

In the complex models implying 2D or 3D reconstruction of heart and torso, it is possible to suit their parameters to the typical dimensions of neonates. The typical conductions and AP waveforms at individual cells seem to be adequately changeable as well. In this way, the resulting ECGs at the body surface would logically represent the cardiac electrical activity of the neonate.

Models from Burke, Schwid, Nowotny and Howlett are able to generate arrhythmias, once they allow a good control on the ECG rhythm. This enables the generation of neonatal rhythms with the same origin as in the adult. McSharry's article is a particular case, presenting a good control in wave amplitudes and instants of occurrence. It suggests a good control for generating neonatal typical wave shapes rather then specific rhythms and/or conduction phenomena. Apparently, Fukushima and Takeushi's models allow a good manipulation of underlying physiology for the generation of different rhythms, and thus to reproduce some typical rhythms of the neonate. The generation of neonatal ECG waveforms is dependent (and limited) to the use of different templates.

Finally, it is known that the importance of the ventricular activity in the adult heart is higher than the atrial. Therefore, of the found models for the adult, some of them only generate ventricular electrical activity (Miller, Lu, Clayton or Hsiao's). The other models are shown (or suggested) to represent both atrial and ventricular activities. These are the ones that would better suit the neonatal adaptation, once the atrial activity of the heart is particularly important in the first weeks of life (Chapter 2).

4.2.5 Multi lead simulation

Modern neonatal ECG analysis involves 12-lead ECG. Considering the available models, only some of them can easily generate such tracings. The 3D models are able to represent potentials at any point on the body surface, requiring the identification of typical electrode positions. The 2D models by Ahlfeldt and Malik both generate

several body surface potentials in the frontal plane, but not the ones underlying the common limb or augmented limb leads. However, it seems possible to expand these models for the generation of potentials underlying these leads. Fukushima and Takeushi present the generation of only one lead. Expansion to include more frontal plane leads seems again possible. The models by Nowotny and Howlett are shown to generate V1, V4 and V5 leads, but the model description is not detailed enough to allow for implementation of other leads. The model by Schwid generates leads II and V5, and the one by Burke lead II. In these electronic single wave form generators, it seems possible to adapt the parameters to generate different leads. McSharry generates a single generic ECG, but explicitly refers to the use of the model to generate multilead ECG.

4.3 Recommendation for neonatal educational simulation

The choice of one or more of the above models to form a basis for further work on educational simulation of neonatal electrophysiology, is based on the requirements for a simulation engine (section 3.3.3). Single analog wave form generators do not fulfil the demands for the simulation of underlying physiology, including conduction events and action potentials, nor would they allow for the creation of different rhythms through manipulation of model parameters with a physiological interpretation. The level of detail reflected in 2D heart models should be enough to meet these requirements, without having to deal with the additional complexity of 3D heart models. Selected model(s) should preferentially have an educational purpose, and be capable to generate at least standard leads I or II, and aVF in the frontal plane. Of the discussed 2D models, the one presented by Fukushima has the closest match to these requirements. Adaptation to the neonate and inclusion of additional ECG leads seems possible, even within the time frame of this thesis. In the next chapter we will start with a more detailed description of this model.

Chapter 5

Model description and adaptation

In the previous chapter, the model proposed by Fukushima et al. [Fukushima, 1984] was chosen as a basis for generation of neonatal ECGs. In this chapter we will briefly describe the most important aspects of the Fukushima et al.'s model. Subsequently, we will present our proposed adaptations and extensions for educational simulation of neonatal electrophysiology and cardiography.

5.1 Description of the selected model

The focus of the Fukushima et al.'s model is on rhythm generation. The model represents both impulse formation and the conduction system of the heart. The various waveform segments of body surface ECG are stored in fixed templates for the P-wave and QRS-T complex, and are presented at the output, depending on the actual activation sequence in the simulated conduction system. The following sections briefly describe impulse formation and conduction system. This will serve as a basis for the presentation of the necessary adaptations for simulation of the neonatal ECG.

5.1.1 Structure

The model consists of 5 pacemaker centres (SA node, Atrium, AV node, bundle of His, Ventricle) and 4 bidirectional pathways connecting these centres (Fig. 5.1). Each centre has its own action potential (AP) defined by a function of time, a refractory period and a threshold firing potential. When the AP of a non-refractory centre exceeds its threshold, it begins to depolarize and sends an impulse to the antegrade and retrograde centres, respecting the corresponding pre-defined conduction times. Centres can fire autonomously or when triggered by another centre. Autonomous firing is caused by a rising resting potential. When stimulated by another centre, the transmembrane potential is increased by a constant value. If the resulting potential is above the centre threshold, it also depolarizes. The atria and ventricles, represented by a single AP each, can also depolarize following a premature stimulus.

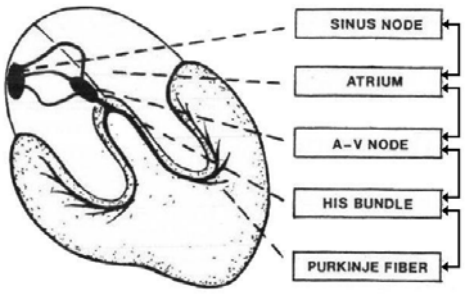

Figure 5.1 - *Structure of the model for simulation of specialized impulse formation and conduction [Fukushima, 1984]*

5.1.2 Parameters

Fukushima et al. explicitly specify 5 parameters for each centre: slope of the AP during the resting period, threshold potential, refractory period, and ante grade and retrograde conduction times to neighbouring centres. These parameters reflect a number of electrophysiological properties. Automaticity is included implicitly and controlled by the potential difference between the initial resting potential (not specified by Fukushima et al.) and the threshold potential, and by the slope of the action potential during the resting period. The parameters can be changed at will or randomly from beat to beat for the simulation of various arrhythmias.

5.1.3 Electrocardiogram generation

Atrial depolarisation is accompanied by the start of a P-wave. Fukushima et al. implemented three possible P-wave templates for a standard lead II: 1. resulting from SA node ante grade conduction (positive), 2. resulting from AV node retrograde conduction (negative), and 3. resulting from atrial autonomous firing or premature stimulation (tall).

Ventricular depolarisation is accompanied by the start of a QRS-T complex. Three possible complexes are implemented for a standard lead II: 1. resulting from AV node ante grade conduction (normal, narrow QRS), 2. resulting from autonomous firing of the bundle of His (wide, bizarre, negative QRS), and 3. resulting from ventricular autonomous firing or premature stimulation (wide, bizarre, positive QRS).

Fig. 5.2 shows examples of P-wave and QRS-T complex templates used in normal antegrade conduction and autonomous ventricular firing.

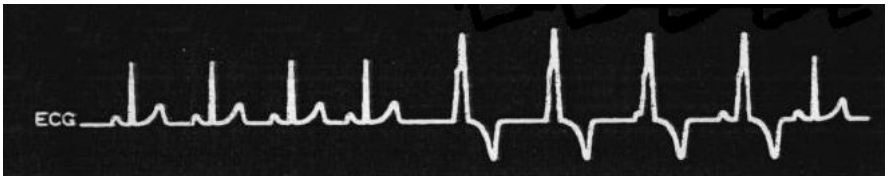

Figure 5.2 - *Simulated lead II ECG for normal rhythm and premature ventricular beat [Fukushima, 1984]*

5.2 Adaptation to neonatal ECG simulation

The model for the adult, presented by Fukushima et al., and summarized in the previous section, constitutes our basis for educational simulation of the neonatal ECG. The following sections describe the adaptations and extensions of the Fukushima model, necessary to reflect the specificity of the neonatal ECG. We also fill in some of the information gaps left by the authors, but necessary for a software implementation.

5.2.1 Parameters

In Fukushima et al., the generation of AP for each centre is the first step in generating ECG waveforms. From the article, we can infer that APs are represented by a piece-wise linear function (Fig. 5.3). The authors assume that this rather rough approximation of the natural AP, adapted to the different parts of the heart, is detailed

enough for the purpose of educational simulation. We observe that in this model, the simulation of APs is not essential for rhythm generation, which only requires specification of the instant of firing, automaticity and refractory period. However, simulated APs give insight in the underlying physiology of complex rhythms, and we will therefore maintain them. Moreover, it will be the basis of our set of parameters, which is constituted as follows:

- At each centre:
  . Amplitudes at flexion points: A_1, A_2, A_3, and A_4;
  . Segment durations: D_1, D_2, D_3, and D_4;
  . Refractory period: RP;
  . Impulse conduction delay: ICD.
- Impulse conduction times between centres: Matrix "Conductions" further described in Chapter 6.

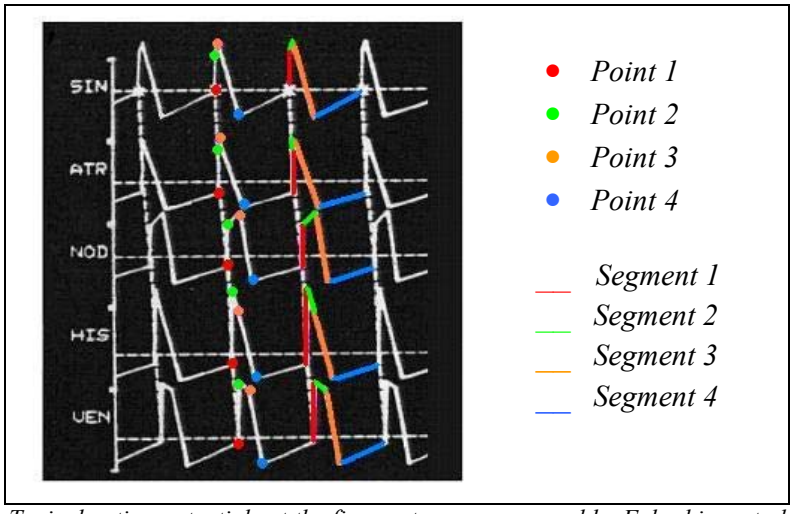

Figure 5.3 - *Typical action potentials at the five centres, as proposed by Fukushima et al.. The flexion points of the pice-wise linear functions are identified by "Point 1, … , Point 4", and the segment durations by "Segment 1, … , Segment 4" [Fukushima, 1984].*

Only the following sub-set of the parameters listed above may be altered during simulations: D_2 (only of the ventricular segment, varying with HR, see section 5.2.5), D_4, RP, ICD, and "Conductions". The remaining parameters are fixed.

For ease of parameter manipulation, the instructor sets the "automaticity" (in bpm) of each centre. This quantity determines the total autonomous firing period T (in ms) of the centre AP:

$$T = \frac{60.000}{automaticity}$$

Because T is equal to the sum of the segment durations, the model parameter D_4 is then determined as follows:

$$D_4 = T - \sum_{i=1}^{3} D_i$$

Note that in the Fukushima model, the threshold potential is used to manipulate AP duration. The threshold potential corresponds to our model parameter A_1, which

is kept fixed during the simulations. Fukushima et al. further use the slope S of the fourth segment, which can be expressed in our model parameters as follows:

$$S = \frac{A_1 - A_2}{D_4}$$

Parameters for impulse conduction are considered separately. To enable the simulation of neonatal arrhythmias, such as the ones involving complex re-entry, or to allow for direct conduction between SA and AV nodes [Guyton, 1991], we lifted the ante grade/retrograde conduction restrictions imposed by Fukushima et al., providing parameters for the triggering of any centre by any other.

Possible delays at the centres are not mentioned by Fukushima et al.. They consider that, as soon as a centre fires, it immediately sends an impulse to the ante grade and retrograde centres. It is known that certain centres, for example the AV node, can present a delay. Delays in this node can even degenerate into important conduction disturbances, such as AV blocks. We therefore provide parameters for delays for all centres.

In this expanded model, the total time between the triggering of centre *(a)* and the subsequent triggering of centre *(b)* is given by is the sum of the delay at centre *(a)* and the impulse propagation time between the two centres.

5.2.2 Parameter estimation for action potential generation

There are no explicit references to the relationships between segments and underlying physiology. Nevertheless, analysis of the presented AP waves suggests the following relationships: *segment 1* represents depolarisation, *segment 2* the transition between depolarisation and repolarisation, *segment 3* repolarisation and *segment 4* the resting phase. From now on, we will assume these relationships and set the parameters for AP generation accordingly.

In Figure 5.3, time and amplitude scales do not carry units, nor do Fukushima et al. list values for AP amplitudes and segment durations. Information given by the authors is limited to the slope of the fourth segment and heart rate. Therefore, to find a complete AP description, we have to use additional sources.

The segment durations were defined based on a target ECG, Fig. 3.1, and observation of APs in [Fukushima, 1984]. Since D_1 is always very short, corresponding to a practically instantaneous transition, it is set to a single step for all centres:

$$D_1 = T_s = \frac{1}{F_s}$$

Where F_s is the sampling frequency, which in our code implementation is equal to 100 Hz. Durations D_2 and D_3 were set under the following physiological constraints related to the target ECG:

- atrial D_2, representing the transition between depolarisation and repolarisation, starts during the P-wave after *segment 1*, and has to end during the PR-interval. Atrial D_3, representing repolarisation, starts during the PR-interval after *segment 2*, and has to end during de QRS-complex.

- ventricular D_2 starts during the QRS-complex after *segment 1*, and ends at the beginning of the T-wave. *Segment 3* represents repolarisation and ventricular D_3 is set equal to the T-wave duration.

At the SA and AV nodes, we kept the same total action potential durations ($D_{AP} = D_1 + D_2 + D_3$) as in the atrium. The same procedure was followed for the bundle of His relative to the ventricle. The individual durations D_2 and D_3 at the SA and AV nodes, and at the bundle of His were slightly adjusted in order to match the AP waveforms presented by Fukushima et al..

Durations D_4 depend on the total autonomous cycle durations T, as explained in the previous section. Table 5.1 contains proposed normal values of automaticity at each centre (for normal sinus rhythm). The derived values for D_4 are listed in to Table 5.3 containing the complete set of model parameters.

Table 5.1 – *Proposed normal values for automaticity and autonomous cycle duration in different heart locations (personal commucation Dr. Peter Andriessen).*

AP settings	SA node	Atrium	AV node	Bundle of His	Ventricle
Automaticity (bpm)	150	80	50	45	45
Autonomous cycle duration – T (ms)	400	750	1200	1333	1333

Amplitudes were set according to data in Table 5.2. Note that from the chapter by Pickoff [Pickoff, 1998], it could not be confirmed if these data are specific for the neonate. Given that the main role of the action potentials in the simulation is visual support rather than determination of rhythms, we decided to leave this issue to future investigation.

Table 5.2 – *Action potential characteristics in different cardiac cells [Pickoff, 1998].*

		SA node	Atrium	AV node	His-Purkinge	Ventricle
Resting Potential	Amplitude (mV)	(-60)-(-50)	(-80)-(-90)	(-60)-(-70)	(-90)-(-95)	(-80)-(-90)
Action Potential *	Amplitude (mV)	60-70	110 - 120	70 - 80	120	110 – 120
	Duration (ms)	100-300	100 - 300	100 - 300	300 – 500	200 – 300

** - The author refers to "Action Potential" as the depolarisation/repolarisation processes, not including the resting potential.*

Amplitudes A_4 are given by the mean values of the resting potentials, Table 5.2. The peak-to-peak value of AP tracings, either A_2-A_4 or A_3-A_4, respect the mean action potential amplitude values in Table 5.2. A_2 and A_3 were adjusted for each centre in order to match the waveforms presented by Fukushima et al.. Amplitudes A_1 were set according to the values proposed by Fukushima et al. for the threshold potentials.

Table 5.3 contains the complete set of model parameters and numerical values. The resulting AP tracings are shown in Fig. 5.4 in a hypothetical case of autonomous depolarisation at all centres.

Note that the action potential duration in the bundle of His is below the minimal limit in Table 5.2 for the His-Purkinge system. In our model, the action potential duration of the bundle of His does not include the influence of Purkinge fibres.

Table 5.3 – *Derived model parameters for normal neonatal AP tracings.*

Parameters		SA node	Atrium	AV node	Bundle of His	Ventricle
Durations (ms)	D_1	10	10	10	10	10
	D_2	40	70	100	80	120
	D_3	120	90	60	150	110
	D_4*	230	580	1030	1103	1103
Amplitudes (mV)	A_1	-40	-50	-40	-58	-60
	A_2	-10	5	0	28	30
	A_3	10	30	10	10	25
	A_4	-55	-85	-65	-92	-85

* - *Values derived from the autonomous cycle durations T.*

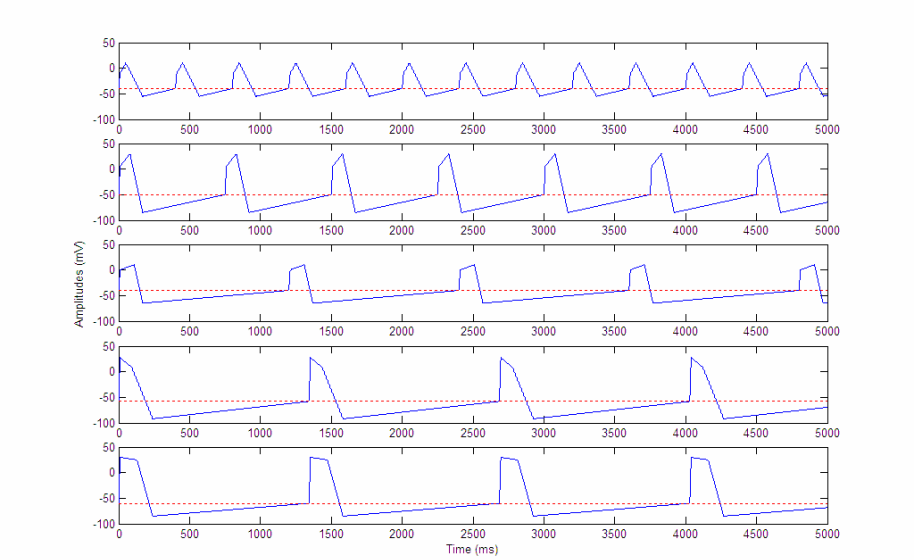

Figure 5.4 – *AP wave forms for a neonatal subject. Hypothetical case of autonomous depolarisation at all centres. Dashed red lines represent threshold potentials.*

5.2.3 Electrocardiogram generation

Like Fukushima et al., this section focuses on generating a standard lead II. The goal is to establish a simple demonstration tool, which, in the same time, constitutes a step towards meeting the general requirement for at least two leads in the frontal plane (lead I or II and aVF).

Selected figures in Fukushima et al. include typical P-waves and QRS-T complexes. They mention, but do not provide, templates for different wave shapes. We separate the QRS-complexes and T-waves, allowing for independent manipulation of the ST segment duration, and explicitly provide the templates (Fig. 5.5).

Three different P-waves are provided depending on the origin of the impulse. QRS-complexes are also provided in three different configurations depending on the origin of the impulse. T-waves are triggered at a specified time after the QRS-complex. They are presented in a single configuration only: a normal T-wave, originating from either ante grade conduction or autonomic ventricular depolarisation.

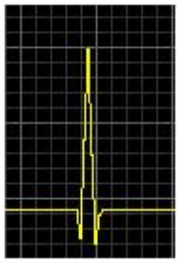

QRS-complex for ante grade conduction from AV node to the ventricle

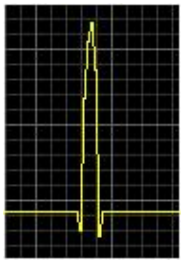

QRS-complex for autonomous firing of the ventricle

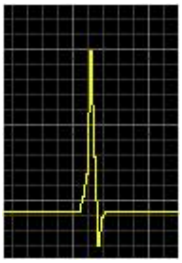

QRS-complex for ante grade conduction from atrium to ventricle (for WPW syndrome)

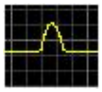

P-wave for ante grade conduction SA node → atrium

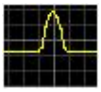

P-wave for atrial autonomous firing

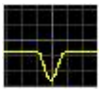

P-wave for retrograde conductions to the atrium

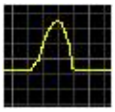

T-wave for all different ventricular repolarisations

Figure 5.5 - *Lead II P-wave, QRS-complex and T-wave simulation templates, 1 division = 40ms x 0.1mV*

The wave shapes were obtained from digitised images of ECG [Tipple, 1999]. Amplitudes and durations are consistent with the typical values listed in the requirements section. In absence of a simulated waveform, a null baseline is generated. Baseline output can occur between T-wave and following P-wave (isoelectric region), between P-wave and following QRS-complex (PQ or PR interval) and between QRS-complex and the following T-wave (ST segment). The isoelectric region and PR interval are only dependent on the time of occurrence of the respective waves. The ST segment varies with heart rate, as described on next section.

5.2.4 Variation of the QT interval with heart rate

The QT interval, from the beginning of the QRS-complex until the end of the T-wave, reflects the time required for both ventricular depolarisation and repolarisation. It varies with HR, but not with age, except in infancy [Park, 1992].

In the neonatal situation, involving high heart rates, unphysiological wave overlap could occur when maintaining the same ST segment for all rates. In our model, we therefore introduce a QT(HR) relationship, based on [Park, 1992], Table 5.4. The range of considered values limited by the minimum and maximum heart rates for sinus rhythms as listed in Chapter 3.

Table 5.4 - *Selected values for heart rate, cycle length, and QT interval for the neonate [Park, 1992].*

Heart Rate (bpm)	Cycle Length (ms)	QT interval average (Upper Limit) (ms)
100	600	310 (340)
109	550	300 (330)
120	500	280 (310)
133	450	270 (290)
150	400	250 (280)
172	350	230 (290)

A graphical representation of average QT interval as a function of HR suggests a linear regression (Fig 5.6). This approximation is used in our model to calculate the QT interval.

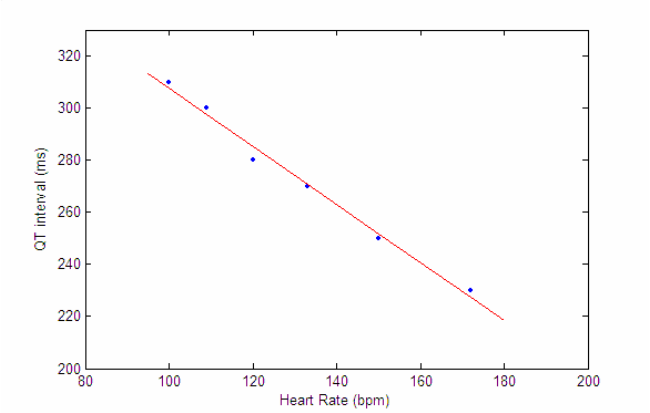

Figure 5.6 - *Graphical representation of the QT interval-HR relationship.*

The underlying assumption of this method is that variations in QT interval can be completely attributed to variations in the ST segment. However, several examples of simulated and real ECGs present variations in T-wave duration. T-waves seem to extend in time at slower rhythms and to get shorter in faster rhythms. Measuring those changes is complicated by the difficulties in the exact delimitation of the T-wave. Because of this uncertainty, we decided to maintain a fixed T-wave in our model.

5.2.5 Ventricular action potential and T-wave morphology

As mentioned in the previous section, changes in QT interval are simulated by changes in ST segment, keeping the T-wave duration constant. This means that once the QT interval (and ST segment) is calculated, the beginning of repolarisation in the ventricle (start of T-wave) is also known. Remembering that in our AP representation, the 3rd segment represents repolarisation with the same fixed duration as the T-wave, the beginning of 3rd segment can thus be defined by the end of ST segment. Therefore, T-waves will always be triggered at the start of 3rd segment of the ventricular AP, Fig. 5.7. Consistency with the tabeled values for QT intervals was verified.

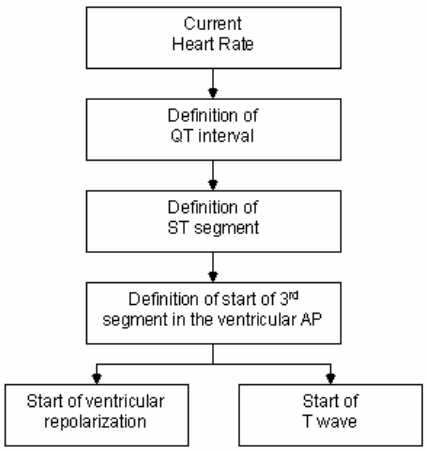

Figure 5.7 - *Sequence for setting the begin of a T-wave and its relationship to the ventricular AP.*

5.3 Parameter estimation for simulation of target rhythms

The adapted model was used to reproduce part of the target rhythms presented in Table 3.1. Examples of ECG strips with these rhythms are available in Appendix II. In this section, we describe the parameter estimation for generating these rhythms. Critical parameter values are presented in Table 5.5. Not all rhythms of Table 3.1 were implemented because of limitations in the software implementation. In Chapter 8 we will come back to this issue.

5.3.1 Sinus rhythms

Normal sinus rhythm (NSR)

For NSR, we focus on the characteristics of the target ECG presented in Fig. 3.1. Values for D_4 were set to fit normal automaticity at each centre, as specified by a clinical expert (Dr. Peter Andriessen): 150 bpm for the SA node, 80 bpm for the atria, 50 bpm for the AV node and 45 bpm for the bundle of His and ventricles. For all centres, refractory periods were set according to values given by Fukushima et al. [Fukushima, 1984]. Conduction pathways between adjacent centres are as given by Fukushima et al.. Besides the pathway via the atria, we also consider a direct path between SA and AV nodes. This conduction represents the influence of "internodal pathways" referred to in Chapter 2. Its duration may be shorter than the total conduction time through the atrium. Conduction times are based on studies by Levin et al. [Levin, 1977]. The AV node delay was also set according to this study.

Sinus tachychardia and sinus bradycardia

The SA node is still the pacemaker. To change HR it is enough to change the automaticity of SA node accordingly. Extreme sinus bradycardias may result in ectopic rhythms described in the next section. The conduction times and refractory periods are as in NSR.

Sinus pause and sinus arrest

Sinus pause is implemented using an occasional null automaticity of the SA node (and thus an infinite resting period). Consequently, the AV node becomes the pacemaker until the SA nodal automaticity returns to normal. Sinus arrest is implemented by permanent null automaticity of the SA node, and blocking the ante grade conductions to the atrium and AV node and the retrograde conduction from the atria to the SA node. Atrial automaticity was decreased in order to make the AV node the pacemaker, obtaining an AV nodal rhythm with inverted P-waves.

5.3.2 Atrial, AV nodal and ventricular disrhythmias

The mechanism for generating ectopic rhythms is simple. They occur when the automaticity of SA node is below the automaticity of at least one of the other centres, making the fastest centre the ectopic pacemaker.

Atrial and nodal tachycardias are obtained by increasing atrial and nodal automaticity above the SA nodal automaticity, respectively. Premature ventricular contractions (PVC) were simulated by occasionally increasing the ventricular automaticity, and triggering isolated QRS-complexes from ventricular self-depolarisation. Ventricular tachycardia was obtained by decreasing SA node

automaticity and increasing ventricular automaticity. The ventricles take over the pacemaker role at a very high rate.

5.3.3 Conduction disturbances

1st degree AV block was generated simply by increasing the delay in the AV nodal conduction. The consequence is an increased delay between atrial and ventricular activity and thus a prolongation of the PR interval on the ECG.

2nd degree AV block (2:1) is implemented as a consequence of high rate sinus tachycardia (by increasing the SA nodal automaticity), rather than as a progression of 1st degree AV blockade. At such high rates, the AV node can only conduct one out of two sinus impulses to the ventricle.

Complete AV block is implemented with complete lack of electrical conduction between upper and lower parts of the heart. This was achieved by setting infinite antegrade/retrograde conduction times between the atria and AV node and infinite direct conduction time between SA and AV nodes. Two centres act as independent pacemakers: the SA node for the atria and the AV node or the venticle centre for the ventricles.

5.3.4 Reentry

SVT – accessory reciprocating AV tachycardia

This is a supraventricular tachycardia characterised by the presence of one accessory pathway – the bundle of Kent – responsible for an abnormal retrograde atrial depolarisation. The ventricles are excited through the normal slow path of the AV node. We simulate this accessory bundle by inserting a direct conduction from ventricles to atria. The conduction time is set so that the impulses reach the atria outside of the refractory period. Retrograde impulses produce inverted P-waves following the QRS-complexes.

Wolff-Parkinson-White syndrome

As in SVT, this syndrome is also caused by the bundle of Kent. However, in this case the direction of conduction is the opposite. We implement this rhythm by inclusion of a direct conduction from atria to ventricles. The conduction time is shorter than the total time for conduction through the AV node. This results in short PR intervals. We also use a template for the QRS-complex which including the characteristic “delta wave”.

5.3.5 Summary of numerical values

Table 5.5 includes numerical values for critical parameters for the rhythms described above. Parameters A_1, A_2, A_3, A_4 and D_1, D_2, D_3 are set according to the values specified in section 5.2.2 for all centres. Parameters D_4 are derived from the automaticities at each centre using equation in section 5.2.1. Ventricular D_2 is derived from the current ventricular rate (section 5.2.4).

Table 5.5 – *Parameters for rhythm generation.*

Target rhythm	HR (bpm)	Centre	Parameter		
			Automaticity (bpm)	Refractory period (ms)	Conduction times/ delays (ms)
Normal sinus rhythm	150	SA	150	30	$\begin{bmatrix} 0 & 10 & 20 & - & - \\ 10 & 0 & 20 & - & - \\ - & 20 & 50 & 10 & - \\ - & - & 10 & 0 & 30 \\ - & - & - & 30 & 0 \end{bmatrix}$
		Atr	80	30	
		AV	50	30	
		Hb	45	30	
		Ven	45	30	
Sinus tachycardia	200	SA	200	30	$\begin{bmatrix} 0 & 10 & 20 & - & - \\ 10 & 0 & 20 & - & - \\ - & 20 & 50 & 10 & - \\ - & - & 10 & 0 & 30 \\ - & - & - & 30 & 0 \end{bmatrix}$
		Atr	80	30	
		AV	50	30	
		Hb	45	30	
		Ven	45	30	
Sinus bradycardia	85	SA	85	30	$\begin{bmatrix} 0 & 10 & 20 & - & - \\ 10 & 0 & 20 & - & - \\ - & 20 & 50 & 10 & - \\ - & - & 10 & 0 & 30 \\ - & - & - & 30 & 0 \end{bmatrix}$
		Atr	80	30	
		AV	50	30	
		Hb	45	30	
		Ven	45	30	
Sinus pause[1]	150 (70)	SA	150 (0)	30	$\begin{bmatrix} 0 & 10 & 20 & - & - \\ 10 & 0 & 20 & - & - \\ - & 20 & 50 & 10 & - \\ - & - & 10 & 0 & 30 \\ - & - & - & 30 & 0 \end{bmatrix}$
		Atr	70	30	
		AV	50	30	
		Hb	45	30	
		Ven	45	30	
Sinus arrest	50	SA	0	30	$\begin{bmatrix} 0 & - & - & - & - \\ - & 0 & 20 & - & - \\ - & 20 & 50 & 10 & - \\ - & - & 10 & 0 & 30 \\ - & - & - & 30 & 0 \end{bmatrix}$
		Atr	40	30	
		AV	50	30	
		Hb	45	30	
		Ven	45	30	
Atrial tachycardia	200	SA	150	30	$\begin{bmatrix} 0 & 10 & 20 & - & - \\ 10 & 0 & 20 & - & - \\ - & 20 & 50 & 10 & - \\ - & - & 10 & 0 & 30 \\ - & - & - & 30 & 0 \end{bmatrix}$
		Atr	200	30	
		AV	50	30	
		Hb	45	30	
		Ven	45	30	
Nodal tachycardia	190	SA	150	30	$\begin{bmatrix} 0 & 10 & 20 & - & - \\ 10 & 0 & 20 & - & - \\ - & 20 & 50 & 10 & - \\ - & - & 10 & 0 & 30 \\ - & - & - & 30 & 0 \end{bmatrix}$
		Atr	80	30	
		AV	190	30	
		Hb	45	30	
		Ven	45	30	
Premature ventricular contractions[2]	150 (160)	SA	150	30	$\begin{bmatrix} 0 & 10 & 20 & - & - \\ 10 & 0 & 20 & - & - \\ - & 20 & 50 & 10 & - \\ - & - & 10 & 0 & 30 \\ - & - & - & 30 & 0 \end{bmatrix}$
		Atr	80	30	
		AV	50	30	
		Hb	45	30	
		Ven	45 (160)	30	
Ventricular tachycardia	150	SA	120	30	$\begin{bmatrix} 0 & 10 & 20 & - & - \\ 10 & 0 & 20 & - & - \\ - & 20 & 50 & 10 & - \\ - & - & 10 & 0 & 30 \\ - & - & - & 30 & 0 \end{bmatrix}$
		Atr	40	30	
		AV	50	30	
		Hb	45	30	
		Ven	150	30	

Table 5.5 (cont) - *Parameters for rhythm generation.*

Target rhythm	HR (bpm)	Centre	Parameter		
			Automaticity (bpm)	Refractory period (ms)	Conduction times/ delays (ms)
1st degree AV block	150	SA	150	30	$\begin{bmatrix} 0 & 10 & 20 & - & - \\ 10 & 0 & 20 & - & - \\ - & 20 & 140 & 10 & - \\ - & - & 10 & 0 & 30 \\ - & - & - & 30 & 0 \end{bmatrix}$
		Atr	80	30	
		AV	50	30	
		Hb	45	30	
		Ven	45	30	
2nd degree (2:1) AV block	150	SA	300	30	$\begin{bmatrix} 0 & 10 & 20 & - & - \\ 10 & 0 & 20 & - & - \\ - & 20 & 50 & 10 & - \\ - & - & 10 & 0 & 30 \\ - & - & - & 30 & 0 \end{bmatrix}$
		Atr	80	30	
		AV	50	30	
		Hb	45	30	
		Ven	45	30	
Complete AV block	60	SA	150	30	$\begin{bmatrix} 0 & 10 & 20 & - & - \\ 10 & 0 & 20 & - & - \\ - & 20 & 50 & - & - \\ - & - & - & 0 & 30 \\ - & - & - & 30 & 0 \end{bmatrix}$
		Atr	80	30	
		AV	50	30	
		Hb	45	30	
		Ven	60	30	
SVT: Accessory reciprocating AV tachycardia	187	SA	150	30	$\begin{bmatrix} 0 & 10 & 20 & - & - \\ 10 & 0 & 20 & - & - \\ - & 20 & 50 & - & - \\ - & - & - & 0 & 30 \\ - & 210 & - & 30 & 0 \end{bmatrix}$
		Atr	80	30	
		AV	50	30	
		Hb	45	30	
		Ven	45	30	
WPW syndrome	150	SA	150	30	$\begin{bmatrix} 0 & 10 & 20 & - & - \\ 10 & 0 & 20 & - & 80 \\ - & 20 & 50 & 10 & - \\ - & - & 10 & 0 & 30 \\ - & - & - & 30 & 0 \end{bmatrix}$
		Atr	80	30	
		AV	50	30	
		Hb	45	30	
		Ven	45	30	

[1,2] - The values in parentheses refer to: 1. occasional change in sinus automaticity and consequently in HR; 2. occasional changes in ventricular automaticity and consequently in HR.

Note that the numerical values for the refractory period refer to the interval starting at the beginning of the resting phase. The centre is also refractory during the depolarisation and repolarisation phases preceding the listed interval.

Chapter 6

Software implementation

We designed a software simulation tool called NEGRA - Neonatal Electrocardiogram Generator for Rhythm Analysis to fulfil (part of) the requirements presented in Chapter 3. It is based on the model of neonatal electrophysiology presented in the previous chapter. This chapter focuses on model implementation. Trainee and instructor interfaces are presented in the next chapter (results). Software implementation of these functions is straight forward and not further discussed here. NEGRA was set up to form the basis for a more complete tool, simulating more rhythms and complex scenarios, but in the context of this work its main purpose is limited to providing a demonstration environment for the developed simulation engine. An executable, based on a code implementation in Microsoft Visual C++, is included in a number of copies of this report, or available upon request to the supervisor.

6.1 Data structures

Current parameter values are stored in matrices with centres identifying rows and parameters columns. One matrix reflects the parameters as introduced in the previous chapter. We also maintain a matrix with parameters as introduced by Fukushima et al. [Fukushima, 1984]. This matrix introduces some redundancy, but, especially in the early design phases, helped keeping a grip on complex parameter relationships. Separate matrices are defined for storing delays and conduction times: "Conductions" and "Current_cond".

Matrix "Conductions"

Table 6.1 shows the structure of this 5x5 matrix. Rows represent conduction times *to* other centres, columns represent conduction times *from* other centres.

Table 6.1 – *Structure for matrixes "Conductions" and "Current_cond". The conductions between adjacent centres (proposed by Fukushima) and delays at each centre are represented in pink and blue blue, respectively (values in ms).*

	1: SA node	2: Atrium	3: AV node	4: His bundle	5: Ventricle
1: SA node	Delay 1	$Cond_{1\to2}$	$Cond_{1\to3}$	$Cond_{1\to4}$	$Cond_{1\to5}$
2: Atrium	$Cond_{2\to1}$	Delay 2	$Cond_{2\to3}$	$Cond_{2\to4}$	$Cond_{2\to5}$
3: AV node	$Cond_{3\to1}$	$Cond_{3\to2}$	Delay 3	$Cond_{3\to4}$	$Cond_{3\to5}$
4: His bundle	$Cond_{4\to1}$	$Cond_{4\to2}$	$Cond_{4\to3}$	Delay 4	$Cond_{4\to5}$
5: Ventricle	$Cond_{5\to1}$	$Cond_{5\to2}$	$Cond_{5\to3}$	$Cond_{5\to4}$	Delay 5

For example, the first row represents conduction times from the SA node to all the other centres. The second column represents conduction times from other centres to the atrium. Note that due to other phenomena, such as refractoriness, some interactions take place more frequently than others. The matrix diagonal contains impulse delays for each centre. Values above the diagonal define ante grade conduction and values below retrograde conduction.

Matrix "Current_cond"

Alongside the matrix "Conductions", there is a matrix called "Current_cond" with the same structure. The purpose of this matrix is to store the current conduction times when the simulation is running. It starts with an infinite value for all possible conductions. Once a centre fires, the corresponding delay and conduction times in "Conductions" are put in the corresponding row in "Current_cond". As simulation time passes, the delay counter is decreased. On zero delay, conduction couters start decreasing. When a conduction counter becomes nonpositive, the target centre depolarises if it is not refractory, and the conduction counter is set to "infinite" again.

This representation is quite flexible, since it allows for the simultaneous simulation of several active centres and conductions. This is expecially helpful in the simulation of pathologic situations.

6.2 Algorithm flowcharts

In this section we provide flowcharts and detailed descriptions of key algorithms in NEGRA.

6.2.1 Main algorithm

The main procedure shown in Fig. 6.1 is called by the simulation engine every time step for each of the five centres. Basically, it checks the matrix C*urrent_cond* and detects if there are any centres depolarising at that time step. Then it calls for the corresponding output and/or update operations.

It begins with AP generation. A numerical value is given for the AP for one centre and time instant. If that value exceeds the established threshold, there is a possible depolarisation. If not, another check is made for conductions from other centres arriving at that instant. This is done by detecting non-positive elements in the corresponding column in the matrix *Current_cond*.

The next step is to check if the possible depolarisation would occur outside of the refractory period. If not, there is no depolarisation. The conductions in the corresponding line in the matrix *Current_cond* are decreased, a null baseline value is sent to the ECG output and the algorithm repeats the same procedure for the remaining centres at that time instant. These procedures for "no depolarisation" are also followed when the AP value does not exceed the threshold and there are not incoming conductions.

When depolarisation occurs our algorithm is slightly different from the approach by Fukushima et al.. In their algorithm, when, for example, the atrium depolarises, its AP is increased by a constant value. Then, the threshold potential is taken into account. In our algorithm, any depolarisation automatically sets the next AP sample with the amplitude A_2, which always exceeds the threshold potential. The consequent depolarisation triggers the following actions:

1. The centre can send impulses to other centres. The matrix *Conductions* is checked for non-infinite values in the corresponding line, as well as a possible delay. The equivalent line is then updated with those values in *Current_cond*.
2. An ECG output request is sent to a buffer. P-wave, QRS-complex or T-wave templates are used in case of atrial or ventricular depolarisation (the output mechanism is described in the next section). Otherwise, a null baseline is requested.

The described procedures will be repeated for the centres that were not yet tested at the same time instant.

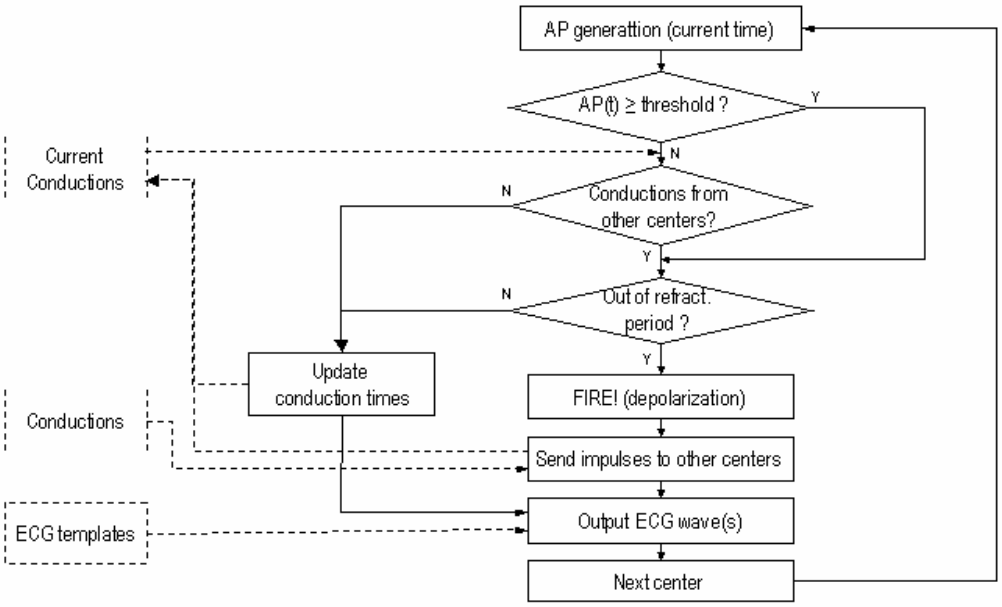

Figure 6.1 – *Flowchart for the representation of the Main procedure. Dotted connections represent the use of external data (ECG templates and matrices for conductions).*

6.2.2 Action potential generation

The algorithm for AP generation is summarized by the flowchart in Fig 6.2. As for the Main algorithm, it is called for each centre at each time instant, in order to get instantaneous AP values.

In Chapter 5 we already presented the approach for AP generation, based on four segments and key flexion points. This algorithm also considers four possible AP phases, which are selected depending on the current time instant. A variable *Curr_time* stores the current time since the last depolarisation for each centre.

The first step is to check if a depolarisation is starting, which means that *Curr_time* = 0. In that case, as described in the previous section, the AP is automatically set to amplitude A_2. Otherwise, the algorithm tests *Curr_time* to check what the current segment is. The corresponding instantaneous AP values are then computed by linear interpolation using functions F_2, F_3 and F_4 (Fig. 6.2).

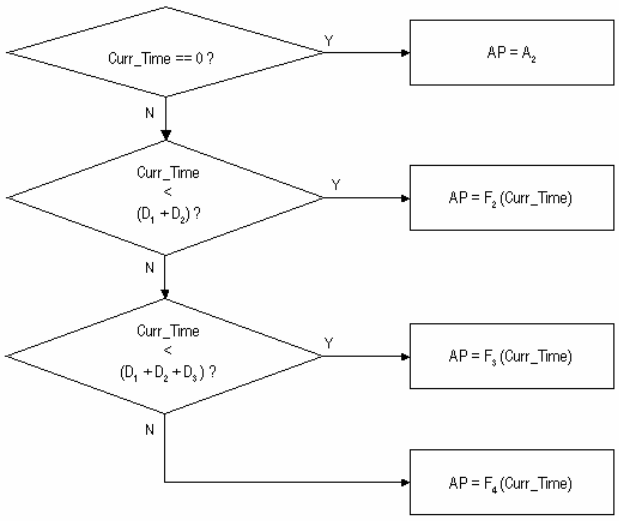

Figure 6.2 – *Flowchart for representation of the algorithm for action potential generation. The duration D_1 is always equivalent to one time step.*

6.2.3 ECG output

The algorithm for ECG output (Fig. 6.3) is executed every time instant, after the "Main" algorithm has run for all separate centres. Five possible ECG outputs are considered: P-wave, QRS-complex and T-wave templates; null ST segment and null baseline. We designed the algorithm for possible simultaneous output of different templates and/or baselines. This was implemented by using a final buffer where the values of currently activated templates and/or baselines are added. The following variables were used to support these functionalities:

- ***CurrWave*:** is a boolean for the separate identification of the currently activated outputs.
- ***CurrPosition*:** contains the value for the position in time for each currently activated output.
- ***STint*:** stores the current time in the ST-segment (determined from the calculation of the QT interval – section 5.2.4).

This algorithm primarily identifies which different outputs are activated at the current instant. This is made by checking *CurrWave*, which contains the current state (activated or not) of the following outputs: Baseline, P-wave, QRS-complex, ST segment and T-wave. The procedures for these outputs are described below:

1. **Baseline:** this output is always activated and puts a null value in the buffer. Obviously, it is only visible in the final ECG if there are not templates activated. This happens on the PR interval and isoelectric region of the ECG.
2. **P-wave:** if this template is active, its value at the right position in time is added to the buffer. Otherwise, the P-wave identifier is set to False and no value is added to the buffer (baseline for PR interval).
3. **QRS-complex:** An analogous procedure is executed when the QRS template is active. At the end of the template the QRS-complex identifier is set to False, the ST segment identifier to True, and no value is added to the buffer (baseline for ST segment).

4. **ST segment:** No templates are used when the ST segment identifier is active. Note that none of the simulated rhythms involved ST segment shifts. No value is added to the buffer and *STint* is decreased if the end of the ST segment duration is not yet reached. At the end of the ST segment (when *STint* becomes null), the ST segment identifier is set to False, the T-wave identifier is set to True and the value of the first T-wave template sample is added to the buffer. It should be kept in mind that the ST segment is considered a particular case of baseline. Even it is characterized by a null amplitude, we consider it a particular segment with a specified duration, only activated between the QRS-complex and T-wave.
5. **T-wave:** Similar steps as for the P-wave and QRS-complex templates are followed for this wave. When it is no longer active the T-wave identifier is set to False and no value is added to the buffer. The T-wave is followed by the isoelectric region.

When all possible outputs are checked, the final ECG value for that instant is given by the summed values in the buffer. Normally, the result is limited to a null baseline or a template value. However, simultaneous templates may be active. A common example is the overlap of the P-wave and the T-wave of the previous beat in high rate rhythms.

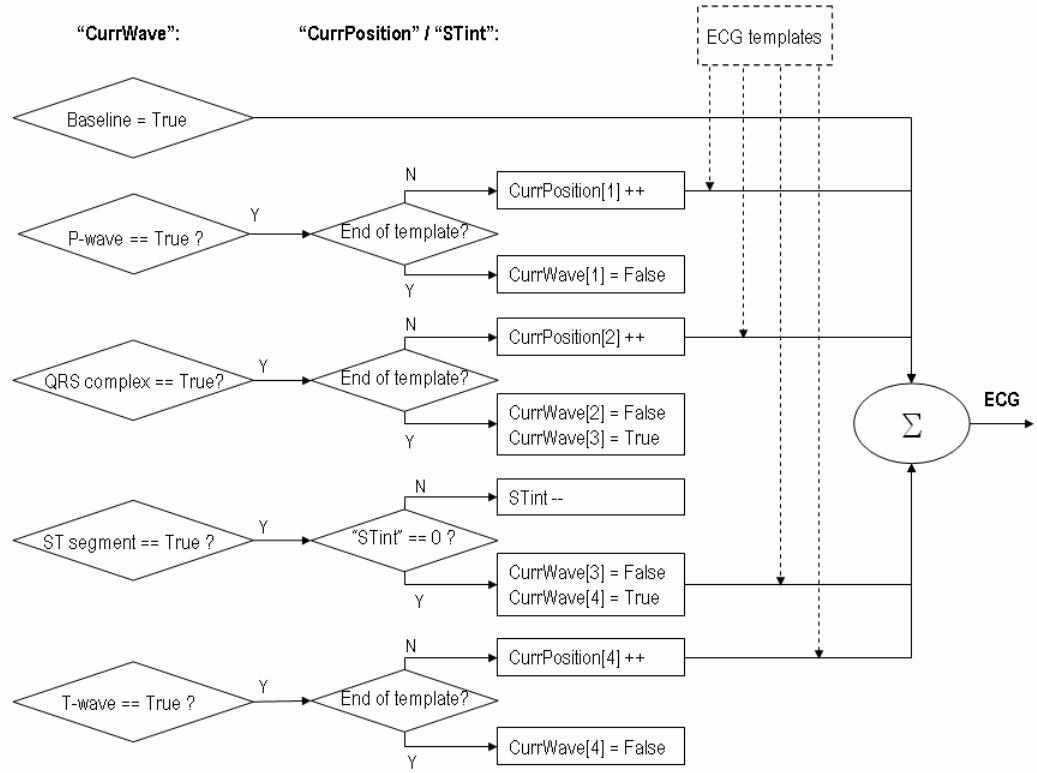

Figure 6.3 – *Flowchart for representation of the algorithm for ECG output. Dotted connections represent the use of external data (ECG templates). Different outputs are numbered from 0 to 4 (0 - Baseline,1 - P-wave, 2 - QRS-complex, 3 – ST segment, 4 – T-wave).*

Chapter 7

Results

The presentation of results closely follows the TNA-TPD-TMS framework for setting simulator and model requirements, Chapter 3. Because the focus was on software and model development, these sections are more elaborate than the sections on training needs and training program. The most extensive section presents the simulation results of the physiologic model and its use for rhythm generation. These results emphasize the power of the model-driven approach for this particular application.

7.1 Training needs

We defined primary: residents in pediatrics, and secondary target audiences for neonatal ECG simulation with as the final goal a full-body training environment for neonatal resuscitation. Three main categories of learning objectives were identified and elaborated upon: 1. Recognition of normal and abnormal rhythms in the ECG, 2. Understanding underlying electrophysiology, and 3. Clinical decision making, therapeutic and diagnostic interventions. Concerning the rhythms, we focus on timely and accurate recognition of dynamic rhythm changes into potentially life threatening conditions. See Chapter 3 for further details on the training objectives.

7.2 Training program

In the context of this study, we outlined a training program consisting of introductory lessons followed by interactive computer based demonstrations. See Chapter 3 for further details on the training program requirements.

7.3 Developed software

We designed and programmed a screen-based demonstration tool - NEGRA – for the simulation of normal and abnormal neonatal cardiac rhythms in real time, Chapter 6. In presenting the results, we will follow the structure of the requirements in Chapter 3, and address trainee interface, instructor interface, and simulation engine. Fig. 7.1 shows a screen shot of NEGRA.

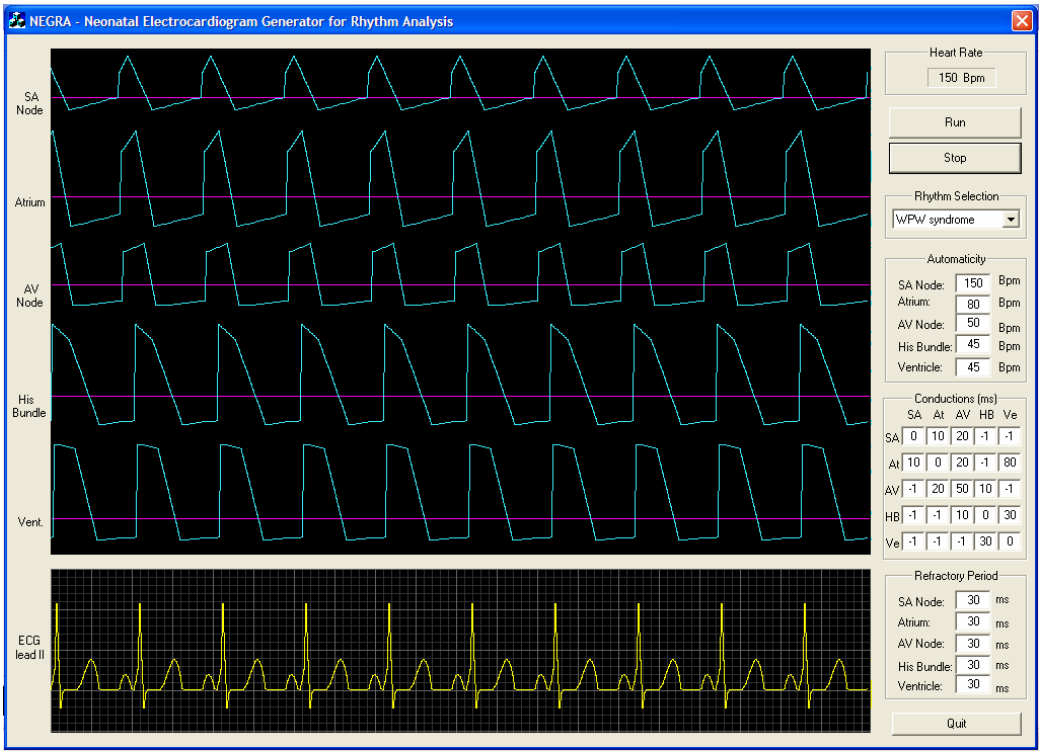

Figure 7.1 - *Screen shot of the NEGRA interface, including identification of Trainee and Instructor interfaces. In this case, a simulation of WPW syndrome is displayed..*

The Trainee Interface (TI) displays stylised real-time AP tracings at 5 different heart locations (SA node, atrium, AV node, bundle of His and ventricle) together with their threshold potentials and a standard lead II ECG tracing. The simulated ECG is displayed as an emulated stylised monitor, and drawn over on a standard grid, where each small square represents 40 ms in time (horizontal axis) and 0,1 mV in amplitude (vertical axis). A numerical value for the instantaneous heart rate is also part of the TI.

The Instructor Interface (II) allows for the selection of a pre-defined rhythm from a list. Each selection automatically sets pre-defined values for automaticity and refractory periods at all centres, and possible conductions and delays. Not all target rhythms presented in Table 3.1 were implemented. Not included in the present list are: atrial flutter, atrial fibrillation, ventricular fibrillation, atrioventricular dissociation, atrial, ventricular and P-wave-triggered pacemaker, and abnormal ventricular repolarisations (QT interval prolongation, long QT syndrome, ST segment depression/elevation).

When the simulation is not running (by controlling “Run” and “Stop” buttons), the instructor can manipulate automaticities, refractory periods, and conductions and delays.

The simulation engine (SE) consist of our proposed model for selected aspects of neonatal electrophysiology, Chapter 6, and has the capability of generating AP and ECG signals corresponding to a subset of the rhythms in Table 3.1. Rhythms reflect

underlying physiology, which can be manipulated by altering model parameters with a physiological interpretation available on the instructor interface. The model can generate abrupt transitions in waveforms and can be further developed to react to therapeutic interventions. Although the model has the capability to reflect gradual transitions in parameter values and resulting waveforms, this feature is not yet used in the present simulator. To make this possible, a state machine should be added to the simulation engine; this was beyond the time-frame of the present study. In the next section we will focus on the simulation results of the physiologic model underlying the simulation engine.

7.4 Physiologic model simulation results

7.4.1 Real vs. simulated ECG wave forms

A simulated ECG is always an approximation of a real ECG. Fig. 7.2 shows a side by side comparison of samples of real ECG and simulated ECG, generated by NEGRA.

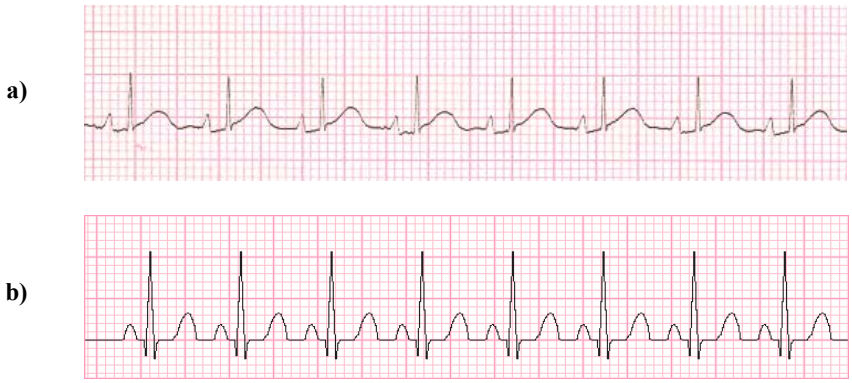

Figure 7.2 – *Real (a) and simulated (b) standard lead II ECGs for a normal sinus rhythm in a 3 weeks-old neonate, HR=150bpm.*

- Wave form amplitudes and time intervals, although visibly different, are within the limits specified in Table 3.2.
- Delimitation of the T-wave, necessary to establish the length of the ST-segment, is more difficult in the real ECG. We also note the absence of Q-waves on Fig. 7.2(a).
- The real ECG presents depressions and elevations on the ST segment, PR interval, and isoelectric region, which were not modelled in the presented approach. Wave segments are not completely distinct from baseline and there seems to be a low-frequency variation in amplitudes.
- The simulated ECG does not contain measurement noise. Even though the real ECG does not contain much noise either, it should be noted that it is common to find noisy ECGs in the neonatal context [Park, 1992].

We will elaborate on these observations in the discussion – Chapter 8.

7.4.2 Simulated rhythms

In Chapter 6 we described the strategy for the generation of target rhythms, and presented the selected parameters values. In this section we present simulated lead II ECG tracings and relevant portions of AP tracings on a rhythm per rhytm basis. All figures are screen shots of the NEGRA software. *Ladder diagrams* [Fukushima, 1984] indicating conduction sequences, are superimposed on these images.

Sinus rhythms

Normal sinus rhythm (NSR)

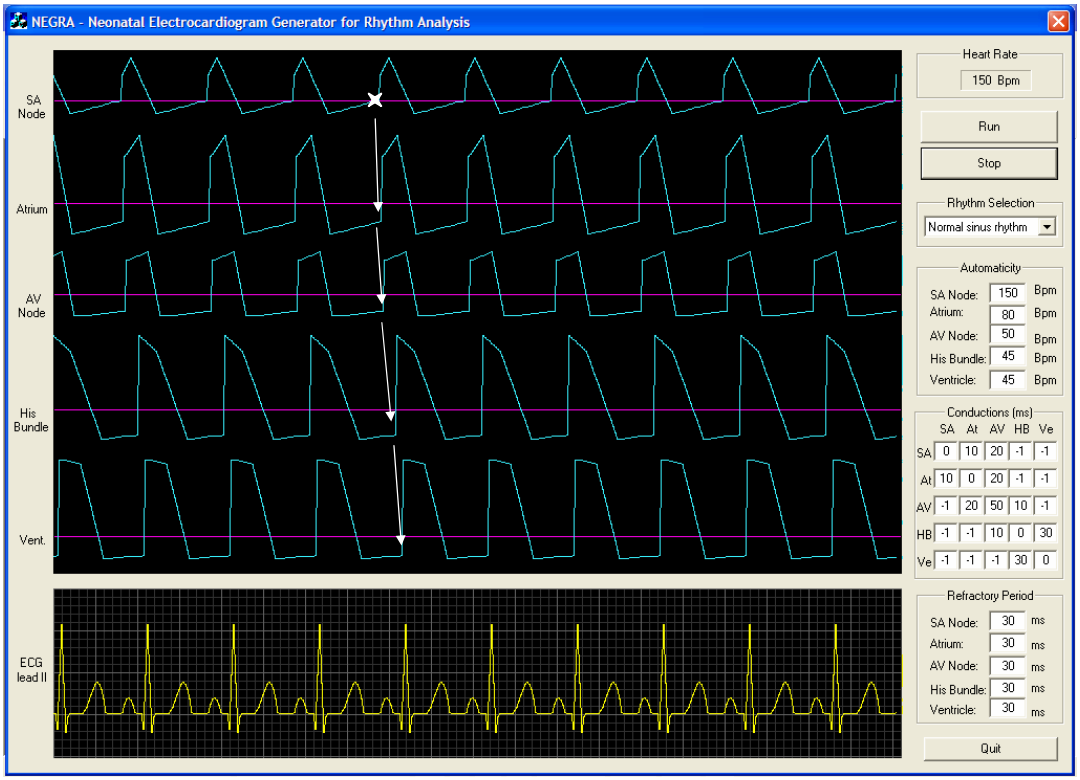

Figure 7.3 - *Screen shot of NEGRA for the simulation of normal sinus rhythm with HR=150 bpm*

In NSR, the SA node always depolarises when the threshold level is reached. Other centres depolarise due to impulse propagation from the SA node to the atrium and from there on to the AV node, bundle of His, and ventricles. Retrograde conductions do not originate in any depolarisations, because they always occur during the refractory period of the "upstream" centre. The templates for P-wave and QRS-complex output reflect normal antegrade conductions to the atria and ventricles, respectively.

Sinus tachycardia

In sinus tachycardia (200 bpm), the same conduction mechanism as in NSR is present and the same templates are displayed. The autonomic nervous system has only influence on the SA node rate, and not on the conduction times, which are maintained. The higher rate shortens the isoelectric interval between the T-wave and the following P-wave, and the ST segment. The PR interval, depending only on the AV nodal delay, remains constant.

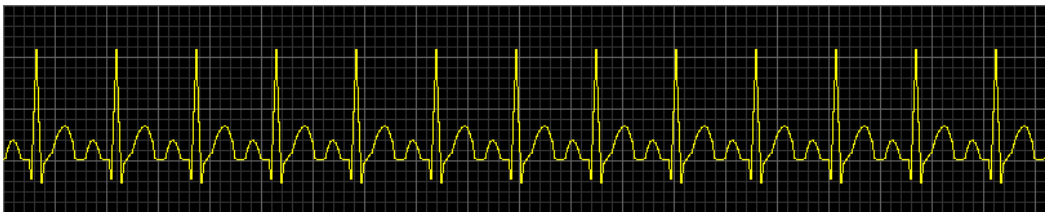

Figure 7.4 – *ECG tracing obtained from NEGRA for simulation of sinus tachycardia, HR=200 bpm.*

Sinus bradycardia

In sinus bradycardia (85 bpm) the conduction mechanism and templates are still the same. Similarly, the PR interval remains constant, and the isoelectric interval and ST-segment are augmented as compared to NSR.

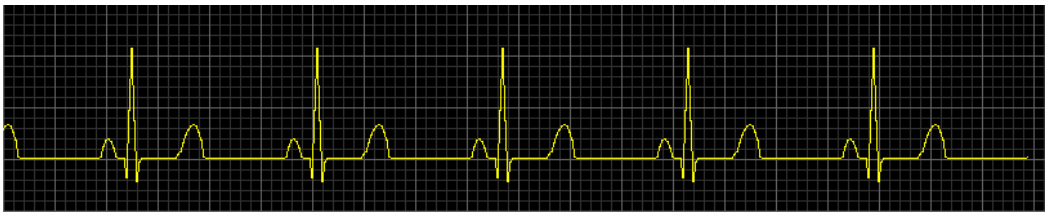

Figure 7.5 – *ECG tracing obtained from NEGRA for simulation of sinus bradycardia, HR=85 bpm.*

Sinus pause

Sinus pause, Fig. 7.6, reflects a momentary sinus failure in which the SA node does not send an electrical impulse. An atrial escape beat results, because this is the structure with the highest intrinsic rate or automaticity. After retrograde conduction and depolarisation, the SA node recovers its primary pacing role.

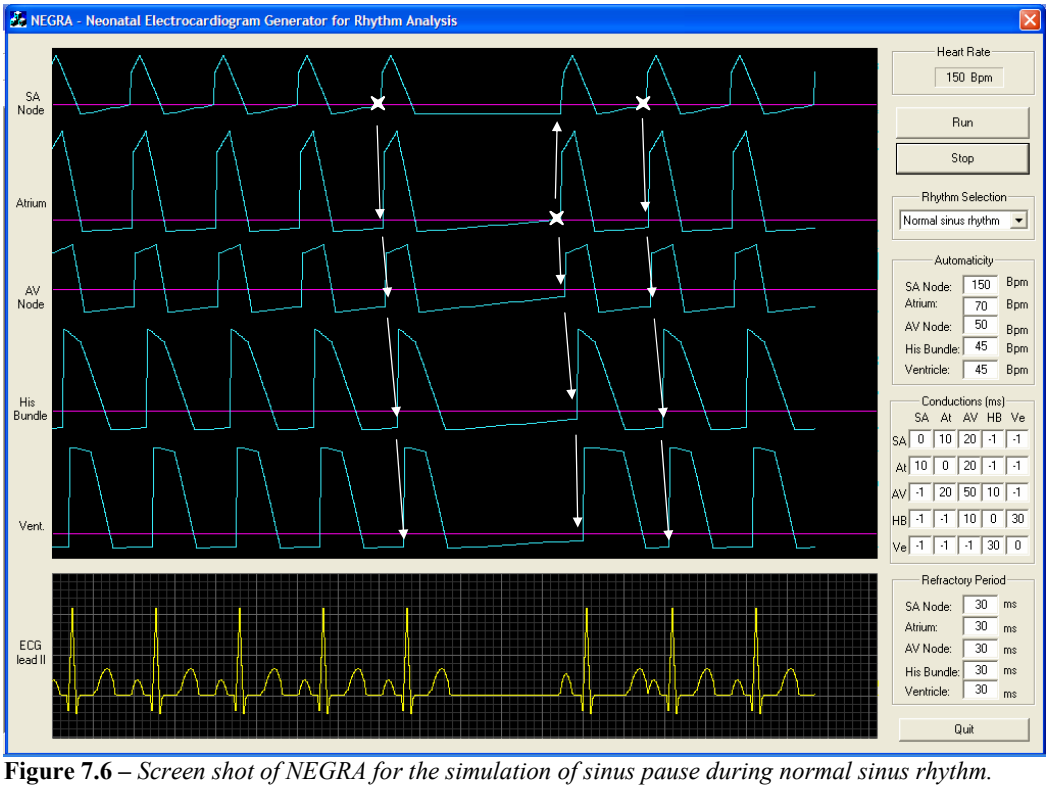

Figure 7.6 – *Screen shot of NEGRA for the simulation of sinus pause during normal sinus rhythm.*

Sinus arrest

With electrically isolated and inactive SA node and low atrial automaticity, the AV node becomes the primary pacemaker, sending antegrade impulses to the bundle of His ventricles, and retrograde impulses to the atria. A normal QRS-complex, but

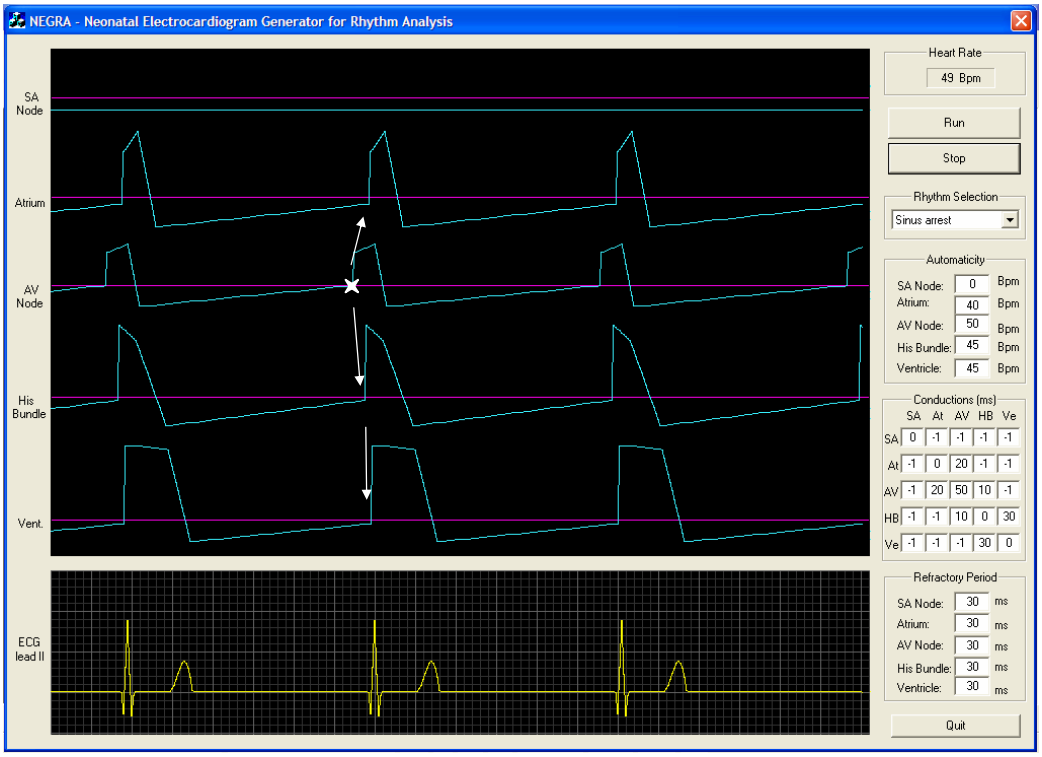

Figure 7.7 – *Screen shot of NEGRA for the simulation of sinus arrest with HR=50 bpm.*

inverted P-wave templates are presented at the output. Note that in Fig 7.7 the inverted P-waves are masked by the overlapping QRS-complexes.

By increasing the retrograde conduction time from AV node to atria, the inverted P-wave becomes visible, Fig. 7.8.

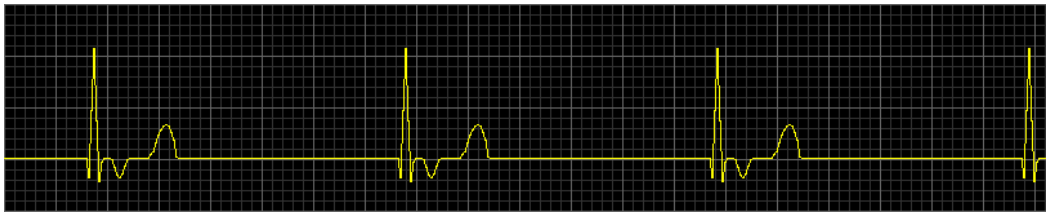

Figure 7.8 – *ECG tracing obtained from NEGRA for simulation of sinus arrest with augmented retroagrade conduction from AV node to atria.*

Atrial, nodal and ventricular disrhythmias

Atrial tachycardia

In atrial tachycardia, the highest atrial automaticity originates taller P-waves due to the use of the adequate template for the autonomic atrial depolarisation. The HR is set by the atrium automaticity and the ventricle is depolarised by antegrade conduction, producing normal QRS-complexes. The isoelectric region and ST-segment are almost inexistent.

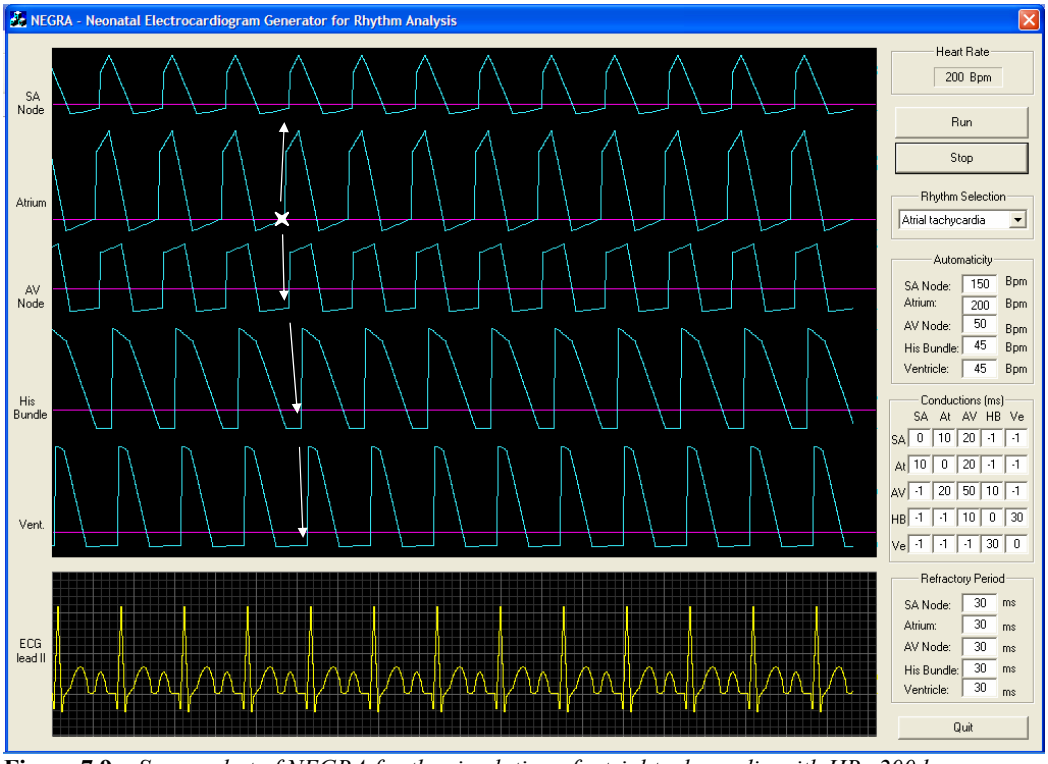

Figure 7.9 – *Screen shot of NEGRA for the simulation of atrial tachycardia with HR=200 bpm.*

Nodal tachycardia

The mechanism for this disrhythmia is similar to the one for atrial tachycardia. However, in this case the rhythm is paced by the AV node, due to its abnormally high automaticity. Consequently, retrograde P-waves and antegrade QRS-complexes are superimposed on the ECG.

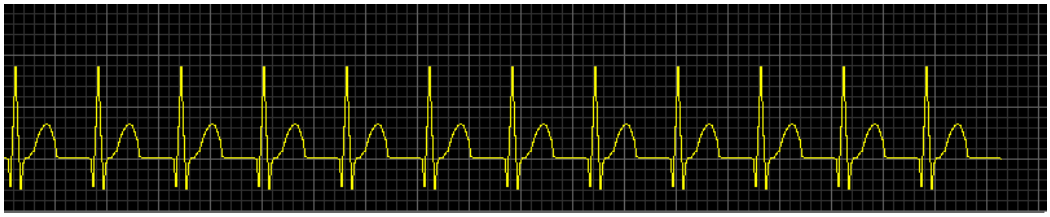

Figure 7.10 – *ECG tracing obtained from NEGRA for simulation of nodal tachycardia, HR=190 bpm*

Ventricular tachycardia

During ventricular tachycardia, the rhythm is paced by the ventricles with a high intrinsic rate. Abnormally wide QRS-complexes are presented and all the other centers are depolarised by retrograde conduction. The apparently bizarre T-waves are the result of simultaneous output of inverted P-waves from atrial depolarisation.

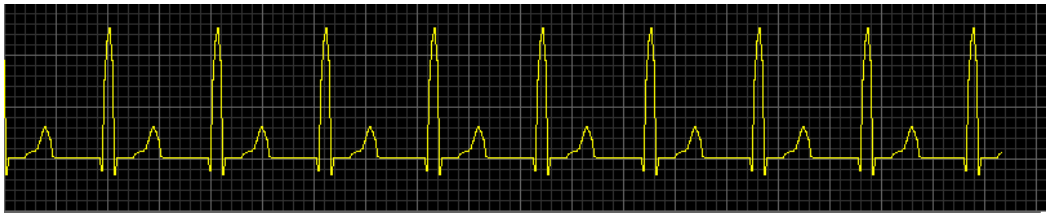

Figure 7.11 – *ECG tracing obtained from NEGRA for simulation of ventricular tachycardia, HR=150bpm.*

PVC – premature ventricular contractions

The analysis of the ventricular AP tracing shows the origin of the PVCs (Fig.7.11). Suddenly, the ventricular automaticity increases and the ventricle depolarises autonomously before the sinus impulse has arrived through the AV node. On the ECG, this is reflected by an abnormally wide and tall QRS-complex and the absence of a PR interval.

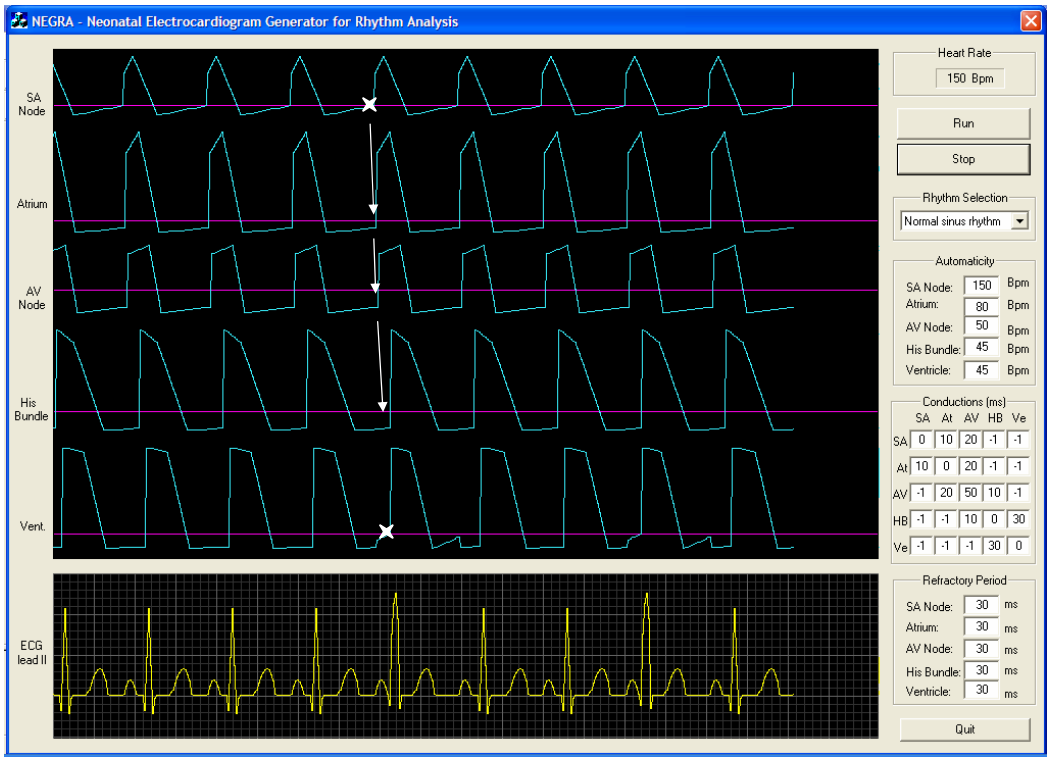

Figure 7.12 – *Screen shot of NEGRA for the simulation of normal sinus rhythm with occasional premature ventricular contractions.*

Conduction disturbances

First degree AV block

The simulated 1st degree AV block presents the commonly diagnosed features: augmented PR-interval due to an augmented delay on the AV node. In case of very long PR intervals, Fig 7.13, we observe atrial depolarisation before the end of the previous ventricular repolarisation.

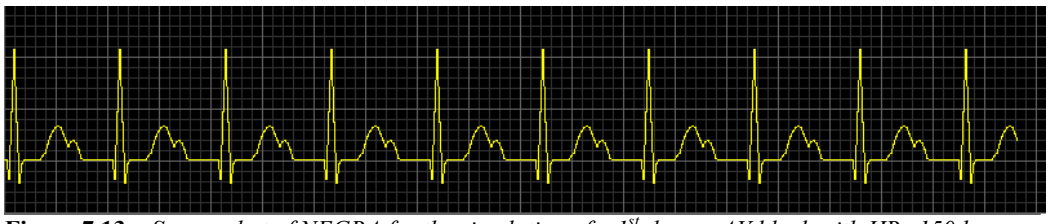

Figure 7.13 – *Screen shot of NEGRA for the simulation of a 1st degree AV block with HR=150 bpm*

Second degree AV block (2:1)

In Fig. 7.14 the sinus node paces at such a high rhythm that it cannot be followed by the AV node. Thus, in every two antegrade impulses reaching the AV node, the second one always falls within the nodal refractory period. The result is a ventricular rate of half of the atrial rate and two P-waves per QRS-complex in the ECG. In this particular case, there is a regular overlap of one out of two P-waves with T-waves.

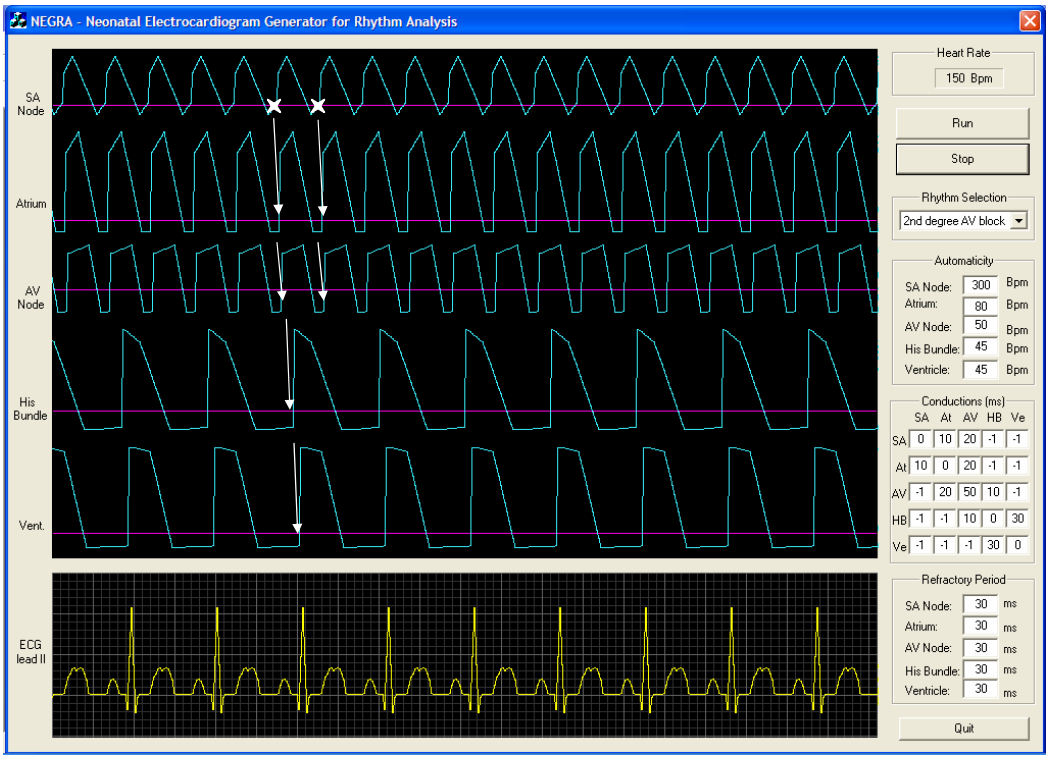

Figure 7.14 – *Screen shot of NEGRA for the simulation of a 2:1 AV block, resultant from high sinus tachycardia (sinus rate = 300 bpm, ventricular rate = 150 bpm).*

Complete AV block

Complete AV block as shown in Fig. 7.15 presents two completely independent electrical activities: one paced by the SA node at 150 bpm and one by the AV node at 60 bpm. Although there are two pacemakers, the HR is still given by the ventricular rate, calculated from the inverse of RR intervals. In the ECG, atrial activity is represented by regular antegrade P-waves, and ventricular activity by regular abnormal QRS-complexes from autonomic depolarisation.

Reentry

SVT - Accessory reciprocating AV tachycardia

The inverted P-waves are indicative of retrograde atrial excitation from the accessory pathway, see the dotted arrow in Fig. 7.16. In this case, they occur after ventricula r repolarisation, with long PR intervals (actually short RP intervals). Normal QRS-complexes result from normal antegrade conduction through the AV node.

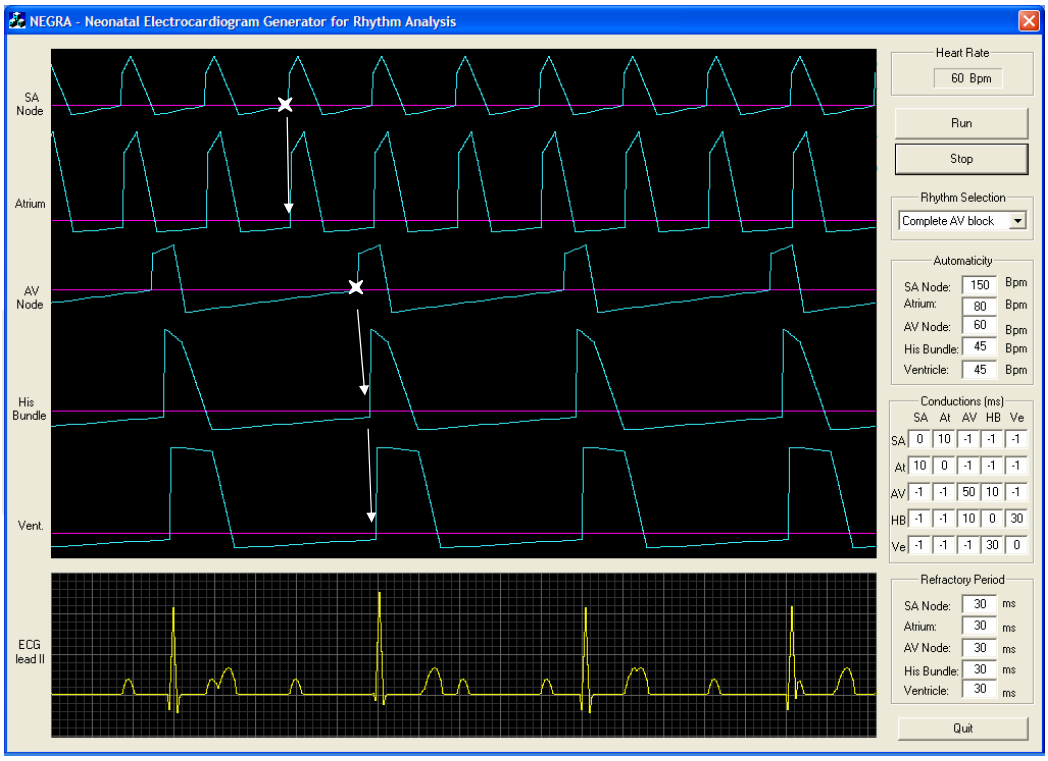

Figure 7.15 – *Screen shot of NEGRA for the simulation of a complete AV block with HR=60 bpm*

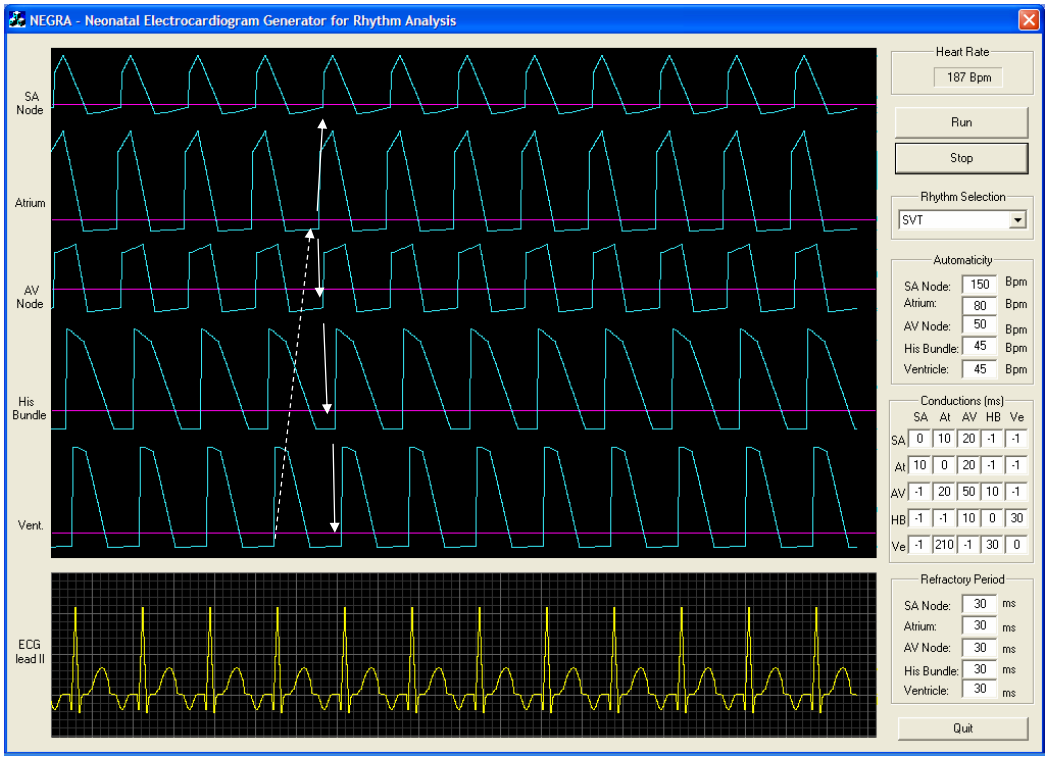

Figure 7.16 – *Screen shot of NEGRA for the simulation of a SVT – reciprocating AV tachycardia with HR=187 bpm*

WPW – Wolff-Parkinson-White syndrome

The ECG in Fig. 7.17 shows a normal sinus rhythm with typical "delta waves" at the beginning of the QRS-complex, also see Chapter 2, and absence of PR intervals. This was implemented using a single template for direct conduction between atria and ventricles, representing the early ventricular depolarisation.

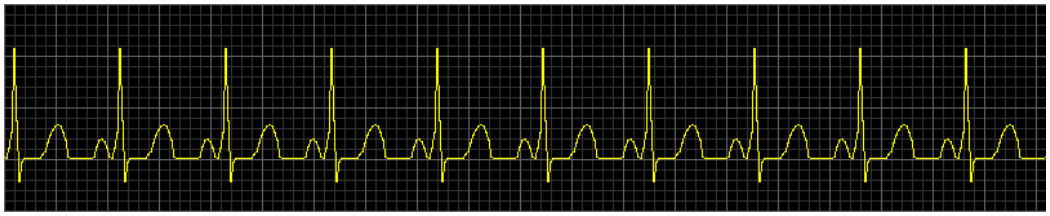

Figure 7.17 – *ECG tracing obtained from NEGRA for simulation of a WPW syndrome, HR=150 bpm*

Chapter 8

Discussion

In this section, we return to Chapters 3 and 7 to discuss to what extent the presented results meet the requirements resulting from the TNA-TPD-TMS process. We also provide some suggestions for future extension of the presented training program and simulator.

8.1 Training needs

Training program, physiologic model, and simulation software were designed to meet all three categories of training objectives: 1. recognition of normal and abnormal rhythms in the ECG, 2. understanding underlying electrophysiology, 3. clinical decision making, therapeutic and diagnostic interventions, for the primary target audience: residents in pediatrics. Mainly because of time constraints, the software implementation does not allow meeting all these objectives yet. However, in our opinion, secondary target audiences could already benefit from the capabilities addressing the second category of learning objectives.

8.2 Training program

The outlined training program, Chapter 3, refers to a screen-based tool for demonstrations by an instructor. Continued development could include TPD for more interactive and/or immersive environments.

8.3 Developed software

The developed NEGRA software meets many, but not all, specified requirements for a screen-based model-driven application. The main goal of this work was to provide a practical example of the application of the systematic approach to specification of simulators, presented by Farmer et al. [Farmer, 1999], in the acute care context. Priority was given to complete this process from start to finish, rather than being all inclusive in terms of rhythms, leads, etc.

The developed Trainee Interface includes practically all required information. The current software and underlying model only simulate one lead in the frontal plane, but can easily be expanded by using adequate wave form templates. Simulation of precordial leads could possibly be accomplished with the same methodology, but further investigation is required.

The developed Instructor Interface does not allow for the selection of all proposed target rhythms; the reasons are further explained in section 8.4.2. Manipulation of physiologic parameters at five locations in the heart is relatively simple, and meets the requirements for the generation of separate rhythms. This interface could be extended with control over a state machine for automatic simulation of gradual changes and abrupt transitions.

The performance and flexibility of the model-driven Simulation Engine are demonstrated by the results presented in section 7.3. Automatic evolution of rhythms and wave forms, possibly in response to therapeutic interventions, can be accomplished by coupling to a state machine, as alluded to above. Coupling to other physiologic models would extend such capabilities even further. Noteworthy limitations of the current simulation engine include that changes in wave shape are limited by discrete templates, only lead II is simulated, also see comments on TI, and action potential wave forms are rough approximations. A number of detailed critical observations on the model and simulation results are included below.

8.4 Model simulation results

A number of observations concerning the wave forms in Fig. 7.2 also hold for most other simulated ECGs. We can easily distinguish the simulated from the real ECG. It may be possible to adapt or design models that generate ECGs that cannot be distinguished from real tracings. For the present application, focussing on identification of rhythms and the association to (simplified) underlying physiology, the likely complexity of such a model may represent prohibitively high costs in terms of time for model development and for manipulation of parameter values to represent other rhythms or situations. How much realism is necessary for "suspense of disbelieve" in a full-scale environment is still an open question [van Meurs, personal communication, 2005]. Specific examples include:

- "The real ECG presents depressions and elevations on the ST segment, PR interval, and isoelectric region, which were not modelled in the presented approach. Wave segments are not completely distinct from baseline and there seems to be a low-frequency variation in amplitudes," Chapter 7. Decisions on which elements to incorporate will have to result from a balanced consideration of medical educational, physiologic modelling, and software engineering arguments. One way to accomplish this would be "another round" in the TNA-TPD-TMS cycle.
- The inclusion of baseline variation and measurement noise could also improve the realism of the simulated ECG. However, they were not considered a major priority in a rhythm simulator for medical education; the presence of measurement noise could even interfere with the identification of ECG waves and their relationship with underlying APs.

Less obvious delimitation of simulated T-waves may be achieved by using different templates. The absence of a perceptible Q-wave in the standard lead II of Fig. 7.2a is confirmed in many examples [Park, 1992]. However, Tipple et al. [Tipple, 1999] show that "complete" QRS-complexes are quite common in Lead II. For educational reasons we choose the option with "classic" complete QRS-T complexes.

Not all target rhythms listed in Chapter 3, were implemented. Atrial flutter would demand the use of new templates for generating F-waves with a typical "sawtooth" configuration. Atrial and ventricular fibrillation are irregular rhythms and hence demand the generation of continuous rhythm transitions with variable configuration of ECG waves. In atrioventricular dissociation an occasional atrial impulses may be conducted via the AV node. Simulation of such rhythm disturbances requires continuous variation of impulse formation and conduction, possibly via a state machine. Pacemaker rhythms demand the use of new templates reflecting artificial depolarisation. The current model has no capabilities for simulating abnormal ventricular repolarisations and associated ST-segment changes. Extension to include these phenomena is straight forward. In appendix III we list a number of supplementary critical observations on a rhythm-per-rhythm basis.

Chapter 9

Conclusions

- Like other areas of acute care medicine, neonatal resuscitation could benefit from realistic full-body, model-driven educational simulation.

- A model for educational simulation of the neonatal electrocardiogram (ECG) is an important component of such a simulator. To our knowledge no such model, or model-driven simulator, is currently described in the scientific literature or commercially available.

- A rigorous methodology for the design of military educational simulations, consisting of subsequent training needs analysis (TNA), training program design (TPD), and training media specification (TMS), was described. After a brief review of neonatal electrophysiology, we applied this methodology to the design of a screen-based, model-driven simulator for the neonatal ECG. This work led to the following presentation and publication: *Pinto JR, van Meurs WL, de Beer NAM, Andriessen P: Systematic approach to specification of acute care training programs, simulators, and physiologic models - neonatal electrophysiology example*, Proceedings of the 10th annual meeting of the Society in Europe for Simulation Applied to Medicine (SESAM), Stockholm, Sweden, June 17-19, 2004, p21.

- TNA resulted in three main categories of learning objectives: 1. Recognition of normal and abnormal rhythms in the ECG, with a focus on timely and accurate recognition of dynamic rhythm changes into potentially life threatening conditions, 2. Understanding underlying electrophysiology, 3. Clinical decision making concerning therapeutic and diagnostic interventions. In the context of this study, the envisioned training program is limited to introductory lessons and interactive computer based demonstrations by an instructor in a classroom setting. Specifications for trainee and instructor interfaces and for a model-driven simulation engine were derived as part of the TMS.

- After a detailed review of the literature, we classified models for ECG generation into: Single analog wave form generators, 2D heart models, and 3D heart and thorax models. The 2D heart model by Fukushima et al. [Fukushima, 1984] for the adult came closest to meeting the model requirements derived as part of the TMS, and was selected as a basis for further elaboration.

- We expanded the Fukushima model with a more flexible structure for representing cardiac conduction and delays, derived parameters and ECG wave form templates for the neonate, and filled in several blanks left by Fukushima et al..

- We designed, implemented, and tested a screen-based, model-driven simulator: Neonatal Electrocardiogram Generator for Rhythm Analysis (NEGRA), which displays action potentials in a number of cardiac structures and a corresponding lead II ECG for a number of rhythms in real-time, and which allows for manipulation of a number of physiologic parameters.

- The simulation results emphasize the power of a model-driven approach for the generation of a large variety of cardiac rhythms and associated action potentials and ECG time signals.

- Simultaneous display of action potentials and corresponding ECG time signal greatly improved the "mental model" of impulse conduction through the heart and its relationship with surface electrocardiograms of the author and supervisors, and is expected to do the same for trainees.

- The developed model forms an essential component of a neonatal acute care simulator. It would gain in versatility if expanded into a 3D configuration and combined with a neonatal torso model.

- The software can be developed further into a practical screen-based application. Addition of a state machine providing gradual rhythm transitions and inclusion of more ECG leads are necessary steps.

- The adapted and followed design methodology is a foundation for further work on all educational acute care simulators.

References

[1] Ahlfeldt H, Tanaka H, Nygards M-E, Furukawa T and Wigertz O: "Computer simulation of cardiac arrhythmias", *Comput Biomed Res.*, vol. 20(4), pp. 305-23, 1987.

[2] Andriessen P, Koolen AMP, Bastin FH, Lafeber HN and Meijler FL: "Supraventricular escape rhythms during transient episodes of bradycardia in preterm infants", *Cardiology in the Young*, vol. 11, pp. 626-31, 2001.

[3] Avery GB, Fletcher MA and McDonald MG: *Neonatology - Pathophysiology & Management of the Newborn*, 5th Edition, Philadelphia: Lippincott Williams & Wilkins, 1999.

[4] Bell C and Kain ZN: *The pediatric anesthesia handbook*, 2nd edition, St. Louis: Mosby Year Book, 1997.

[5] Berenfeld O and Abboud S: "Simulation of cardiac activity and the ECG using a heart model with a reaction-diffusion action potential", *Med. Eng. Phys.*, vol. 18(8), pp. 615-625, 1996.

[6] Burke MJ and Nasor M: "An accurate programmable ECG simulator", *Journal of Medical Engineering & Technology*, vol. 25(3), pp. 97-102, 2001.

[7] Charand KX: *Action potentials*, Department of physics and astronomy - Georgia State University, Atlanta, USA, 2001. http://hyperphysics.phy-astr.gsu.edu/hbase/biology/actpot.html

[8] Clayton RH and Holden AV: "Simulating the ECG of Ventricular Tachyarrhythmias", *IEEE Computers in Cardiology*, vol. 29, pp. 321-24, 2002.

[9] Couto CS: "A model for educational simulation of neonatal cardiovascular physiology", [MSc thesis on Biomedical Engineering]. University of Porto College of Engineering, 2002.

[10] Davignon A, Rautaharju P, Boiselle E, Soumis F, Megelas M and Choquette A: "Normal ECG standards for infants and children", *Pediatric Cardiology*, vol. 1, pp. 123-52, 1979.

[11] Farmer E, Rooij JV, Riemersma J, Jorna P and Moraal J: *Handbook of Simulator-Based Training*, Aldershot: Ashgate, 1999.

[12] Fukushima M, Inoue M, Fukunami M, Ishikawa K, Inada H and Abe H: "Computer-Assisted Education System for Arrhythmia (CAESAR)", *Computers and Biomedical Research*, vol. 17, pp. 376-388, 1984.

[13] Guyton AC: *Textbook of medical physiology*, 8th Edition, Philadelphia: W.B. Saunders Company, 1991.

[14] Halamek LP, Kaegi DM, Gaba DM, Sowb YA, Smith BC, Smith BE and Howard SK: "Time for a new paradigm in pediatric medical education: teaching neonatal resuscitation in a simulated delivery room environment." *Pediatrics*, vol. 106(4), pp. E45, 2000.

[15] Hernandez AI, Carrault G, Mora F and Bardou A: "Overview of CARMEN: a new dynamic quantitative cardiac model for ECG monitoring and its adaptation to observed signals", in *Acta Biotheoretica*, vol. 48, The Netherlands, 2000.

[16] Howlett PJ and Pearson SA: "Simple e.c.g. arrhythmia simulator." *Med Biol Eng Comput.*, vol. 16(2), pp. 217-8, 1978.

[17] Hsiao CH and Kao T: "Constructing a 3-D Mesh Model for Electrical Cardiac Activity Simulation", *Computers and Biomedical Research*, vol. 33, pp. 23-42, 2000.

[18] Kimball JW: *Kimball's Biology Pages*, 2004. http://users.rcn.com/jkimball.ma.ultranet/BiologyPages/E/ExcitableCells.html

[19] Klaus MH and Fanaroff AA: *Care of the High-Risk Neonate*, 5th Edition, Philadelphia: W. B. Saunders Company, 2001.

[20] Levin AR, Haft JI, Engle MA, Ehlers KH and Klein AA: "Intracardiac conduction intervals in children with congenital heart disease: comparison of His bundle studies in 41 normal children and 307 patients with congenital cardiac defects." *Circulation*, vol. 55(2), pp. 286-94, 1977.

[21] Lu W: "Microcomputer-based cardiac field simulation model", *Med Biol Eng Comput.*, 1993.

[22] MacLeod R: *Electrocardiography*, Notes for Bioengineering, 2004. http://www.cvrti.utah.edu/~macleod/bioen/be6010/notes/electro-ecg-color.pdf

[23] Malik: "Computer Simulation of Cardiac Rhythm and Artificial Pacemakers Using a Ten-Element Heart Model", *Comput. Biomed. Res.*, vol. 19, pp. 237-53., 1986.

[24] Matthews GG: *Neurobiology: Molecules, Cells and Systems*, Blackwell Publishing, 2004. http://www.blackwellpublishing.com/matthews/actionp.html

[25] McSharry PE, Clifford GD, Tarassenko L and Smith LS: "A Dynamical Model for Generating Synthetic Electrocardiogram Signals", *IEEE Transactions on Biomedical Engineering*, vol. 50(3), 2003.

[26] Meurs WL van, Good ML and Lampotang S: "Functional anatomy of full-scale patient simulators", *Journal of Clinical Monitoring*, vol. 13, pp. 317-324, 1997.

[27] Miller WT and Geselowitz DB: "Simulation studies of the electrocardiogram. I. The normal heart", *Circulation Research*, vol. 43(2), pp. 301-15, 1978.

[28] Miller WT and Geselowitz DB: "Simulation studies of the electrocardiogram. II. Ischemia and infarction", *Circulation Research*, vol. 43(2), pp. 315-23, 1978.

[29] Nowotny R: "Simple e.c.g. simulation by pulse-shaping techniques", *Medical and Biological Engineering*, 1976.

[30] Park MK and Guntheroth WG: *How to read pediatric ECGs*, 3rd Edition, St Louis: Mosby-Year Book, 1992.

[31] Pickoff AS: "Developmental electrophysiology in the fetus and neonate", in *Fetal and neonatal physiology*, vol. 1, 2nd ed. Philadelphia: W.B. Saunders Company, 1998, pp. 892.

[32] Rijnbeek PR, Witsenburg M, Schrama E, Hess J and Kors JA: "New normal limits for the pediatric electrocardiogram", *European Heart Journal*, vol. 22, pp. 702-711, 2001.

[33] Schwartz PJ, Garson A, Paul T, Stramba-Badiale M, Vetter VL, Villain E and Wren C: "Guidelines for the interpretation of the neonatal electrocardiogram. A Task Force of the European Society of Cardiology", *European Heart Journal*, vol. 23, pp. 1329-1344, 2002.

[34] Schwid HA: "Electrocardiogram Simulation Using a Personal Computer", *Comput-Biomed. Res.*, vol. 21(6), pp. 562-569, 1988.

[35] Schwid HA: "A flight simulator for general anesthesia training", *Comput-Biomed. Res.*, vol. 20(1), pp. 64-75, 1987.

[36] Sheidt S: *Basic Electrocardiography*, 5th Edition, USA: Novartis, 2000.

[37] Siregar P, Sinteff JP, Julen N and Beux P Le: "An Interactive 3D Anisotropic Cellular Automata Model of the Heart", *Computers and Biomedical Research*, vol. 31, pp. 323-47, 1998.

[38] Stat: *Heart and stroke statistical update*, American heart association, 2002. http://www.americanheart.org

[39] Stedman TL: *Stedman's concise medical dictionary*, 3rd edition, Philadelphia: Williams and Wilkins Company, 1997.

[40] Takeuchi A, Ikeda N, Nara Y, Miyahara H and Mitobe H: "WinArrhythmia: a Windows based application for studying cardiac arrhythmias", *Computer Metods and Programs in Biomedicine*, vol. 55, pp. 199-206, 1998.

[41] Tipple M: "Interpretation of electrocardiograms in infants and children", *Images in Paediatric Cardiology*, vol. 1, pp. 1-13, 1999.

[42] Weixue L and Ling X: "Computer simulation of epicardial potentials using a heart-torso model with realistic geometry", *IEEE Transactions on Biomedical Engineering*, vol. 43(2), pp. 211-17, 1996.

Appendix I

Basic electrophysiology and electrocardiography

I.1 Electrical activity at cellular level

The human body has the capacity of generating electrical activity at the cellular level. Electrical potentials exist across the membranes of almost all cells of the body, namely the nervous cells. The basic nervous cells - neurons - are "excitable", which means that they can self-generate electrochemical impulses at their membranes and transmit/receive those impulses to/from neighboring cells (Fig. AI.1).

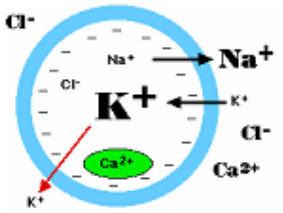

Figure AI.1 – *Cellular membrane diffusion [Kimball, 2004]*

Chemicals in the body are called ions when they have an electrical charge. The most important ions in the nervous system are Sodium (Na) and Potassium (K), both having one positive charge (+); Calcium (Ca), having two positive charges (++); and Chloride (Cl), having one negative charge (-).

All the nervous cells are surrounded for a semi-permeable membrane that blocks the passage of some ions and allows some other to pass through. This selective property of the membrane, together with the variation of the concentrations of the mentioned ions is the phenomena underlying the generation of electrical potential at the membrane.

I.1.1 The nerve resting membrane potential

A neuron is "at rest" when its inside is negative relative to the outside and is not sending an electrical signal. Although the concentrations of the different ions attempt to balance out on both sides of the membrane, they cannot because the cell membrane allows only some ions to cross through channels (ion channels).

At rest, (K^+) ions can easily cross through the membrane, and ions (Cl^-), (Na^+) have a more difficult crossing. In addition to these selective ion channels, there is a pump - the sodium-potassium pump (Fig. AI.1) - which uses energy to move three (Na^+) ions out of the neuron for every two (K^+) ions it puts in.

When all these forces balance out and the difference in the voltage between the inside and outside of the neuron is detectable, the resting potential is generated. The resting membrane potential of a neuron is about -90 mV in the most part of nervous human cells [Guyton, 1991], which means that the inside of the neuron is 90 mV less than the outside. At rest, there are relatively more sodium ions outside the neuron and more potassium ions inside that neuron.

I.1.2 - The nerve action membrane potential

Nerve signals are transmitted by action potentials, which are rapid changes in the membrane potential. Whereas the resting potential refers to what happens when a

neuron is at rest, an action potential occurs when a neuron sends information along the nerve fibre until it comes to its end. Each action potential begins with a sudden change from the normal resting negative potential to a positive membrane potential and than ends with an almost equally rapid change back again to the negative potential.

The successive stages of the action potential are shown on Fig. AI.2, including three main phases:

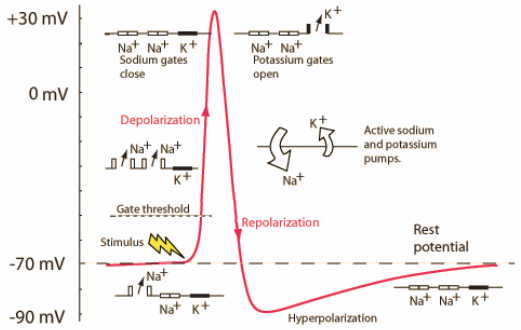

Figure AI.2 - *Example of a modelled action potential of a human nerve cell, with nominal resting potential of –70 mV [Charand, 2001].*

Depolarisation:

Suddenly, the membrane becomes very permeable to ions Na^+, allowing a strong flow of these ions from the outside to the inside. The normal "negatively polarized" state is lost and the potential rapidly rises in the positive direction. If it exceeds the threshold potential, it triggers a new depolarisation**.** Depending on the size of the nerve fibres, the membrane potential may "overshoot" beyond the zero level and becomes positive (large fibres) or just to approach the zero level and not overshooting the positive state (small fibres).

Repolarisation:

After the membrane becomes highly permeable to sodium ions, the sodium channels begin to close, and the potassium channels open more than the normal. Then, a rapid diffusion of potassium ions to the exterior re-establishes the normal negative resting membrane potential.

By the end of repolarisation, the resting potential may be overshoot. It would seem to be counterproductive, but it actually prevents the neuron from receiving another stimulus during this time, or at least raises the threshold for any new stimulus, ensuring that the signal is only proceeding in one direction. Then, the Na^+/K^+ pumps eventually bring the membrane back to its resting potential.

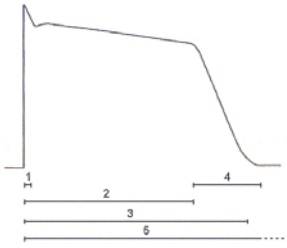

Figure A1.3 – *An action potential with the following periods demonstrated: 1-depolarisation, 2-absolute refractory, 3-total refractory, 4-repolarisation, 5-automaticity cycle length [Ahlfeldt, 1987].*

Refractory period:

All the excitable tissues (including the cardiac muscle) are refractory to restimulation during their action potentials. The refractory period is the time interval where normal impulses can not stimulate an already excited

area of the muscle. The *absolute refractory period* covers practically all the action potential duration, whereas the *relative refractory period* is an additional period where stimulations are only hardly allowed.

I.1.3 Propagation of the action potential

An action potential occurred at any point of a membrane usually excites adjacent points of the membrane, thus resulting in the propagation of the action potential. This mechanism is illustrated in Fig. AI.4, starting from a normal resting nerve fibre:

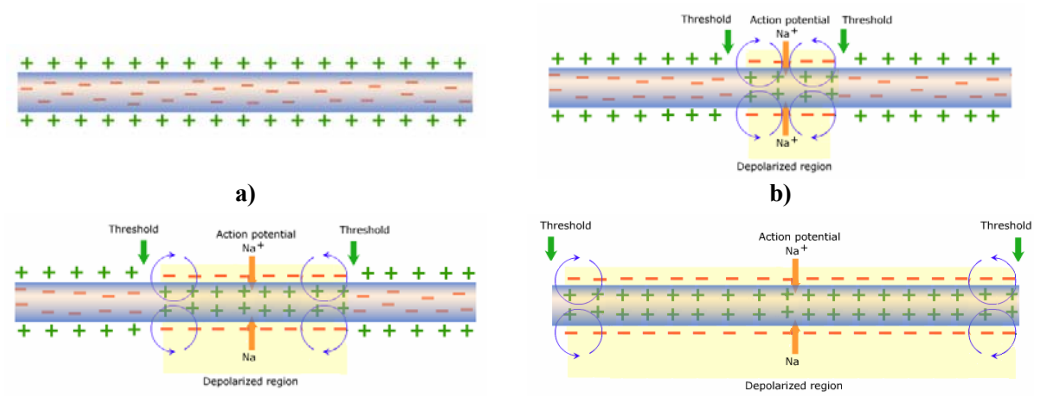

Figure A1.4 - *Propagation of an action potential through a nerve fibre portion. a) fibre portion at normal resting state; b) excitation of the fibre at its midpoint; c) excitation of the "neighbourhood"; d) fibre portion totally depolarised [Matthews, 2004].*

Assume that the nerve fibre gets excited in its midportion. The arrows illustrate a "local circuit" of current flowing between the depolarised areas and the adjacent resting membrane areas. Positive electrical charges carried by the inward (Na^+) ions flow inward through the depolarised membrane. These positive charges increase the voltage to above the threshold value for initiating an action potential.

Consequently, the Sodium channels immediately activate in the new areas around. These new polarized areas cause more local current circuits of current flow still further along the membrane, thus creating further depolarisations.

Finally, the action potential spreads all over the fibre and the depolarisation process travels along the entire extent of the fibre. The following repolarisation will take place with the outflow of (K^+) ions. It will start in the same location of the earlier depolarisation and will spread along the fibre in analogous way.

I.1.4 The cardiac conduction system

Electrical potentials generated by the heart are a sum of individual amounts of electricity generated from single cardiac specialized nerve cells (producing individual action potentials). These cells are so joined that electrical activity can easily spread from one cell to the next. There are specialized groups of cardiac cells designed to rapidly produce and transmit electrical activity through the heart: the sinoatrial (SA) node, the atrioventricular (AV) node, the bundle branches, the bundle of His and the Purkinje fibres. Fig. AI.5 shows the location of these groups of cells in the heart and their typical action potential waveforms.

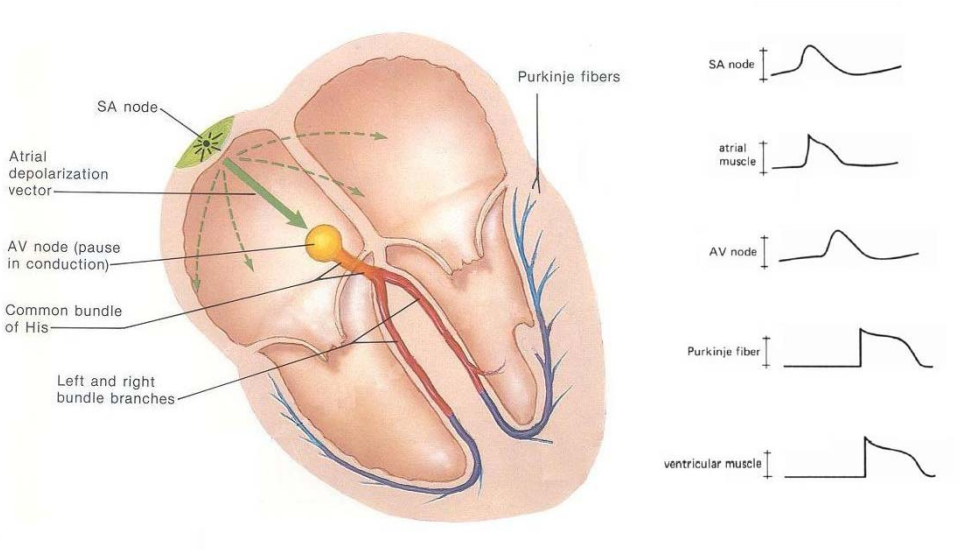

Figure AI.5 - *Anatomy of the adult cardiac conduction system and typical waveforms of action potential at specialized conduction cells [MacLeod, 2004, Sheidt, 2000].*

The SA node is very a small structure located at the junction of the superior vena cava and the upper right atrium. Under normal conditions, this is the area that depolarises more rapidly, although it is such a weak depolarisation that can not be detected on the body surface. Once the SA node is located at the superior right border of the heart, the spread of atrial activation is made generally downward and to the left (green arrows – Fig. AI.5). Since the atria have thin walls with little muscular mass, only relatively little electrical activity results from their depolarisation, but usually detectable on the body surface.

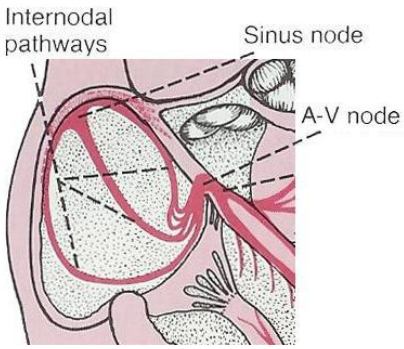

Figure AI.6 – *The simplified right upper part of the cardiac conduction system, including the internodal pathways between the SA node and the AV node [Guyton, 1991].*

Electrical impulses can be conducted to the AV node through the atria or "internodal pathways", connecting directly the SA node and AV node (Fig. AI.6). They consist of some specialized conduction fibbers along the atrial muscle. These fibbers are similar to the very rapidly conducting Purkinge fibbres, having more rapid velocity of conduction than the entire atrial muscle mass [Guyton, 1991].

The wave of depolarisation goes on until reaching the AV node, which provides the only electrical connection between the atria and the ventricles. The AV node is such a small and thin structure that allows only a small amount of electrical activity to pass through, causing a delay on the electrical conduction to the lower part of the heart. Its electrical activity is considerably weak and can not be detected on the body surface.

From the AV node, the depolarisation wave is conducted along the bundle of His and then to the ventricles. Normally, the first part of the ventricular myocardium being depolarised is the interventricular septum, from left to right, and downwards - Fig. AI.7b). Depolarisation then spreads along the ventricular conduction system, to the bundle branches - Fig. AI.7c), and Purkinje fibres - Fig. AI.7d), respecting the

following sequence: septum → apex → bulk of the left/right ventricular free walls. It finishes in the most superior portion of the left ventricular free wall or the right ventricular outflow tract. As depolarisation of both ventricles normally occurs simultaneously, the greater muscle mass of the left ventricle generates stronger electrical activity, and thus the electrical forces are directed downward and somewhat to the left.

After the total depolarisation of the ventricles, there's little activity until repolarisation - the return of myocardial cells to their resting negative potential - beginning from endocardium to epicardium. Again, the resulting vector of electrical forces (current) tends to be to the left and downward in the direction of the main muscle mass of the left ventricle - Fig. AI.7b). When the repolarisation is concluded, there is again a period of electrical inactivity, until the next depolarisation cycle starting at the SA node, under normal conditions.

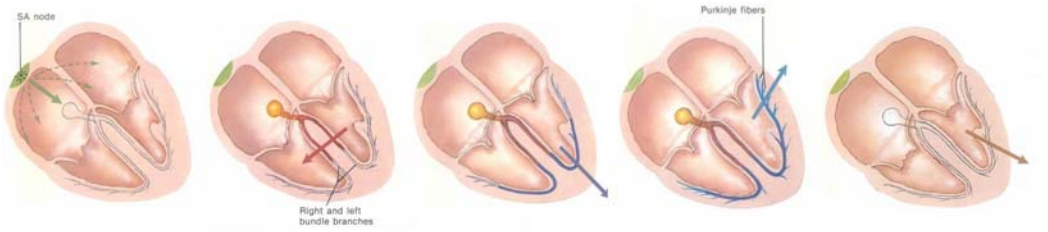

Figure AI.7 - *Cardiac conduction sequence and resultant vectors of electrical activity. a) atrial depolarisation; b) propagation through AV node, bundle of His and bundle branches; c) early depolarisation of interventricular septum; d) late ventricular depolarisation at Purkinje fibres; e) ventricular repolarisation [Sheidt, 2000].*

I.2 Fundaments of electrocardiography

I.2.1 The basic ECG

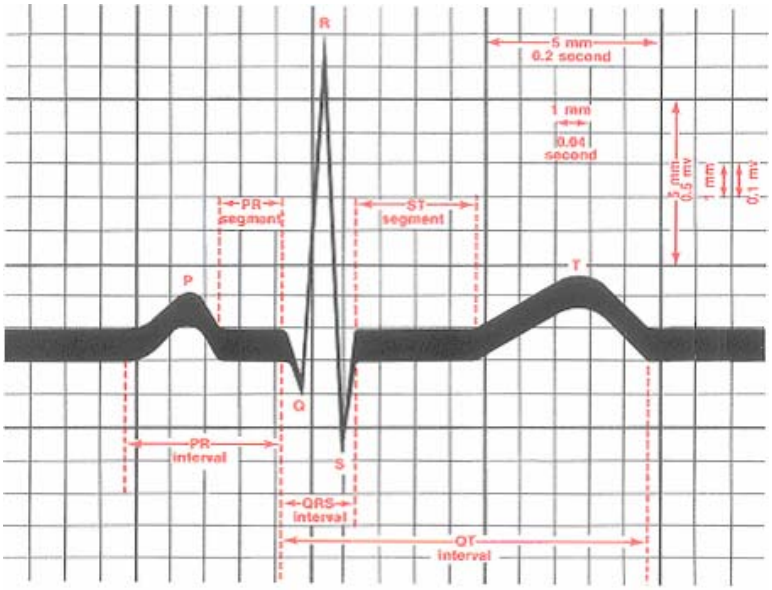

Figure AI.8 - *Morphology of a mean PQRST complex of a normal human ECG [Sheidt, 2000].*

An electrocardiogram (ECG) is a representation of the electrical activity of the heart along the time. Electrocardiograms are recorded from electrodes disposed on the body surface, providing differences of potential. These potentials present an almost cyclic variation in time, where each cycle has the following typical configuration:

From the analysis of Fig. AI.8, we can primarily register the presence of a P-wave, a QRS-complex (Q, R and S waves) and a T-wave. The P-wave is caused by electrical potential generated by the atrial depolarisation, originating an atrial contraction. The QRS-complex is caused by potentials generated when the ventricles depolarise and then, contract. During this phase, the atria also repolarise, but in comparison with the ventricles, they generate such a small electrical activity that it is completely overlapped by the ventricular depolarisation. The T-wave reflects the electrical activity related with ventricular repolarisation.

I.2.2 Relationship between atrial/ventricular contractions and ECG waves

Before the occurrence of any muscular contraction, depolarisation has to propagate through the muscle in order to start the chemical processes for contraction (Fig. AI.9). Therefore, the P-wave occurs immediately before the beginning of atrial contraction and QRS-complex occurs immediately before the beginning of ventricular contraction. Ventricles still contracted until some milliseconds after the end of ventricular repolarisation, which means after the end of T-wave. The ventricular muscle commonly starts its repolarisation around 200-350ms after the beginning of the depolarisation wave. Atrial repolarisation usually occurs 150-200ms after the end of P-wave, simultaneously with the ventricular depolarisation [Guyton, 1991].

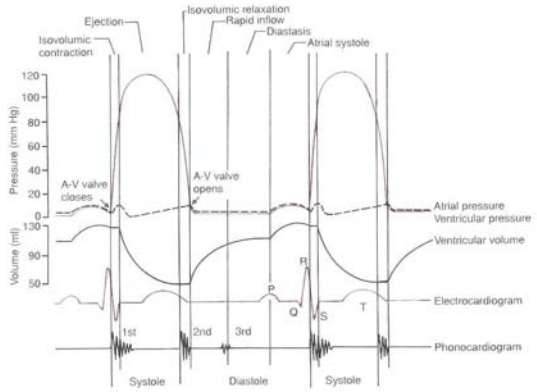

Figure AI.9 – *Diagram for the contractions during the cardiac cycle, showing the related left atrial pressure, left ventricular pressure, the electrocardiogram and the phonocardiogram [Guyton, 1991].*

I.2.3 Basic measurements

In this section, we present the basic measurements that are commonly used to read and interpret ECGs. Depending on the age, family pathological history and other factors, different measures may be more relevant or important to analyse.

Heart Rate (HR) - in bpm (beats per minute)

The heart rate represents the frequency that the heart (and the pacemaker) is beating and is given by the inverse of the RR interval. The most common unit of measurement is bpm (beats per minute), which can be obtained by simply multiplying the inverse of the RR interval by 60.

Intervals / Durations - in seconds (s) or milliseconds (ms)

- **P-wave duration:** is measured from the onset to the end of the P-wave.
- **PQ (PR) interval:** is measured from the onset of the P-wave to the beginning of the QRS-complex and therefore it is sometimes called PQ interval. The denomination *PR interval* is due to the possible absence of Q-wave on the ECG and thus the QRS-complex is considered to begin at the onset of R-wave.
- **QRS duration:** is measured from the onset of Q-wave (or R-wave, if Q-wave is absent) to the termination of S-wave.
- **QT interval:** is measured from the onset of the Q-wave to the end of the T-wave. The same precautions applicable to detect the beginning of PR interval and QRS-complex should be taken.
- **ST segment:** is measured from the end of the QRS-complex (normally the end of S-wave) to the onset of the T-wave.
- **T-wave duration:** is measured from the onset to the end of the T-wave.

Wave Amplitudes - in volt (V) or millivolt (mV)

- **P-wave, QRS-complex, T-wave amplitudes:** these amplitudes are inspected routinely. Amplitudes for positive deflections are measured from the upper margin of the baseline to the top of the positive deflection. The amplitude of negative deflections is measured from the lower margin of the baseline to the lowest point of the wave.

R/S ratio

The R/S ratio compares the individual amplitudes of R and S waves. It is commonly used on the diagnosis of ventricular hypertrophy (section 2.2.2).

QRS axis

The QRS axis represents the direction of the vector of ventricular depolarisation. It can also be seen as an approximation of the mean frontal plane vector of the QRS loop in the vectocardiogram [Sheidt, 2000]. This quantity is important on the diagnosis of ventricular hypertrophy, bundle branch block and other ventricular conduction disturbances. Its calculation may be performed by different methods, such as the *Graph*, the *Successive Approximation* or the *Two Vector Plot* methods [Park, 1992].

P axis and T axis

The same methods for determining the QRS axis can be used for the P axis and T axis. The P axis represents the direction of the atrial depolarisation vector and therefore gives information about the pacemaker site and the location of the SA node. The T axis represents the mean vector of ventricular repolarisation and is important on detecting severe ventricular hypertrophy, ventricular conduction disturbances and other myocardial disorders.

QRS-T angle

The QRS-T angle is the angle formed by the QRS axis and the T axis, relating the ventricular depolarisation and repolarisation activities. It is frequently used together with the mentioned angles on the diagnosis of severe ventricular hypertrophy, ventricular conduction disturbances and other repolarisation disorders on the ventricles.

I.2.4 The 12-Lead Electrocardiogram

In section I.2.1, we mentioned that the electrocardiogram is a representation along the time of the electrical activity of the heart, recorded by electrodes on the body surface. And how is this electrical activity recorded?

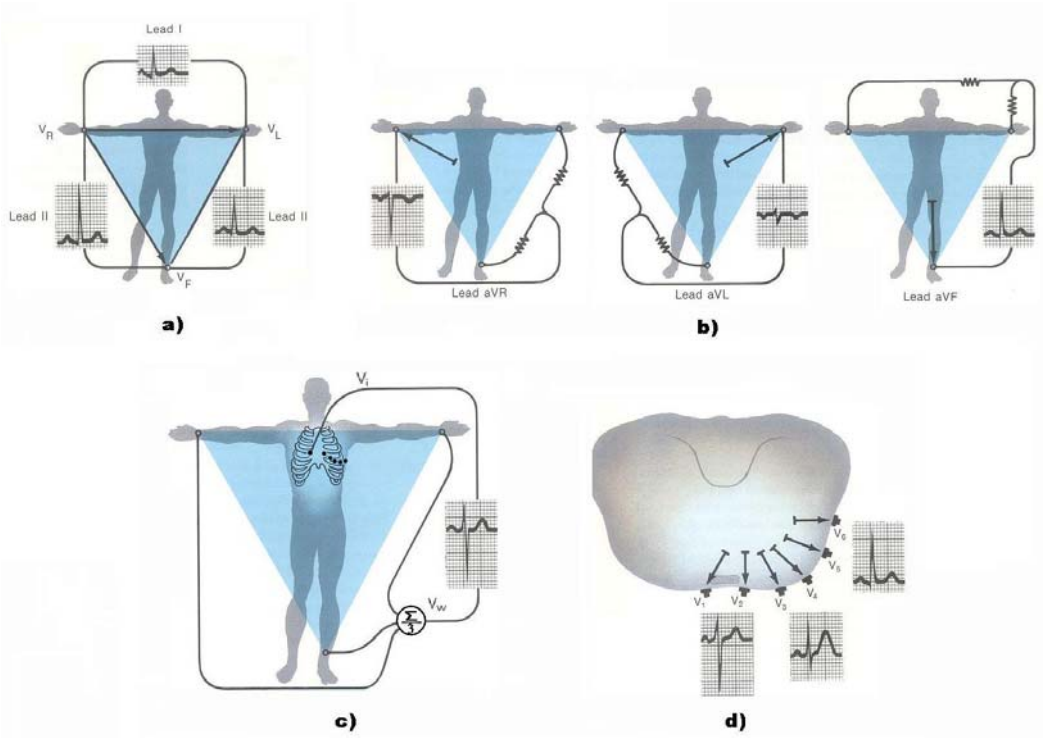

Figure AI.10 – *12-lead ECG: a) limb leads; b) augmented limb leads; c) precordial leads; d) electrode displacement for precordial leads (horizontal plane) [Sheidt, 2000].*

Electrical activity of the heart is captured by the potentials recorded at several electrodes disposed on the body surface and then connected to an electrocardiograph Fig. AI.10. The electrocardiogram results in a representation of the variation in time of the potential difference between two of those electrodes (or combination of electrodes). It can be seen as the projection of the electrical activity along the axis defined by two electrodes in a certain plane of the heart.

Since the first ECG recorded by Willem Einthoven in 1903, a lot of different ways of disposing the electrodes on the body surface have been used. Nowadays, the most commonly used configuration is the 12-lead ECG, providing 12 differences of potential ("leads") in frontal and horizontal planes, using 9 electrodes disposed as show on Fig. AI.10.

Limb leads (leads I, II and III): are derived from the called **"**Einthoven Triangle**"** in the frontal plane, with the poles as shown on Fig. AI.10a). Leads II and III use V_F as the positive pole and V_R, V_L as the negative poles. Lead I uses V_L as the positive pole and V_R as the negative pole.

$$I = V_L - V_R \qquad II = V_F - V_R \qquad III = V_F - V_L$$

Augmented limb leads (leads aVR, aVL and aVF): are derived from the limb leads. V_R, V_L and V_F, respectively, are used as positive poles. The negative poles (ground) are given by the combination of the remainder electrodes in each case Fig. AI.10b).

$$aVR = \frac{2V_R - V_L - V_F}{2} \qquad aVL = \frac{2V_L - V_R - V_F}{2} \qquad aVF = \frac{2V_F - V_L - V_R}{2}$$

Precordial leads (V1, V2, V3, V4, V5, V6): were introduced several decades after the first electrocardiograph, resulting from the need of examination of cardiac events in more than one plan. These leads examine cardiac electrical activity in the horizontal plane - Fig. AI.10d). The positive poles are given by electrodes V_i and the common negative pole is always a ground arranged in the electrocardiograph by connecting V_R, V_L and V_F together - Fig. AI.10c):

$$V_i = v_i - V_w \quad (i = 1 \text{ to } 6)$$

Appendix II

Abnormal neonatal electrocardiograms

Sinus tachycardia

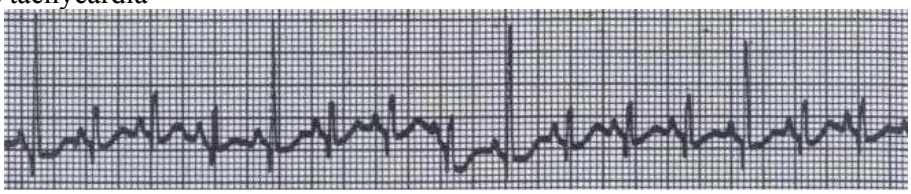

Figure AII.1 – *Tracing from a 4-month-old infant with tetralogy of Fallot and hypoxic spells, showing sinus tachycardia with respiratory variations in QRS voltage [Park, 1992].*

Sinus bradycardia

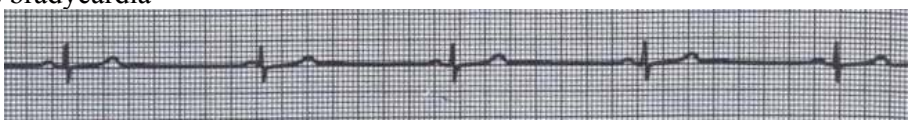

Figure AII.2 – *Tracing from a 14-year-old boy in whom sinus node dysfunction developed following repair of an atrial septal defect, with profound sinus bradycardia and AV nodal escape beat (the second QRS-complex) [Park, 1992].*

Sinus pause

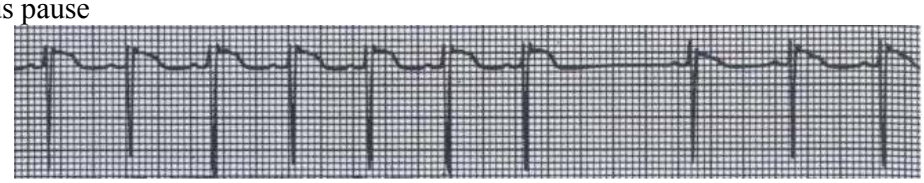

Figure AII.3 – *Tracing from a 11-year-old boy Down's syndrome, endocardial cushion effect, and severe pulmonary hypertension. There is a long pause, which is interrupted by a sinus beat with regular PR interval [Park, 1992].*

Sinus arrest

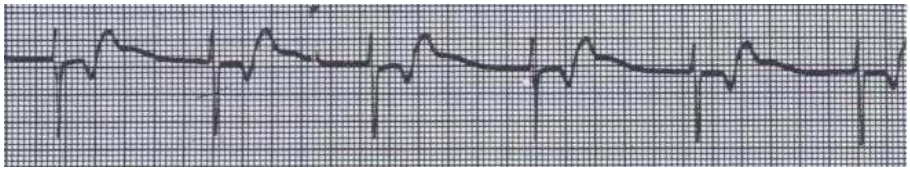

Figure AII.4 – *Tracing from a 4-year-old infant with two left atria, and therefore no SA node. A sinus arrest is present with AV nodal rhythm and retrogradely conducted P-waves [Park, 1992].*

Atrial tachycardia

Figure AII.5 – *Tracing from a 3-day-old neonate who received digoxin for congenital atrial tachycardia. The atrial rate is 235 bpm, too fast to be sinus tachycardia, and fast enough to be atrial tachycardia. Together with atrial tachycardia, the conduction ration 5:4 suggests a 2nd-degree AV block [Park, 1992].*

Atrial flutter

Figure AII.6 – *Tracing from a newborn infant with tachycardia, showing atrial flutter with varying ventricular response [Park, 1992].*

Atrial fibrillation

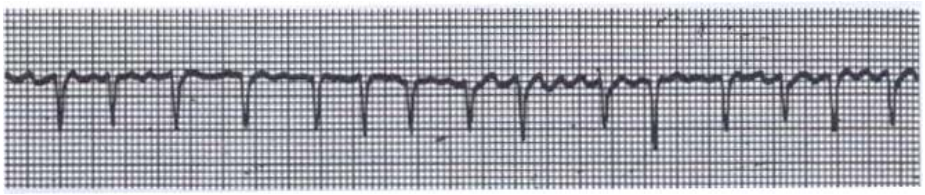

Figure AII.7 – *Tracing from a healthy-looking newborn infant with atrial flutter and fibrillation. The latter is identified by the irregularly irregular atrial rhythm, the former is identified the "sawtooth" typical shape of some P-waves [Park, 1992].*

Nodal tachycardia

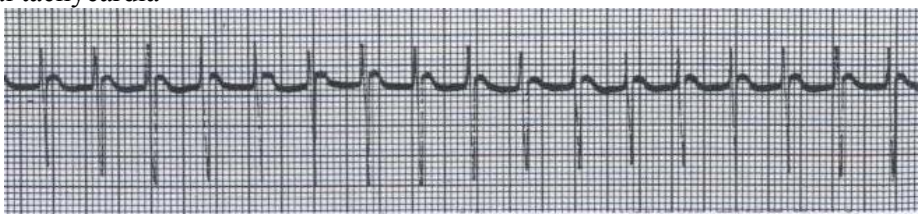

Figure AII.8 – *Rhythm strip from a 3-month-old infant with signs of congestive heart failure. A regularly regular nodal tachycardia (188 bpm) is present together with no visible P-waves [Park, 1992].*

PVC – Premature ventricular contractions

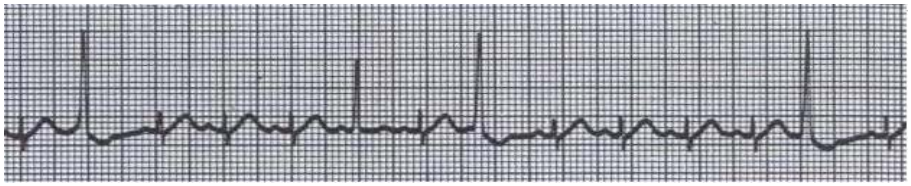

Figure AII.9 – *Tracing form a 7-month-old infant with myocarditis, showing premature ventricular contractions and one ventricular fusion complex (the 6th QRS-complex) [Park, 1992].*

Ventricular tachycardia

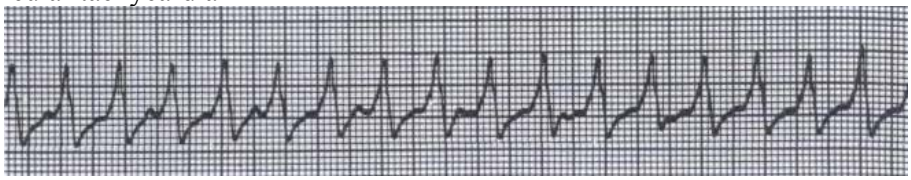

Figure AII.10 – *Tracing form an 8-year-old child who had corrective surgery for tetralogy of Fallot. The rhythm is regular with rapid HR (176 bpm) and the QRS duration is wide with no regular preceding P-wave [Park, 1992].*

Ventricular fibrillation

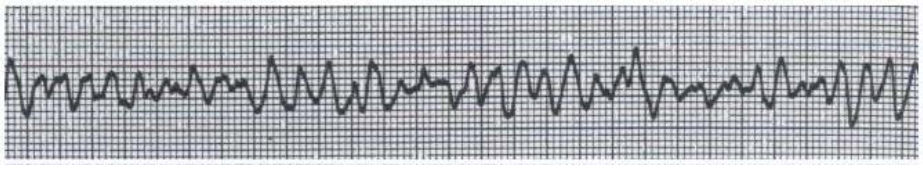

Figure AII.11 – *Rhythm strip showing clear ventricular fibrillation obtained in the operating room from a 9-month-old infant who was undergoing surgery for tetralogy of Fallot [Park, 1992].*

1st degree AV block

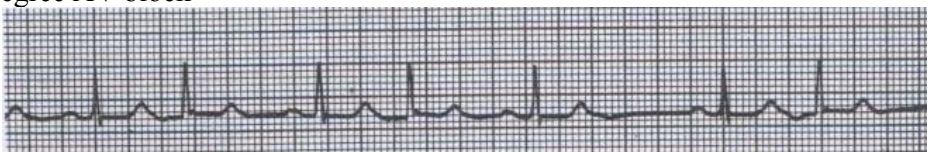

Figure AII.12 – *Tracing from a 6-year-old child who had repair of a secundum atrial septal defect. There is a 1st degree AV block (before 3rd, 5th, 7th QRS-complexes) and several ectopic atrial contractions (before 2nd, 4th, 7th QRS-complexes) [Park, 1992].*

2nd degree AV block

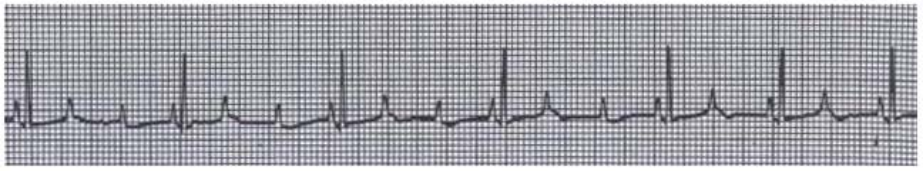

Figure AII.13 – *Tracing from a 3-day-old neonate born to a morphine-addicted mother, showing 2:1 and 3:1 second-degree AV block [Park, 1992].*

Complete AV block

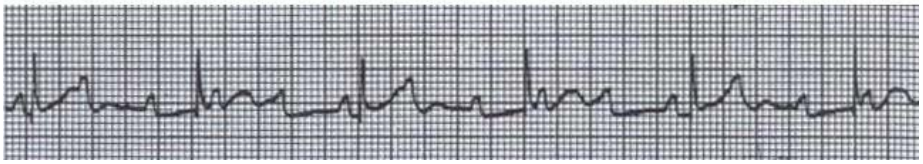

Figure AII.14 – *Tracing from a 2-day-old neonate with a slow heart rate, showing a complete AV block of suprahisian type (AV nodal rhythm with complete AV block) [Park, 1992].*

AV dissociation

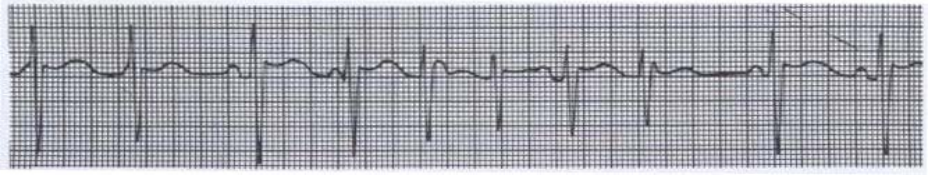

Figure AII.15 – *Tracing from a 3-year-old child, immediately after the repair of ventricular septal defect. The paper speed was 50/min, twice the usual. The atrial rate is regular, the QRS-complex and its rate in the midportion is about 230 bpm. The 3rd and last QRS-complexes are of sinus origin [Park, 1992].*

Ventricular pacemaker

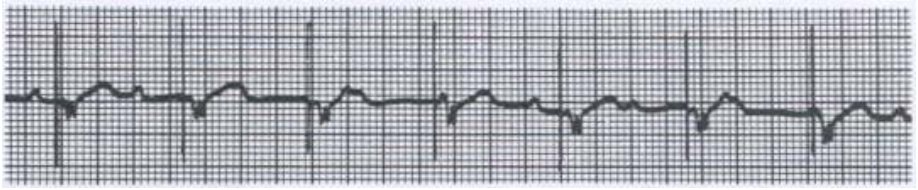

Figure AII.16 – *Example of a fixed-rate ventricular pacemaker tracing with large electronic spikes followed by relatively wide and small-voltage QRS-complexes [Park, 1992].*

Atrial pacemaker

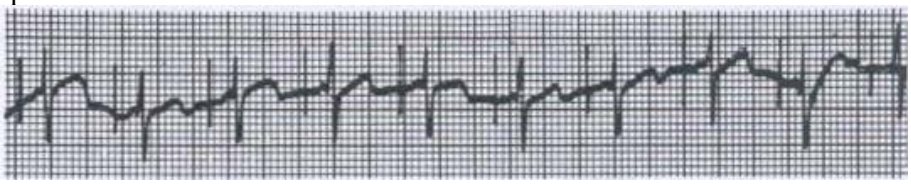

Figure AII.17 – *Example of an atrial pacemaker tracing from a 2-year-old child in whom extreme, symptomatic sinus bradycardia developed following surgical repair for transposition of the great arteries. There is an atrial complex following the atrial electronic spike [Park, 1992].*

P-wave triggered ventricular pacemaker

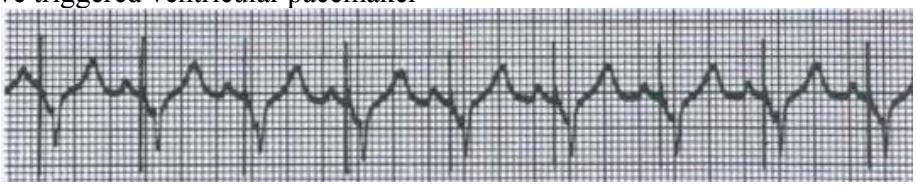

Figure AII.18 – *Example of a P-wave triggered ventricular pacemaker tracing from an infant who developed surgically induced heart block, for which an artificial pacemaker was implanted. The rate of ventricular pacing varies with the rate of the patient's own P-wave [Park, 1992].*

QT prolongation

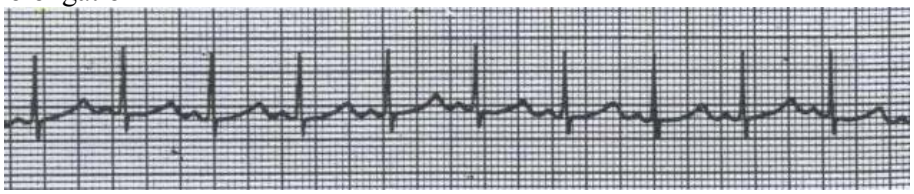

Figure AII.19 – *ECG tracing from an infant of a diabetic mother, showing a regular sinus rhythms, and long QT interval suggestive of hypocalcemia [Park, 1992].*

LQTS – Long QT syndrome

Figure AII.20 – *ECG tracing of a newborn with LQTS diagnosed in the first months of life [Schwartz, 2002].*

ST depression

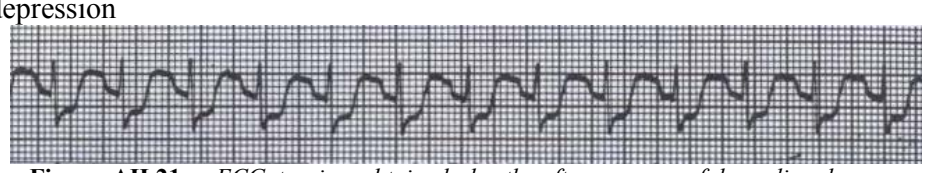

Figure AII.21 – *ECG tracing obtained shortly after a successful cardiopulmonary resuscitation on a 4-year-old child. There is a sinus tachycardia with ST-segment depression and P-waves buried in previous T-waves [Park, 1992].*

SVT - Reciprocating AV tachycardia

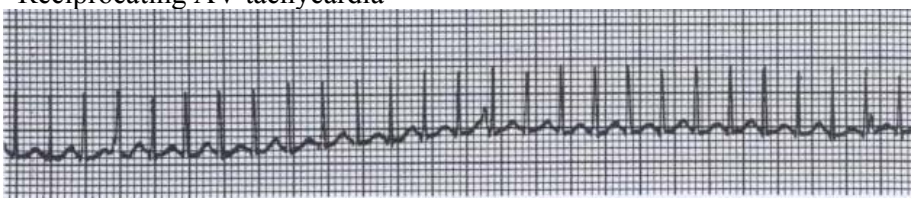

Figure AII.22 – *Tracing from a 3-month-old infant with cardiomegaly and rales, indicating a supraventricular tachycardia, probably reciprocating AV tachycardia [Park, 1992].*

Wolff-Parkinson-White syndrome

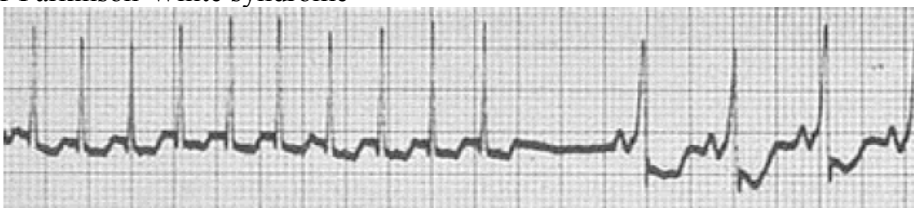

Figure AII.23 – *Tracing from a neonate with Wolff Parkinson-White syndrome [Schwartz, 2002].*

Appendix III

Detailed discussion of simulation results

On below, we make some comments about the results from simulations presented in Chapter 7, together with some considerations on how the simulated results reproduce the examples of target rhythms, with ECGs shown in Appendix III.

Sinus rhythms

Despite the differences mentioned on the previous section, we consider that the simulated and real ECGs of normal sinus rhythm at 150 bpm (Fig. 7.2) are concordant. They are both regular rhythms, resulting from the normal impulse formation at the SA node and conduction to the ventricles. In this and all the other simulations, the ST-segment varies correctly with the HR, according to section 5.2.4.

Sinus tachycardia and bradycardia result from accelerated or decelerated sinus automaticity (values concordant with the proposed by [Park, 1992, Schwartz, 2002]). The example of sinus tachycardia (Fig. AII.1) differs from the simulated ECG as it presents respiratory variations on QRS and baseline voltage. Its HR is about 150 bpm (our proposed normal HR), but we should note that in the patient's age – 4 months old – the normal HR is usually lower than a 3-weeks-old neonate. The target example of regular and stable tbradycardia (Fig. AII.2) is quite similar to the simulated ECG on Fig. 7.5, even thoug with a slower rate, normal for sinus bradycardia in a 14-year-old boy.

The method for simulating the sinus pause (Fig. 7.6) resulted in a good reproduction of the ECG example shown on Fig. AII.3 from an 11-year-old boy. The use of a script or state machine that could occasionally alter the sinus automaticity would be a better solution in case of a script-controlled model-driven simulator.

On the simulation of a sinus arrest, the atrial automaticity was decreased in order to let the AV node take the pacemaker role. The ECG on Fig. 7.8, with augmented AV node↔atrium conduction, clearly shows the retrograde P-wave between the QRS-complex and T-wave, as in the target example on Fig. AII.4.

Atrial, nodal and ventricular disrhythmias

The simulated atrial tachycardia presents a typical rate (200 bpm) close to the rate in the target example in Fig. AII.5 (235 bpm), as well as tall P-waves (similar to the T-waves). In Fig. 7.9, the variable ventricular rate is due to a 2nd degree AV block.

The ECG of simulated nodal tachycardia is similar to the one presented for sinus arrest. The difference is that the SA node does not fail, but has a slower rate. P-waves are still not visible, being superimposed on previous QRS-complexes. The same happens on the target example in Fig. AII.8.

PVCs were simulated using the same strategy for the sinus pause. In this case, the simulation had to be stopped for altering the ventricular automaticity. Although we consider the resulting ECG a good reproduction of the example on Fig. AII.9, the random occurrence of PVCs could be generated over script or state-machine control.

The simulated ventricular tachycardia presented expected high ventricular rate, wide and tall QRS-complexes, and superimposed P and T-waves. The example of

target rhythm in Fig. AII.10 also presents wide QRS-complexes, absence of QRS preceding P-waves, and inverted T-waves. As the mechanism for T-wave inversion in neonates is not clearly defined in [Fukushima, 1984] nor [Park, 1992], we didn't include such templates in our model.

Conduction disturbances

On the 1st degree AV block, the generated PR interval is large, but inside of the limits on Table 3.2, and originates superposition of P-waves on the previous T-waves. The target example on Fig. AII.12 shows episodes of AV block in slower rhythm, but combined with other rhythm disturbances.

Our simulated 2nd degree AV block was based on the limited capacity of the AV node to conduct impulses at a high rate, due to its typical delay. The target example on Fig. AII.13, shows a combination of a 2:1 and 3:1 block, which apparently results from the same mechanism. In a script or state-machine controlled simulator, this kind of block could also be simulated by regularly blocking the AV node or the bundle of His.

The simulated ECG of complete AV block on Fig. 7.15 is highly concordant with the target example shown in Fig. AII.14. They both present regular atrial and ventricular rates of approx. 150 bpm and 60 bpm, respectively. In both cases, normal P-waves from normal sinus impulse formation and QRS-complexes from AV nodal pacing are irregularly superimposed.

Reentry

The simulated accessory reciprocating AV tachycardia shows a rhythm similar to the normal sinus rhythm with inverted P-waves. However, the retrograde atrial depolarisation has its origin in the accessory pathway from the ventricle. In this case, the time for that conduction makes the P-wave occur after the current ventricular depolarisation and repolarisation. In the example of Fig. AII.22, at a higher rate, P-waves are usually superimposed with the QRS-complexes.

The proposed simulation of WPW syndrome represents efficiently the origin of the delta waves, and is in agreement with the target example in Fig. AII.23 (even if the latter presents a higher HR). The use of two templates for representation of normal and accessory ventricular depolarisations starting at different time instants (Fig. AIII.1) could be another good solution for generating QRS-complexes with delta-waves.

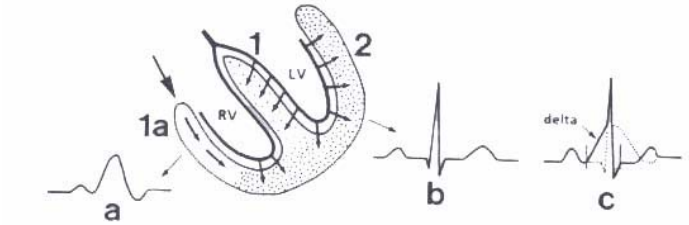

Figure AIII.1 – *Sequence of ventricular depolarisation in the WPW syndrome and the mechanism for generation of abnormal QRS-complex. When the ventricle is depolarised through the abnormal pathway, the QRS is wide (1a); normal depolarisation of the remainder of the ventricle originates normal QRS (1b). The end result is superimposition of "a" and "b", the typical QRS of WPW syndrome (1c) [Park, 1992].*